VOLUME 2 (1956/57) No. 6

NUCLEAR PHYSICS

MONTHLY JOURNAL DEVOTED TO THE EXPERIMENTAL AND THEORETICAL STUDY OF ATOMIC NUCLEI, NUCLEAR FIELDS AND THE FUNDAMENTAL ASPECTS OF COSMIC RADIATION

EDITOR: L. ROSENFELD - MANCHESTER

H. R. ROBL. Kern-Anregung durch Elektronen 641

P. ROMÁN, On the isocovariance properties of leptons . . . 651

G. BERTOLINI, Upper limit for the lifetimes of excited states of Fe^{56} and Ti^{46} 660

G. TRUMPY, Measurement of circularly polarized gamma-radiation following polarized neutron capture 664

T. LINDQVIST and E. HEER, Directional correlation measurements in Fe^{57} 680

N. N. DELYAGIN, A. A. SOROKIN, N. V. FORAFONTOV and V. S. SHPINEL, Decay scheme for Zr^{97} and Nb^{97} 687

V. GLASER and G. KÄLLÉN, A model of an unstable particle 706

A. Z. DOLGINOV, On the information about β-interaction and nuclear levels derived from the polarization of X-ray quanta 723

M. D'HONT and A. DE LATTRE, Note on the isotopic effect in the fractional decomposition of potassium fluoborate . . 736

Book review 737

AUTHOR INDEX 738

INDEX BOOK REVIEWS 742

SUBJECT INDEX 742

NORTH-HOLLAND PUBLISHING COMPANY - AMSTERDAM

February 1957

EDITORIAL BOARD

AUSTRIA:	B. Karlik (Vienna), H. Thirring (Vienna)
BELGIUM:	M. de Hemptinne (Louvain), J. Verhaeghe (Ghent)
CANADA:	G. Volkoff (Vancouver)
DENMARK:	C. Møller (Copenhagen), S. Rozental (Copenhagen)
EGYPT & ARAB COUNTRIES:	F. El Bedewi (Alexandria), M. G. Nooh (Cairo)
FINLAND:	L. Simons (Helsinki)
FRANCE:	A. Berthelot (Saclay), S. Gorodetzky (Strasbourg), F. Joliot (Paris)
GERMANY (FED. REP.):	W. Gentner (Freiburg i. B.), J. H. D. Jensen (Heidelberg)
GERMANY (DEM. REP.):	G. Hertz (Leipzig)
GREAT BRITAIN:	S. Devons (Manchester)
HUNGARY:	L. Janossy (Budapest)
INDIA:	H. Bhabha (Bombay), B. Peters (Bombay), R. Ramanna (Trombay)
IRISH REPUBLIC:	J. McConnell (Maynooth)
ISRAEL:	G. Racah (Jerusalem)
ITALY:	E. Amaldi (Rome)
JAPAN:	S. Kikuchi (Tokyo), S. Tomonaga (Tokyo)
NETHERLANDS:	H. Brinkman (Groningen), S. R. de Groot (Leiden)
NORWAY:	E. Hylleraas (Oslo), A. Lundby (Oslo), H. Wergeland (Trondheim)
POLAND:	L. Infeld (Warsaw)
PORTUGAL:	J. M. Araújo (Porto), J. R. de Almeida Santos (Coimbra)
SOUTH AMERICA:	G. Beck (Saõ Paulo), J. Leite Lopes (Rio de Janeiro)
SPAIN:	J. M. Otero (Madrid), C. Sanchez del Rio (Madrid)
SWEDEN:	O. Klein (Stockholm), K. Siegbahn (Uppsala), I. Waller (Uppsala)
SWITZERLAND:	P. Huber (Basel), P. Scherrer (Zürich)
U.S.S.R.:	M. A. Markov (Moscow), I. S. Shapiro (Moscow), D. V. Skobeltzyn (Moscow)
YUGOSLAVIA:	I. Supek (Zagreb)
U.S.A. & MEXICO:	V. Weisskopf (Cambridge, Mass.)
AUSTRALIA & NEW ZEALAND:	H. Messel (Sydney), M. L. Oliphant (Canberra)

CONTRIBUTIONS may be sent to the Editor, Professor L. Rosenfeld, Dept. of Theoretical Physics, The University, Manchester, either directly, or preferably through the intermediary of one of the members of the Editorial Board of the country or region in which the author is working. They may be written in English, French or German.

BOOKS FOR REVIEW should be sent to Professor Rosenfeld.

NUCLEAR PHYSICS is published in monthly issues. The subscription price of a volume of 700 pages is fl 57.00; 114s; $ 15.00. Postfree.

SUBSCRIPTIONS should be sent to the publishers, NORTH-HOLLAND PUBLISHING COMPANY, P.O.Box 103, Amsterdam or to any subscription-agent. Subscriptions for U.S.A. are to be sent exclusively to INTERSCIENCE PUBLISHERS, INC., 250 Fifth Avenue, New York 1, N.Y.

Printed in the Netherlands.

Nuclear Physics **2** (1956/57) 641—650; *North-Holland Publishing Co., Amsterdam*

KERN-ANREGUNG DURCH ELEKTRONEN

H. R. ROBL
Office of Ordnance Research, U. S. Army

Received 12 October 1956

Abstract: The excitation of nuclei by electrons is considered as the inverse process to electron scattering in transitions of nuclei to states of lower energy. The calculation of the cross-sections does not make explicit use of nuclear matrix elements, but involves only the mean life-times of the excited states. The cross-sections are given for magnetic and electric multipole transitions of arbitrary order. The total cross-sections for an electron energy of 10 mc^2 and for excitation energies between 0.2 and 5 mc^2 are shown in the figure.

Die unelastische Streuung von Elektronen an Atomkernen ist schon in mehreren theoretischen Arbeiten behandelt worden [1]). Die vorliegende Arbeit unterscheidet sich von den früheren Berechnungen hauptsächlich dadurch, daß sie die Kern-Anregung durch Elektronen als inversen Prozeß zur Streuung von Elektronen bei Übergängen von angeregten Atomkernen in Zustände mit niedrigerer Energie betrachtet. Die mathematische Beschreibung einer solchen Streuung von Elektronen steht in enger Beziehung zur inneren Paarerzeugung. Man kann daher die von Rose [2]) angegebenen Faktoren für innere Paarerzeugung sofort in Wirkungsquerschnitte für die Kern-Anregung durch Elektronen umschreiben.

Zur Berechnung der Kern-Anregung durch Elektronen ist es aber zweckmäßig, an Stelle der von Rose durchgeführten Integrationen über alle Richtungen der Achse des Multipolfeldes, als ausgezeichnete Richtung des Multipolfeldes die Richtung des übertragenen Impulses zu wählen [3]). Es zeigt sich nämlich, daß in Bezug auf die ausgezeichnete Richtung nur Übergänge mit der Richtungsquantenzahl -1, $+1$ und 0 zur Streuung beitragen. Diese Auswahlregel ermöglicht die Bestimmung der Richtungsverteilung der Lichtquanten, die nach der Anregung von Atomkernen emittiert werden.

Ein bemerkenswerter Vorteil der hier verwendeten Methode besteht darin, daß Kern-Matrixelemente explizit in die Rechnung überhaupt nicht eingehen. Dafür enthält der Wirkungsquerschnitt die mittlere Lebensdauer des angeregten Zustandes. Die Messung

des Wirkungsquerschnittes ermöglicht daher eine indirekte Bestimmung der Lebensdauer des angeregten Zustandes. Dieses Verfahren erscheint besonders vorteilhatt, wenn die Lebensdauer zu kurz ist, um eine direkte Messung zu gestatten. Die indirekte Bestimmung einer sehr kurzen Lebensdauer wird dadurch begünstigt, daß der Wirkungsquerschnitt für die Kern-Anregung durch Elektronen der Lebensdauer des angeregten Zustandes verkehrt proportional ist.

Es soll zunächst der Wirkungsquerschnitt für die Streuung von Elektronen durch Multipolpotentiale angegeben werden. Wir setzen $\hbar = c = m = 1$ und verwenden die von Rose [2]) angegebenen Multipolpotentiale

$$\begin{aligned} \mathbf{A} &= \left[\frac{2}{\pi l(l+1)}\right]^{\frac{1}{2}} h_l(kr)\mathbf{L}Y_l^m(\vartheta,\varphi) \\ V &= 0 \end{aligned} \tag{1}$$

mit $\mathbf{L} = -i\mathbf{r}\times\mathrm{grad}$ für magnetische Übergänge und

$$\begin{aligned} \mathbf{A} &= \left[\frac{2}{\pi l(l+1)}\right]^{\frac{1}{2}} h_{l-1}(kr)\mathbf{R}Y_l^m(\vartheta,\varphi) \\ V &= i\left[\frac{2l}{\pi(l+1)}\right]^{\frac{1}{2}} h_l(kr)Y_l^m(\vartheta,\varphi) \end{aligned} \tag{2}$$

mit $\mathbf{R} = r\ \mathrm{grad} + l(\mathbf{r}/r)$ für elektrische Übergänge. Die Multipolpotentiale enthalten die sphärischen Hankel-Funktionen $h_l(\varrho) = (\pi/2\varrho)^{\frac{1}{2}}H^{(1)}_{l+\frac{1}{2}}(\varrho)$ und die normierten Kugelflächenfunktionen $Y_l^m(\vartheta,\varphi)$. Mit den hier benützten Einheiten ist k die Energie der Multipolquanten. Die Potentiale entsprechen der Emission von $1/\pi^2 k$ Quanten pro Zeitinheit.

Es sei t die mittlere Lebensdauer eines angeregten Zustandes. Für die Wahrscheinlichkeit des Überganges eines Elektrons von dem Impuls $\mathbf{p}$ zu dem Impuls $\mathbf{p}_0$ in den Raumwinkel $\mathrm{d}\Omega_0$ pro Zeiteinheit ergibt sich dann

$$\mathrm{d}w_0 = L^3\frac{\alpha}{4}\frac{k}{t}\frac{1}{2l+1}\,\mathrm{S}_m\mathrm{S}_0\,\tfrac{1}{2}\mathrm{S}\left|\int \psi_0^*(V+\boldsymbol{\alpha}\cdot\mathbf{A})\psi\,\mathrm{d}^3\mathbf{r}\right|^2 p_0 E_0\,\mathrm{d}\Omega_0; \tag{3}$$

L^3 ist das Normierungsvolumen. Die Feinstrukturkonstante $\alpha = 1/137$ rührt von der Elementarladung her. $\frac{1}{2}\mathrm{S}$ bedeutet Mittelung über die Spineinstellungen im Anfangszustand, S_0 Summation über die Spineinstellungen im Endzustand und $(2l+1)^{-1}\mathrm{S}_m$ Mittelung über die Einstellungen der Achse des Multi-

polpotentials. $\boldsymbol{\alpha}$ ist der Dirac'sche Matrixvektor, $E_0 = (p_0^2+1)^{\frac{1}{2}}$ die Energie des Elektrons im Endzustand. Wir verwenden ebene Wellen $\psi = L^{-3/2} u \exp i(\mathbf{p}\cdot\mathbf{r})$ mit Dirac'schen Amplituden u. Wegen $\mathrm{d}\sigma_0 = L^3(E/p)\mathrm{d}w_0$ mit $E = (p^2+1)^{\frac{1}{2}}$ ergibt sich für den Wirkungsquerschnitt der Streuung

$$\mathrm{d}\sigma_0 = \frac{\alpha}{8}\frac{k}{t}\frac{1}{2l+1}\,\mathrm{S}_m\,\mathrm{S}_0\,\mathrm{S}|M|^2\frac{p_0}{p}E_0\,E\,\mathrm{d}\Omega_0 \tag{4}$$

wobei $M = u_0^*(Q+\boldsymbol{\alpha}\cdot\mathbf{P})u$ und

$$Q = \int V\mathrm{e}^{i\mathbf{q}\cdot\mathbf{r}}\mathrm{d}^3\mathbf{r}, \qquad \mathbf{P} = \int \mathbf{A}\mathrm{e}^{i\mathbf{q}\cdot\mathbf{r}}\mathrm{d}^3\mathbf{r} \tag{5}$$

mit $\mathbf{q} = \mathbf{p}-\mathbf{p}_0$.

Der inverse Prozeß besteht offensichtlich in dem Übergang eines Elektrons aus einem Anfangszustand mit dem Impuls $-\mathbf{p}_0$ in einen Endzustand mit dem Impuls $-\mathbf{p}$. Es ist $E = E_0-k$. Auf Grund des Prinzips der Detailed Balance besteht zwischen dem Wirkungsquerschnitt $\mathrm{d}\sigma_0$ und dem Wirkungsquerschnitt $\mathrm{d}\sigma$ des inversen Prozesses die Beziehung $\mathrm{d}\sigma_0/\mathrm{d}\sigma = gp^2\mathrm{d}\Omega/g_0p_0^2\mathrm{d}\Omega_0$, wobei g und g_0 die Multiplizität der Endzustände in beiden Prozessen bedeutet. Es sei der Kernspin im Grundzustand I und im angeregten Zustand I^*. Dann ist $g/g_0 = (2I^*+1)/(2I+1)$. Daraus ergibt sich für den gesuchten Wirkungsquerschnitt der Kern-Anregung durch Elektronen

$$\mathrm{d}\sigma = \frac{2I^*+1}{2I+1}\frac{\alpha}{8}\frac{k}{t}\frac{1}{2l+1}\,\mathrm{S}_m\,\mathrm{S}_0\,\mathrm{S}|M|^2\frac{p}{p_0}E_0\,E\,\mathrm{d}\Omega. \tag{6}$$

Wenn die mittlere Lebensdauer des angeregten Zustandes t in Sekunden eingesetzt wird und der Wirkungsquerschnitt in cm^2 angegeben werden soll, so ist mit dem Faktor λ_0^3/c zu multiplizieren.

Die Spinsummationen liefern bei Verwendung der Gleichung $M = u_0^*(Q+\boldsymbol{\alpha}\cdot\mathbf{P})u$

$$\mathrm{S}_0\,\mathrm{S}|M|^2 = \frac{1}{E_0\,E}\{(E_0\,E-\mathbf{p}_0\cdot\mathbf{p}-1)(\mathbf{P}^*\cdot\mathbf{P})+(E_0\,E+\mathbf{p}_0\cdot\mathbf{p}+1)(Q^*Q)$$
$$+[(\mathbf{p}_0\cdot\mathbf{P}^*)(\mathbf{p}\cdot\mathbf{P})+E_0Q^*(\mathbf{p}\cdot\mathbf{P})+EQ^*(\mathbf{p}_0\cdot\mathbf{P})+\mathrm{c.c.}]\} \tag{7}$$

Hierbei bedeutet c.c. den konjugiert komplexen Ausdruck. Nach Gl. (6) wird daher

$$\mathrm{d}\sigma = \frac{2I^*+1}{2I+1}\frac{\alpha}{8}\frac{k}{t}\frac{p}{p_0}\frac{1}{2l+1}\sum_{m=-l}^{m=+l}\{(E_0\,E-\mathbf{p}_0\cdot\mathbf{p}-1)(\mathbf{P}^*\cdot\mathbf{P}) \tag{8}$$
$$+(E_0\,E+\mathbf{p}_0\cdot\mathbf{p}+1)Q^*Q+[(\mathbf{p}_0\cdot\mathbf{P}^*)(\mathbf{p}\cdot\mathbf{P})$$
$$+E_0Q^*(\mathbf{p}\cdot\mathbf{P})+EQ^*(\mathbf{p}_0\cdot\mathbf{P})+\mathrm{c.c.}]\}\,\mathrm{d}\Omega.$$

Der in der geschweiften Klammer stehende Ausdruck ist nun getrennt für magnetische und für elektrische Übergänge zu berechnen.

Für magnetische Übergänge ist nach Gl. (5) $Q = 0$ und

$$\mathbf{P} = \left[\frac{2}{\pi l(l+1)}\right]^{\frac{1}{2}} \int e^{i\mathbf{q}\cdot\mathbf{r}} h_l(kr)\mathbf{L}Y_l^m(\vartheta, \varphi)\mathrm{d}^3\mathbf{r}. \tag{9}$$

Für die Komponenten des Drehimpulsoperators gilt

$$\begin{aligned}(L_x \pm iL_y)Y_l^m &= [(l \mp m)(l \pm m+1)]^{\frac{1}{2}} Y_l^{m\pm 1}\\ L_z Y_l^m &= mY_l^m.\end{aligned} \tag{10}$$

Fällt die z-Achse des Koordinatensystems in die Richtung des übertragenen Impulses $\mathbf{q}$, dann ist

$$e^{i\mathbf{q}\cdot\mathbf{r}} = (4\pi)^{\frac{1}{2}} \sum_{\lambda=0}^{\infty} i^\lambda (2\lambda+1)^{\frac{1}{2}} j_\lambda(qr) Y_\lambda^0(\vartheta, \varphi) \tag{11}$$

mit den sphärischen Bessel-Funktionen $j_\lambda(\varrho) = (\pi/2\varrho)^{\frac{1}{2}} J_{\lambda+\frac{1}{2}}(\varrho)$. Da $Y_\lambda^0 = Y_\lambda^{0*}$, findet man auf Grund der Orthogonalitätsrelationen der Kugelflächenfunktionen

$$\begin{aligned}P_x \pm iP_y &= 2i^l[2(2l+1)]^{\frac{1}{2}} I_l \delta_{\mp 1}^m\\ P_z &= 0\end{aligned} \tag{12}$$

oder

$$\begin{aligned}P_x &= i^l[2(2l+1)]^{\frac{1}{2}} I_l(\delta_{+1}^m + \delta_{-1}^m)\\ P_y &= i^{l+1}[2(2l+1)]^{\frac{1}{2}} I_l(\delta_{+1}^m - \delta_{-1}^m)\\ P_z &= 0\end{aligned} \tag{13}$$

wobei

$$I_l = \int_0^\infty h_l(kr) j_l(qr) r^2 \,\mathrm{d}r. \tag{14}$$

Man sieht, daß nur die Richtungsquantenzahlen $m = +1$ und $m = -1$ einen Beitrag liefern.

Zur Berechnung von I_l verwendet man das unbestimmte Integral [4])

$$\int h_l(kr) j_l(qr) r^2 \,\mathrm{d}r = \frac{r^2}{k^2 - q^2}[q h_l(kr) j_{l-1}(qr) - k h_{l-1}(kr) j_l(qr)]. \tag{15}$$

Mit Hilfe der asymptotischen Darstellung der sphärischen Bessel-Funktionen und sphärischen Hankel-Funktionen für kleines und großes Argument findet man

$$I_l = \frac{i}{k^2 - q^2} \frac{q^l}{k^{l+1}}. \tag{16}$$

NUCLEAR PHYSICS

EDITORIAL BOARD

AUSTRIA:	B. Karlik (Vienna), H. Thirring (Vienna)
BELGIUM:	M. de Hemptinne (Louvain), J. Verhaeghe (Ghent)
CANADA:	G. Volkoff (Vancouver)
DENMARK:	C. Møller (Copenhagen), S. Rozental (Copenhagen)
EGYPT & ARAB COUNTRIES:	F. El Bedewi (Alexandria), M. G. Nooh (Cairo)
FINLAND:	L. Simons (Helsinki)
FRANCE:	A. Berthelot (Saclay), S. Gorodetzky (Strasbourg), F. Joliot (Paris)
GERMANY (FED. REP.):	W. Gentner (Freiburg i. B.), J. H. D. Jensen (Heidelberg)
GERMANY (DEM. REP.):	G. Hertz (Leipzig)
GREAT BRITAIN:	S. Devons (Manchester)
HUNGARY:	L. Janossy (Budapest)
INDIA:	H. Bhabha (Bombay), B. Peters (Bombay), R. Ramanna (Trombay)
IRISH REPUBLIC:	J. McConnell (Maynooth)
ISRAEL:	G. Racah (Jerusalem)
ITALY:	E. Amaldi (Rome)
JAPAN:	S. Kikuchi (Tokyo), S. Tomonaga (Tokyo)
NETHERLANDS:	H. Brinkman (Groningen), S. R. de Groot (Leiden)
NORWAY:	E. Hylleraas (Oslo), A. Lundby (Oslo), H. Wergeland (Trondheim)
POLAND:	L. Infeld (Warsaw)
PORTUGAL:	J. M. Araújo (Porto), J. R. de Almeida Santos (Coimbra)
SOUTH AMERICA:	G. Beck (Saõ Paulo), J. Leite Lopes (Rio de Janeiro)
SPAIN:	J. M. Otero (Madrid), C. Sanchez del Rio (Madrid)
SWEDEN:	O. Klein (Stockholm), K. Siegbahn (Uppsala), I. Waller (Uppsala)
SWITZERLAND:	P. Huber (Basel), P. Scherrer (Zürich)
U.S.S.R.:	M. A. Markov (Moscow), I. S. Shapiro (Moscow), D. V. Skobeltzyn (Moscow)
YUGOSLAVIA:	I. Supek (Zagreb)
U.S.A. & MEXICO:	V. Weisskopf (Cambridge, Mass.)
AUSTRALIA & NEW ZEALAND:	H. Messel (Sydney), M. L. Oliphant (Canberra)

NUCLEAR PHYSICS

MONTHLY JOURNAL DEVOTED TO THE EXPERIMENTAL AND THEORETICAL STUDY OF ATOMIC NUCLEI, NUCLEAR FIELDS AND THE FUNDAMENTAL ASPECTS OF COSMIC RADIATION

EDITOR: L. ROSENFELD · MANCHESTER

VOLUME II

SEPTEMBER 1956—FEBRUARI 1957

NORTH-HOLLAND PUBLISHING COMPANY - AMSTERDAM

PRINTED IN THE NETHERLANDS BY
BOEKDRUKKERIJ VOORHEEN GEBROEDERS HOITSEMA N.V., GRONINGEN

Mit den oben angegebenen Komponenten von $\mathbf{P}$ ergibt sich

$$\frac{1}{2l+1}\sum_{m=-l}^{m=+l}\mathbf{P}^*\cdot\mathbf{P}=8\,|I_l|^2. \tag{17}$$

Bezeichnet man in dem durch $\mathbf{p}-\mathbf{p}_0=\mathbf{q}$ bestimmten Dreieck die den Vektoren $\mathbf{p}$, $\mathbf{p}_0$ und $\mathbf{q}$ gegenüberliegenden Winkel mit ω_0, ω und θ, dann besitzen die Impulse in einem geeignet gewählten Koordinatensystem die Komponenten $q_x=q_y=0$, $q_z=q$ und

$$\begin{aligned} p_{0x}&=p_0\sin\omega_0 & p_x&=p\sin\omega\\ p_{0y}&=0 & p_y&=0\\ p_{0z}&=-p_0\cos\omega_0 & p_z&=p\cos\omega. \end{aligned} \tag{18}$$

Wegen $\sin\omega_0/\sin\theta=p/q$ und $p_0/q=\sin\omega/\sin\theta$ gilt $\sin\omega_0\sin\omega=(p_0p/q^2)\sin^2\theta$. Daraus folgt

$$\frac{1}{2l+1}\sum_{m=-l}^{m=+l}[(\mathbf{p}_0\cdot\mathbf{P}^*)(\mathbf{p}\cdot\mathbf{P})+\text{c.c.}]=8|I_l|^2\left(\frac{p_0p}{q}\right)^2\sin^2\theta. \tag{19}$$

Man erhält daher für Gl. (8)

$$\begin{aligned} \mathrm{d}\sigma_M&=\frac{2I^*+1}{2I+1}\frac{\alpha}{t}\frac{q^{2l}}{k^{2l+1}}\frac{1}{(q^2-k^2)^2}\frac{p}{p_0}\\ &\times\left\{E_0E-1+\frac{p_0p}{q^2}(p_0p\sin^2\theta-q^2\cos\theta)\right\}\mathrm{d}\Omega. \end{aligned} \tag{20}$$

Eine kurze Umformung liefert

$$\begin{aligned} \mathrm{d}\sigma_M&=\frac{2I^*+1}{2I+1}\frac{\alpha}{t}\frac{1}{k}\left(\frac{q}{k}\right)^{2l}\frac{1}{(q^2-k^2)^2}\frac{p}{p_0}\\ &\times\left\{E_0E-1+\frac{p_0p}{q^2}(p_0-p\cos\theta)(p-p_0\cos\theta)\right\}\mathrm{d}\Omega. \end{aligned} \tag{21}$$

Für elektrische Übergänge ist nach Gl. (2) und Gl. (5)

$$\begin{aligned} \mathbf{P}&=\left[\frac{2}{\pi l(l+1)}\right]^{\frac{1}{2}}\int \mathrm{e}^{i\mathbf{q}\cdot\mathbf{r}}h_{l-1}(kr)\mathbf{R}Y_l^m(\vartheta,\varphi)\mathrm{d}^3\mathbf{r}\\ Q&=i\left[\frac{2l}{\pi(l+1)}\right]^{\frac{1}{2}}\int \mathrm{e}^{i\mathbf{q}\cdot\mathbf{r}}h_l(kr)Y_l^m(\vartheta,\varphi)\mathrm{d}^3\mathbf{r}. \end{aligned} \tag{22}$$

Für die Komponenten des Operators $\mathbf{R}$ gilt [5])

$$\begin{aligned} (R_x\pm iR_y)Y_l^m&=\pm\left[\frac{(2l+1)(l\mp m)(l\mp m-1)}{(2l-1)}\right]^{\frac{1}{2}}Y_{l-1}^{m\pm1}\\ R_zY_l^m&=\left[\frac{(2l+1)(l+m)(l-m)}{(2l-1)}\right]^{\frac{1}{2}}Y_{l-1}^m. \end{aligned} \tag{23}$$

Mit der schon früher angegebenen Entwicklung von $\exp i(\mathbf{q}\cdot\mathbf{r})$ findet man

$$\mathbf{P} = i^{l+1}\,2\left[\frac{2(2l+1)}{l+1}\right]^{\frac{1}{2}} I_{l-1}\,\mathbf{B} \tag{24}$$

mit

$$\begin{aligned} B_x &= (l+1)^{\frac{1}{2}}\,\tfrac{1}{2}(\delta^m_{+1}-\delta^m_{-1}) \\ B_y &= (l+1)^{\frac{1}{2}}\,\frac{i}{2}\,(\delta^m_{+1}+\delta^m_{-1}) \\ B_z &= -l^{\frac{1}{2}}\,\delta^m_0. \end{aligned} \tag{25}$$

Bei Verwendung der Beziehung $I_l = (q/k)I_{l-1}$ ergibt sich

$$Q = i^{l+1}\,2\left[\frac{2(2l+1)}{l+1}\right]^{\frac{1}{2}} I_{l-1}\,C \tag{26}$$

wobei

$$C = l^{\frac{1}{2}}\,\frac{q}{k}\,\delta^m_0. \tag{27}$$

Der in Gl. (8) angegebene Wirkungsquerschnitt erhält daher die Gestalt

$$\begin{aligned} \mathrm{d}\sigma_{\mathrm{E}} = {} & \frac{2I^*+1}{2I+1}\,\frac{\alpha}{l}\,\frac{1}{k}\left(\frac{q}{k}\right)^{2l-2}\frac{1}{(q^2-k^2)^2}\,\frac{1}{l+1}\,\frac{p}{p_0} \\ & \times \sum_{m=-l}^{m=+l}\{(E_0E-\mathbf{p}_0\cdot\mathbf{p}-1)(\mathbf{B}^*\cdot\mathbf{B})+(E_0E+\mathbf{p}_0\cdot\mathbf{p}+1)C^2 \\ & +[(\mathbf{p}_0\cdot\mathbf{B}^*)(\mathbf{p}\cdot\mathbf{B})-E_0C(\mathbf{p}\cdot\mathbf{B})-EC(\mathbf{p}_0\cdot\mathbf{B})+\text{c.c.}]\}\,\mathrm{d}\Omega. \end{aligned} \tag{28}$$

Nach Gl. (25) und Gl. (27) ist

$$\begin{aligned} \mathbf{B}^*\cdot\mathbf{B} &= (l+1)\,\tfrac{1}{2}\,(\delta^m_{+1}+\delta^m_{-1})+l\delta^m_0 \\ C^2 &= l\frac{q^2}{k^2}\,\delta^m_0 \end{aligned} \tag{29}$$

$$(\mathbf{p}_0\cdot\mathbf{B}^*)(\mathbf{p}\cdot\mathbf{B})+\text{c.c.} = p_0p[(l+1)\sin\omega_0\sin\omega\cdot\tfrac{1}{2}(\delta^m_{+1}+\delta^m_{-1}) - 2l\cos\omega_0\cos\omega\cdot\delta^m_0]$$

$$EC(\mathbf{p}_0\cdot\mathbf{B})+E_0C(\mathbf{p}\cdot\mathbf{B})+\text{c.c.} = 2l\,\frac{q}{k}\,(Ep_0\cos\omega_0-E_0p\cos\omega)\delta^m_0.$$

Man erkennt, daß bei elektrischen Übergängen sowohl die Richtungsquantenzahlen $m = -1, +1$, als auch $m = 0$ beitragen.

Wir zerlegen den Wirkungsquerschnitt $\mathrm{d}\sigma_{\mathrm{E}}$ in einen Teil $\mathrm{d}\sigma_0$ der von den Übergängen mit $m = 0$ herrührt und in $\mathrm{d}\sigma_1$ für Übergänge mit $m = -1$ und $m = +1$. Bei Verwendung der Beziehungen

$$\cos\omega_0\cos\omega = (1/q^2)(p_0-p\cos\theta)(p-p_0\cos\theta)$$

und

$$(q/k)(Ep_0\cos\omega_0-E_0p\cos\omega) = E_0E+1+p_0p\cos\theta$$

erhält man

$$\begin{aligned}\mathrm{d}\sigma_0 = {}&\frac{2I^*+1}{2I+1}\frac{\alpha}{t}\frac{1}{k}\left(\frac{q}{k}\right)^{2l-2}\frac{1}{(q^2-k^2)^2}\frac{l}{l+1}\frac{p}{p_0}\\ &\times\left\{(E_0E-1-p_0p\cos\theta)+\left(\frac{q^2}{k^2}-2\right)(E_0E+1+p_0p\cos\theta)\right.\\ &\left.-2\frac{p_0p}{q^2}(p_0-p\cos\theta)(p-p_0\cos\theta)\right\}\mathrm{d}\Omega.\end{aligned}\tag{30}$$

Die Summation über $m=-1$ und $m=+1$ liefert

$$\begin{aligned}\mathrm{d}\sigma_1 = {}&\frac{2I^*+1}{2I+1}\frac{\alpha}{t}\frac{1}{k}\left(\frac{q}{k}\right)^{2l-2}\frac{1}{(q^2-k^2)^2}\frac{p}{p_0}\\ &\times\left\{E_0E-1+\frac{p_0p}{q^2}(p_0-p\cos\theta)(p-p_0\cos\theta)\right\}\mathrm{d}\Omega.\end{aligned}\tag{31}$$

Für den gesamten Wirkungsquerschnitt $\mathrm{d}\sigma_E = \mathrm{d}\sigma_0+\mathrm{d}\sigma_1$ erhält man daher

$$\begin{aligned}\mathrm{d}\sigma_E = {}&\frac{2I^*+1}{2I+1}\frac{\alpha}{t}\frac{1}{k}\left(\frac{q}{k}\right)^{2l-2}\frac{1}{(q^2-k^2)^2}\frac{1}{l+1}\frac{p}{p_0}\\ &\times\left\{(2l+1)(E_0E-1-p_0p\cos\theta)+l\left(\frac{q^2}{k^2}-2\right)(E_0E+1+p_0p\cos\theta)\right.\\ &\left.+(l+1)p_0p\cos\theta-(l-1)\frac{p_0p}{q^2}(p_0-p\cos\theta)(p-p_0\cos\theta)\right\}\mathrm{d}\Omega.\end{aligned}\tag{32}$$

Für Elektronen hoher Energie ($E^2_0\gg 1$) und niedrige Anregungsenergie ($k^2\lesssim 1$) läßt sich die Winkelverteilung näherungsweise durch

$$\mathrm{d}\sigma_M/\mathrm{d}\Omega \propto \sin^{2l-4}(\theta/2)[1+\sin^2(\theta/2)],$$
$$\text{bzw. } \mathrm{d}\sigma_E/\mathrm{d}\Omega \propto \sin^{2l-4}(\theta/2)[1-\sin^2(\theta/2)]$$

darstellen. Die Winkelverteilung von elastisch gestreuten Elektronen großer Energie ist näherungsweise $\mathrm{d}\sigma_{el}/\mathrm{d}\Omega \propto \sin^{-4}(\theta/2)\cos^2(\theta/2)$.

Zur Ausführung der Winkelintegrationen verwendet man die von Rose [2]) angegebene Methode. Die Substitution $q^2 = k^2x$ liefert $\cos\theta = (p_0^2+p^2-k^2x)/2p_0p$ und $\sin\theta\,\mathrm{d}\theta = (k^2/2p_0p)\mathrm{d}x$. Die totalen Wirkungsquerschnitte enthalten dann die Integrale

$$K_l = \int_{x_1}^{x_2} \frac{x^l}{(1-x)^2}\,\mathrm{d}x \tag{33}$$

mit

$$x_1 = \frac{1}{k^2}(p_0-p)^2, \qquad x_2 = \frac{1}{k^2}(p_0+p)^2. \tag{34}$$

Die Integrale K_l genügen der Rekursionsformel

$$K_{l+2}-2K_{l+1}+K_l = \frac{1}{l+1}(x_2^{l+1}-x_1^{l+1}). \tag{35}$$

Für die beiden ersten Integrale erhält man

$$K_0 = p_0 p, \qquad K_1 = K_0 + 2\log\frac{k}{E_0 E-1-p_0 p}. \tag{36}$$

Aus Gl. (21) ergibt sich für den totalen Wirkungsquerschnitt von magnetischen Übergängen

$$\sigma_M = \frac{2I^*+1}{2I+1}\frac{\pi\alpha}{tk^3 p_0^2}\left\{(E_0E-1)K_l + \frac{k^2}{4}(K_{l+1}-x_1x_2K_{l-1})\right\}. \tag{37}$$

Für den totalen Wirkungsquerschnitt von elektrischen Übergängen findet man nach Gl. (32)

$$\begin{aligned}\sigma_E = {} & \frac{2I^*+1}{2I+1}\frac{\pi\alpha}{tk^3 p_0^2}\frac{1}{l+1} \\ & \times\left\{\tfrac{1}{4}(l-1)(E_0+E)^2K_{l-2} + [E_0E-l-1-\tfrac{3}{2}l(E_0^2+E^2)]K_{l-1}\right. \\ & \left. + \left[2lE_0E + \frac{k^2}{4}(7l+1)\right]K_l - \tfrac{1}{2}lk^2K_{l+1}\right\}.\end{aligned} \tag{38}$$

Die Umrechnung der in Gl. (37) und Gl. (38) angegebenen Wirkungsquerschnitte auf cm² erfordert Multiplikation mit dem Faktor $\lambda\!\!\!^{-}_0^3/c = \lambda\!\!\!^{-}_0^2 t_0$ wobei $t_0 = \lambda\!\!\!^{-}_0/c$. Es erscheint zweckmäßig, die Wirkungsquerschnitte in der Form

$$\sigma = \frac{t_0}{t}\frac{2I^*+1}{2I+1}F_l \tag{39}$$

darzustellen.

Numerische Werte von F_{M1}, F_{M2}, F_{E1} und F_{E2} sind für die Elektronenenergie $E_0 = 10\ mc^2$, das sind 4.6 MeV kinetische Energie und für Anregungsenergien zwischen 0.2 und 5 mc^2, also zwischen 102 keV und 2.55 MeV in Fig. 1 graphisch dargestellt. Zur Abschätzung der tatsächlichen Wirkungsquerschnitte sind Formeln für die Wahrscheinlichkeit $1/t$ von Ein-Partikel-Übergängen [6])

verwendet worden. Es zeigte sich, daß die rasche Abnahme der Faktoren F mit zunehmender Anregungsenergie k durch eine entsprechende Abnahme der Lebensdauer t fast kompensiert wird. Bei Annahme eines Kernradius von 6×10^{-13} cm ergab sich für

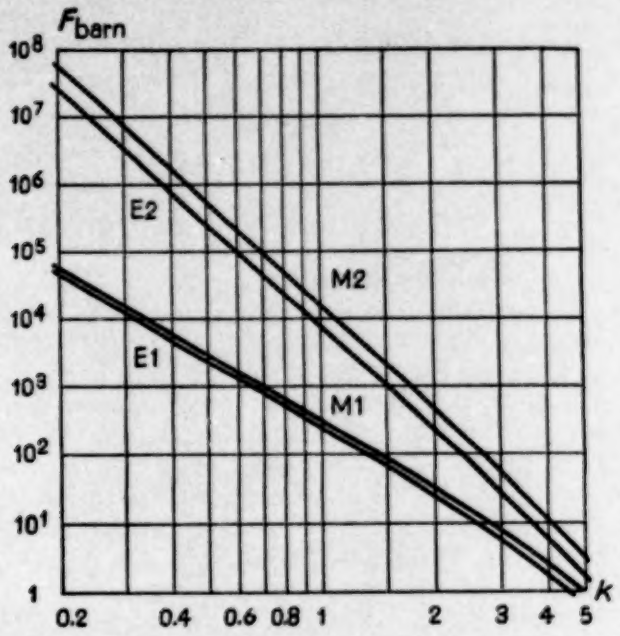

Fig. 1. Anregungsfunktionen F_E und F_M für elektrische und magnetische Übergänge für die Elektronenenergie $E_0 = 10\ mc^2$. Die Anregungsenergie k ist in Einheiten von mc^2 angegeben. Der totale Wirkungsquerschnitt ist $\sigma = (\lambda_0/ct)(2I^*+1)(2I+1)^{-1} F_t$, wobei t die Lebensdauer des angeregten Zustandes bedeutet und der Kernspin vor und nach der Anregung mit I und I^* bezeichnet ist.

$\sigma_{E1}(2I+1)/(2I^*+1) = (t_0/t)F_{E1}$ und für $\sigma_{E2}(2I+1)/(2I^*+1) = (t_0/t)F_{E2}$ die Grössenordnung 10^{-28} cm^2 und 10^{-30} cm^2. Die entsprechenden Werte für magnetische Übergänge sind etwa 50 mal kleiner.

Wir haben die Elektronen durch ebene Wellen beschrieben und die Kern-Übergänge durch die Multipolpotentiale in Gl. (1) und Gl. (2) dargestellt. Es muß daher einerseits die Bedingung $Z\alpha(E/p) \ll 1$ für die Gültigkeit der Born'schen Näherung erfüllt sein, anderseits darf die endliche Ladungs- und Stromverteilung im Kern und die dadurch bedingte Abweichung der Potentiale von Gl. (1) bzw. Gl. (2) auf die Ergebnisse keinen merklichen Einfluß haben. Hierfür ist maßgebend der Einfluß des Integranden in Gl. (14) für kleine r. Es zeigt sich, daß der Wert des Integrals von der unteren Integrationsgrenze r^* näherungsweise unabhängig ist, wenn $kr^* \ll 1$ und $qr^* \ll 1$. Die Abweichung der Potentiale im

Innern eines Atomkerns mit dem Radius R von Gl. (1) bzw. Gl. (2) wird daher vernachlässigbar sein, wenn $kR \ll 1$ und $qR \ll 1$. Dies bedeutet, daß der Kernradius viel kleiner sein muß als die Wellenlängen, die der Anregungsenergie und dem übertragenen Impuls entsprechen. Die obere Grenze für die Energie der einfallenden Elektronen wird daher je nach der Anregungsenergie etwa 10 bis 20 MeV betragen.

Literatur

1) Amaldi, Fidecaro u. Mariani, Nuovo Cimento **7** (1950) 553, 757
R. Gatto, Nuovo Cimento **10** (1953) 1559
J. H. Smith, Phys. Rev. **95** (1954) 271
Thie, Mullin u. Guth, Phys. Rev. **87** (1952) 962
L. Schiff, Phys. Rev. **96** (1954) 765
2) M. E. Rose, Phys. Rev. **76** (1949) 678
3) Baumann u. Robl, Z. f. Naturf. **9a** (1954) 511, Fußnote 6
4) Morse u. Feshbach, Methods of Theoretical Physics (Mc Graw-Hill Book Comp., 1953) p. 1574
5) Morse u. Feshbach, Methods of Theoretical Physics (Mc Graw-Hill Book Comp., 1953) p. 1898
6) Blatt und Weisskopf, Theoretical Nuclear Physics (John Wiley and Sons, 1952) Gleichungen (6.8) und (6.9)

Nuclear Physics **2** (1956/57) 651—659; *North-Holland Publishing Co., Amsterdam*

ON THE ISOCOVARIANCE PROPERTIES OF LEPTONS

P. ROMÁN

Institute for Theoretical Physics of the R. Eötvös University, Budapest, Hungary †

Received 11 October 1956

Abstract: On the basis of a simple postulate regarding the weak interactions of baryons and leptons the transformation character of leptons in isobaric space is determined and various selection rules are studied. The slow decay of strange particles is also considered.

1. Fundamental Postulate

The systematization of heavy particles (different mesons and baryons) was accomplished some time ago by Gell-Mann [1, 2]). Also selection rules were obtained in complete agreement with experiment. The explanation of this phenomenological model was given recently by d'Espagnat and Prentki [3, 4, 5]). According to this, the transformation character of the field operator of a particle in isobaric space is given by the value of the isobaric spin, T, and of the isoparity operator, U. For future reference we list in the table below the transformators for different possible isocovariant entities, for the case of rotation by an angle α_i around some axis X_i, for inversion on the origin and for reflection on the X_1X_2 plane. Reflection on plane X_1X_2 is constructed from a rotation around X_3 with $\alpha_3 = 180°$ and an inversion on the origin.

TABLE 1

Character	Rotation	Inversion (i^U)	Reflection
Scalar	$+1$	$+1$	$+1$
Pseudoscalar	$+1$	-1	-1
Vector	$\exp(i\xi_i\alpha_i)$	-1	$-\exp(i\xi_3\pi)$
Pseudovector	$\exp(i\xi_i\alpha_i)$	$+1$	$+\exp(i\xi_3\pi)$
Spinor of 1st kind	$\exp(\frac{1}{2}i\tau_i\alpha_i)$	$+i$	$+i\exp(\frac{1}{2}i\tau_3\pi)$
Spinor of 2nd kind	$\exp(\frac{1}{2}i\tau_i\alpha_i)$	$-i$	$-i\exp(\frac{1}{2}i\tau_3\pi)$

Here ξ_i is the spin operator for spin-1 particles (cf. Votruba [6])) and τ_i that for spin-$\frac{1}{2}$ particles. Further, it turned out that the strangeness quantum number of Gell-Mann is nothing else but

† Now at the Department of Theoretical Physics of the University, Manchester, England.

$$S = N - U, \tag{1}$$

where N is the number of baryons and U the isoparity. It was also shown that the charge operator for any field can be written as

$$Q = T_3 + \tfrac{1}{2}U. \tag{2}$$

In other words, charge conservation means invariance under reflection on plane X_1X_2.

The strong (or Yukawa) interactions are invariant under any rotation and reflection in isobaric space, so they conserve T, T_3, U, S and Q as well. Electromagnetic (or Maxwell) interactions are invariant for arbitrary reflections, but only for rotations around X_3; therefore T_3, U, S and Q are here good quantum numbers. Finally, the weak interactions (leading to the decay of heavy unstable particles) are invariant neither for rotations nor for inversions; they are invariant only for reflections on the plane X_1X_2. Therefore only Q is conserved (but not T, T_3, U, S).

Concerning the transformation properties of leptons in isobaric space only little has been known so far. In an early work Votruba[6, 7]) treated the negaton, neutrino and positon as an isobaric triplet (pseudovector), basing himself on the assumption of the Majorana neutrino, which now seems not to exist; and besides, nothing was said about muons. Later Sachs [8]) considered this question, but his phenomenological postulates led to the physically unreasonable result of isoparity $|U| = \frac{1}{2}$ for all leptons. Recently Duimio [9]) has treated the problem within the framework of the four-dimensional isobaric space formalism of Polkinghorne and Salam [10]); but this scheme is questionable, and moreover, according to Duimio also uncharged muons would exist, in contradiction with our present experimental knowledge.

Lately Gell-Mann suggested [11]) that the slow decay of hyperons may be interpreted on the basis of some intermediate weak interaction between baryons (and possibly leptons). We take now as a *fundamental postulate* that *all* interactions between baryons and leptons are weak in the sense that they *are invariant only with respect to reflections on plane X_1X_2, but are not invariant for rotations and inversion.* (The only quantity conserved is the total charge Q.) This postulate makes it possible to determine the isocovariance properties of all leptons.

2. Electron and Neutrino

Let us start with the simplest Fermi process

$$n \to p^+ + e^- + \bar{\nu}.$$

The interaction reads

$$\mathcal{I}_1 = \bar{\psi}_p \psi_n \bar{\varphi}_e \varphi_\nu + \text{h.c.}$$

Besides this there are also possible interactions $\mathcal{I}_2$, $\mathcal{I}_3$, $\mathcal{I}_4$, $\mathcal{I}_5$ which differ from $\mathcal{I}_1$ only by insertion of the matrices γ_i, $\gamma_{[ik]}$, $\gamma_{[5i]}$, γ_5, which is now irrelevant. Further, it is well known (cf. Good [12])) that *all* possible Fermi interactions between nucleons, electrons and neutrinos may be expressed through a linear combination $\mathcal{I} = \sum_{\alpha=1}^{5} c_\alpha \mathcal{I}_\alpha$. We may therefore restrict ourselves to the consideration of $\mathcal{I}_1$.

The nucleon field should be characterized by

$$\psi = \begin{bmatrix} \psi_p \\ \psi_n \end{bmatrix}.$$

As ψ is an isospinor of the 1st kind, we have

	T	U	N	S	Q.
Nucleon:	$\frac{1}{2}$	1	1	0	$(+1, 0)$.

Which properties must φ_e resp. φ_ν have so as to ensure that our postulate be fulfilled for the interaction $\mathcal{I}_1$? There are two possibilities. It may be that neutrino and electron form a charge doublet,

$$\varphi = \begin{bmatrix} \varphi_\nu \\ \varphi_e \end{bmatrix},$$

that is, φ forms an isospinor of the 2nd kind:

		T	U	N	S	Q
a)	φ isospinor 2nd kind:	$\frac{1}{2}$	-1	0	1	$(0, -1)$.

Or, electron and neutrino are separate singulets. That means, the electron has to be an isopseudoscalar and the neutrino an isoscalar:

		T	U	N	S	Q
b)	φ_e- isopseudoscalar:	0	-2	0	2	-1
	φ_ν isoscalar:	0	0	0	0	0.

Because of eq. (2) there are no other possibilities. Which of these possibilities are in agreement with our postulate? In case a) $\mathcal{I}_1$ is to be written in the form

$$\mathcal{I}_1 = \bar{\psi}\tau_+\psi \cdot \bar{\varphi}\tau_-\varphi + \text{h.c.},$$

where

$$\tau_{\pm} = \tfrac{1}{2}(\tau_1 \pm i\tau_2).$$

We see from table 1 that this is invariant under inversion (and also under rotations around X_3), contrary to our postulate. But in case b) $\mathscr{I}_1$ reads

$$\mathscr{I}_1 = \bar{\psi}\tau_+\psi \cdot \bar{\varphi}_e \cdot \varphi_\nu + \text{h.c.}$$

This is no longer invariant either for rotation or inversion, thus $\mathscr{I}_1$ fulfils our requirements. Moreover, it is invariant for reflection on plane X_1X_2, as can be seen by remembering that $\bar{\psi}\tau_+\psi$ is a linear combination of the first and second component of an isopseudovector, simply changing its sign in the case of the mentioned reflection, for which $\bar{\varphi}_e\varphi_\nu$ also changes sign.

Summing up, we find that case b) is fully compatible with our basic postulate: the electron has to be an isopseudoscalar, the neutrino an isoscalar. We notice that this choice establishes in the case of pure electromagnetic interactions of electrons the conservation of T, T_3, U, S and Q. The interaction term is in fact

$$M = \bar{\varphi}_e\gamma_i\varphi_e A_i,$$

where, as is well known, the photon field A_i is an isoscalar. Besides, the isoparity operator for electrons may be written explicitly

$$U = -2\int \bar{\varphi}_e\gamma_4\varphi_e \mathrm{dV} = -2\Sigma(a_r^+ a_r - b_r^+ b_r).$$

For a negaton state this gives $U = -2$ and for a positon state $U = +2$. (This has to be so, because now $Q = T_3 + \frac{1}{2}U = \frac{1}{2}U$.) From (3) follows also the conservation of U in the case of electromagnetic interactions.

3. Muon

Now we turn to the *properties of muons*. The fundamental process is here the capture of a μ^-:

$$\mathrm{p}^+ + \mu^- \to \mathrm{n} + \bar{\nu}.$$

The interaction reads

$$\mathscr{H}_1 = \bar{\psi}_n\psi_p\varphi_\nu\bar{\varphi}_{\mu^+} + \text{h.c.}$$

As the nucleon is an isospinor of the 1st kind and the neutrino an isoscalar, this may be written

$$\mathscr{H}_1 = \bar{\psi}\tau_-\psi \cdot \varphi_\nu \cdot \bar{\varphi}_{\mu^+} + \text{h.c.},$$

where only φ_μ has unknown properties. There are now two basic

possibilities: either an uncharged muon does exist or it does not. In the second case μ has to be a charge singulet, that is, it can only be a pseudoscalar. According to Mahmoud and Konopinski [13]) and also Marx [14]) the μ^+ has to be the "particle" and μ^- the "anti-particle" (so as to conserve the number of fermions). Therefore μ^+ has to be a pseudoscalar with $U = +2$:

	T	U	N	S	Q.
α) μ^+ isopseudoscalar:	0	2	0	-2	$+1$

But if an uncharged μ^0 also exists, there are again two possibilities: (μ^+, μ^0) forms a charge doublet, it is an isospinor; or (μ^+, μ^0, μ^-) is a charge triplet with the transformation property of an isopseudovector:

	T	U	N	S	Q
β) (μ^+, μ^0) isospinor 1st kind:	$\frac{1}{2}$	1	0	-1	$(+1, 0)$
γ) (μ^+, μ^0, μ^-) isopseudovector:	1	0	0	0	$(+1, 0, -1)$.

Let us consider cases α), β), γ) separately. As easily seen, $\mathscr{K}_1$ is never invariant for rotations. We have only to investigate the reflections. In case α) $\mathscr{K}_1$ changes its sign for an inversion (note that $\bar{\psi}\tau_-\psi$ is again a linear combination of the first and second component of an isopseudovector). Thus $\mathscr{K}_1$ is not invariant, as required. Further, in case of reflection on plane X_1X_2, $\mathscr{K}_1$ remains unchanged (because $\bar{\psi}\tau_-\psi \to -\bar{\psi}\tau_-\psi$), thus ensuring the conservation of Q.

Taking now possibility β) we again find that $\mathscr{K}_1$ is not invariant with respect to an inversion, but possibility β) is excluded because $\mathscr{K}_1$ also changes its sign for a reflection on plane X_1X_2, thus violating the principle of conservation of charge.

Finally, case γ) is not allowed either, because $\mathscr{K}_1$ would then be invariant under an inversion, contrary to our postulate.

Thus only possibility α) can be accepted† and from this follows *the non-existence of uncharged muons*. The μ-particle is an isopseudoscalar. The isoparity operator is similar to that of the electron: the μ^- has $U = -2$.

4. Isocovariance of Leptons

We now list in the table below the isocovariance properties of leptons.

† Recently also the possibility that (μ^+, ν, e^-) forms an isopseudovector triplet was considered by Votruba [15]). However, the enormous mass difference of the particles leads to a very strange form of the mass operator.

The difference between photons and neutrinos lies evidently in the different *Lorentz*-transformation properties (the photon being a Lorentz vector, the neutrino a Lorentz spinor). The difference

TABLE 2

Name	Type	T	U	N	S	Q
Photon	isoscalar	0	0	0	0	0
Negaton	isopseudoscalar	0	−2	0	+2	−1
Positon		0	+2	0	−2	+1
Neutrino	isoscalar	0	0	0	0	0
Antineutrino		0	0	0	0	0
μ^+-meson	isopseudoscalar	0	+2	0	−2	+1
μ^--meson		0	−2	0	+2	−1

between electrons and muons is a much more intricate problem. Both are of course Lorentz spinors, but it may well be that the one is transformed by Lorentz-space inversions by $+\gamma_4$, the other by $-\gamma_4$. One should also consider the possibility that the muon is a "bound state" of an electron and two neutrinos, brought about by a Fermi interaction. In any case our table shows close connection between electrons and muons.

Now the question arises, whether the coexistence of isoscalar and isopseudoscalar fields does not lead to some contradiction of the type mentioned by d'Espagnat and Prentki [3]). Especially, we have to examine the interaction

$$V = \bar{\varphi}_e^c \gamma_i \varphi_{\mu^+} A_i = -\tilde{\psi}_e C^{-1} \gamma_i \varphi_{\mu^+} A_i .$$

It is seen that this expression is invariant under any rotation or reflection and no conservation rules are violated. (However, the process $\mu \to e+\gamma$ is forbidden because of the conservation of the number of fermions: V is not invariant under the phase transformartion $\psi_e \to \exp(i\alpha) \cdot \psi_e$, $\varphi_\mu \to \exp(i\alpha) \cdot \varphi_\mu$.) A problem similar to that treated by d'Espagnat and Prentki would arise only, if also isopseudovectors or isospinors would occur among the leptons. But such particles are to be found only in the family of heavy particles. The example (5.1) on page 48 of d'Espagnat's and Prentki's [3]) paper would be

$$\tilde{\varphi}_e^* \beta \varphi_\theta^T C \psi_N + \tilde{\varphi}_e^* \beta \varphi_\theta^{*T} \psi_\Sigma ;$$

this really contradictory expression is, however, excluded because of the conservation of the number of baryons.

We investigate now some other processes according to the scheme

given in table 2. First of all, the interaction leading to the muon decay

$$\mu^+ \to e^+ + \nu + \nu$$

reads

$$L = \bar{\varphi}_{e^+} \bar{\varphi}_\nu \bar{\varphi}_\nu \varphi_{\mu^+} = \varphi_{e^-} \bar{\varphi}_\nu \bar{\varphi}_\nu \varphi_{\mu^+}.$$

We find easily that this is an invariant in the Lorentz space as well as in the isobaric space: T, T_3, U, S, Q are all conserved.

Another important process is the pion decay:

$$\pi^+ \to p^+ + \bar{n} \to \mu^+ + \tilde{\nu}.$$

The first step is a well-known strong interaction and the second is described by the term

$$\mathscr{P} = \psi_p \psi_{\bar{n}} \bar{\varphi}_{\mu^+} \bar{\varphi}_\nu = \psi_p \bar{\psi}_n \bar{\varphi}_{\mu^+} \varphi_\nu = \bar{\psi} \tau_- \psi \cdot \bar{\varphi}_{\mu^+} \cdot \varphi_\nu.$$

In the isobaric space this expression is neither rotation nor inversion invariant. It is, however, invariant under reflection on plane $X_1 X_2$, as it should be †.

5. Selection Rules

Finally, let us register the change in strangeness occurring in different weak interactions.

a) In the case of weak interactions in which only leptons participate,

$$\mu^+ \to e^+ + \nu + \nu,$$
$$\mu^- \to e^- + \tilde{\nu} + \tilde{\nu},$$

the change in strangeness is

$$\Delta S = 0.$$

b) In the case of weak interactions between leptons and nucleons, such as

$$n \to p^+ + e^- + \tilde{\nu},$$
$$p^+ + \mu^- \to n + \tilde{\nu},$$
$$p^+ + \bar{n} \to \mu^+ + \tilde{\nu},$$

etc. we have

$$|\Delta S| = 2.$$

c) In the (hypothetical) case of Fermi interaction between hyperons and leptons, e.g.

† It may well be that the process $\pi^+ \to e^+ + \nu$ having a very small (if any) probability is excluded just because of the aforementioned difference in space parity of muons and electrons.

$$\Lambda^0 \to p^+ + e^- + \bar{\nu},$$
$$\Sigma^0 \to p^+ + e^- + \bar{\nu},$$

etc. we have in general

$$|\Delta S| = 1.$$

We are inclined to attribute the slow decay of hyperons to similar processes, as illustrated in fig. 1. In the first vertex

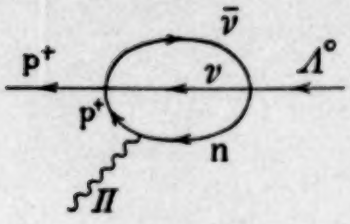

Fig. 1.

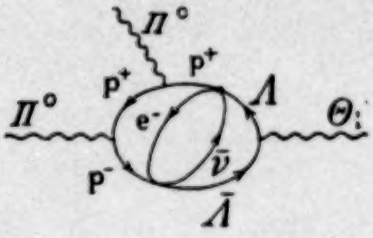

Fig. 2.

$\Lambda^0 \to n + \nu + \bar{\nu}$, with $|\Delta S| = 1$. Similarly, the decay of K-mesons may be explained by the graph shown in fig. 2, where in the intermediate Fermi vertices

$$\Lambda^0 \to p^+ + e^- + \bar{\nu},$$
$$\Lambda^0 + \bar{\nu} + e^- \to p^-,$$

we have again $|\Delta S| = 1$.

The decay processes of the types $K_{\mu 2}$, $K_{\mu 3}$, K_{e3}, which are not yet well-established, may have similar mechanisms, as shown in fig. 3. The first vertex is a strong interaction [and since K^+ has the strangeness -1, $(p^+, \bar{n})$ pairs cannot be created]. In the final Fermi vertex processes again occur, for which $|\Delta S| = 1$.

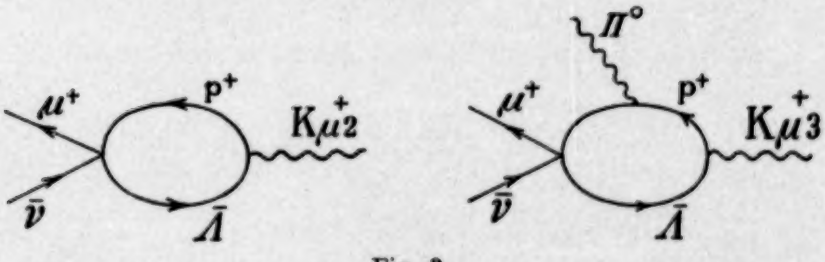

Fig. 3.

We note as an interesting fact that in all processes treated we could have studied instead of the change in S also *the change of* U, and *would have obtained the same values.*

Summing up, we register the following facts: 1) In the case of Fermi interactions between leptons alone or between nucleons and leptons the change in the value of isoparity is $|\Delta U| = 0$ or

$|\Delta U| = 2$, respectively. 2) If also hyperons participate in the process, then $|\Delta U| = 1$. Tentatively we may thus say that processes with even change of $U(|\Delta U| = 0,2)$ are somewhat privileged as against those in which the ispoarity has an odd change in value ($|\Delta U| = 1$). The latter processes occur only when the high mass value cannot be stabilized in any other way.

This fact may be expressed as a tendency to conserve the number of isofermions and isobosons, resp. (Isofermions, i.e. isospinors of the 1st and 2nd kind have $|U| = 1$, isobosons, i.e. iso-scalars, iso-pseudoscalars, iso-pseudovectors, have $|U| = 0,2$.) Thus we may speak of the (approximative) *conservation rule of the "parity of isoparity"*.

Concluding, the author wishes to express his gratitude to the Hungarian as well as to the Czecho-Slovak Academy of Sciences for having granted him a short stay in Prague, during which this paper was prepared. Special thanks are due to Professor Vaclav Votruba of the Charles University in Prague for stimulating interest and valuable discussions.

References

1) M. Gell-Mann and A. Pais, Proc. of the Glasgow Conference on nuclear and meson physics (1954) p. 342
2) M. Gell-Mann, Phys. Rev. **92** (1953) 833
3) B. d'Espagnat and J. Prentki, Nuclear Physics **1** (1956) 33
4) B. d'Espagnat and J. Prentki, Compt. Rend. **240** (1956) 2486
5) B. d'Espagnat and J. Prentki, Phys. Rev. (to be published)
6) V. Votruba and M. Lokajicek, Czechsl. Journ. of Phys. **2** (1953) 1
7) V. Votruba and M. Lokajicek, Phys. Rev. **86** (1952) 206
8) R. G. Sachs, Phys. Rev. **99** (1955) 1573
9) F. Duimio, Nuovo Cimento **3** (1956) 595
10) A. Salam and J. C. Polkinghorne, Nuovo Cimento **2** (1955) 685
11) M. Gell-Mann, Intern. Phys. Conf. Pisa (1955)
12) R. Good, Rev. Mod. Phys. **27** (1955) 187
13) E. J. Konopinski and H. M. Mahmoud, Phys. Rev. **92** (1953) 1045
14) G. Marx, Zeitschr. f. Naturf. **9a** (1954) 1051
15) V. Votruba, private communication (1956)

Nuclear Physics **2** (1956/57) 660—663; *North-Holland Publishing Co., Amsterdam*

UPPER LIMIT FOR THE LIFETIMES OF EXCITED STATES OF Fe^{56} AND Ti^{46}

G. BERTOLINI

Istituto di Fisica Sperimentale del Politecnico, Milano

Received 27 October 1956

E. Gatti *et al.* of C.I.S.E. Laboratories of Milan have developed a new type of millimicroseconds time analyser of high resolution[1]). With this instrument an upper limit of $\approx 10^{-11}$ sec for the lifetimes of the two excited states of Fe^{56} following the β^+ decay with $E_{max} = 1.5$ MeV of Co^{56} and for the lifetime of the first excited level of Ti^{46} has been determined. From previous measurements both gamma rays of 1.24 and 0.845 MeV of Fe^{56} [2-5]) and the γ-ray of 1.12 MeV of Ti^{46} [6-10]) are known to be electric quadrupole. Weisskopf's theoretical relation [11]) for the lifetimes of the 0.845 and 2.09 MeV levels of Fe^{56} and the 1.12 MeV level of Ti^{46} yield lifetimes of $\approx 8\times10^{-11}$ sec, $\approx 0.8\times10^{-11}$ sec, and $\approx 1\times10^{-11}$ sec respectively.

The radioactive sources were placed between two plastic crystals (16 mm diameter, 8 mm thick), each facing a 6342 R.C.A. photomultiplier. Between the source and the crystals two polythene absorbers (6 mm thick) can be interposed preventing any betas from reaching the two crystals (γ-γ coincidences) or only from one at a time (β-γ coincidences).

Three coincidence experiments were performed: 1) a γ-γ coincidence experiment with Sc^{46} using Co^{60} as a "prompt" source, 2) a γ-γ coincidence experiment with Co^{56} using Sc^{46} as a "prompt" source, 3) and a β^+-γ "self-comparison" experiment involving only a Co^{56} source.

The first experiment determines the lifetime of the first excited state of Ti^{46} by comparing the γ-γ resolution curve with that of Co^{60} (an upper limit of 10^{-11} sec has been measured by Bay *et al.* [12]) for the first excited state of Ni^{60}). Considering that the amplitude distribution of gamma-rays of Ni^{60} and Ti^{46} are almost identical, the comparison has not been done with a selection channel but only with amplitude discrimination.

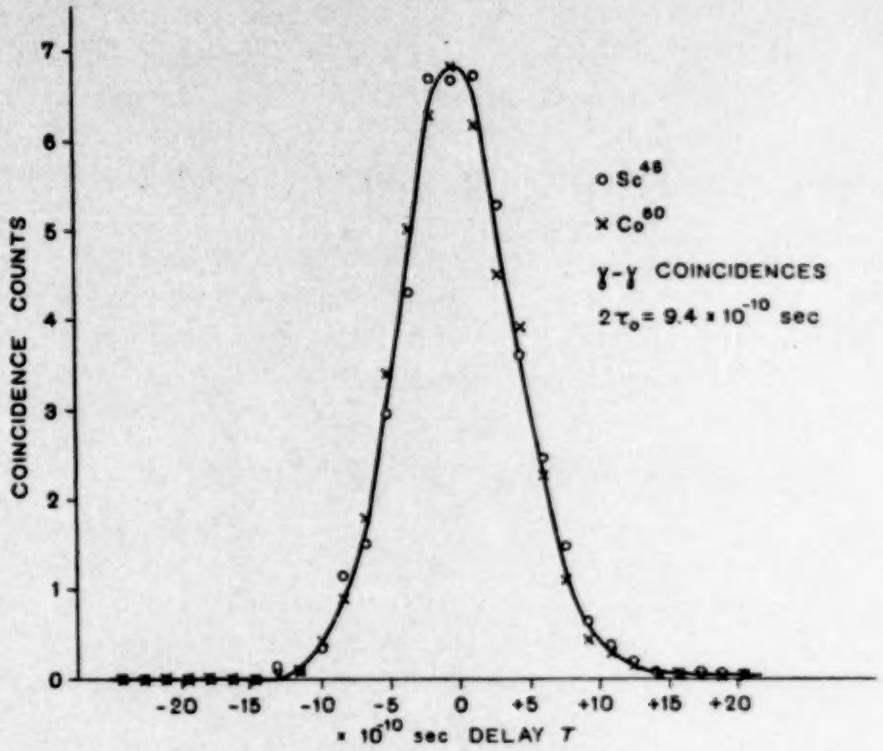

Fig. 1. γ-rays accepted symmetrically in the crystals A and B. Bias $\geqq$ 600 keV.

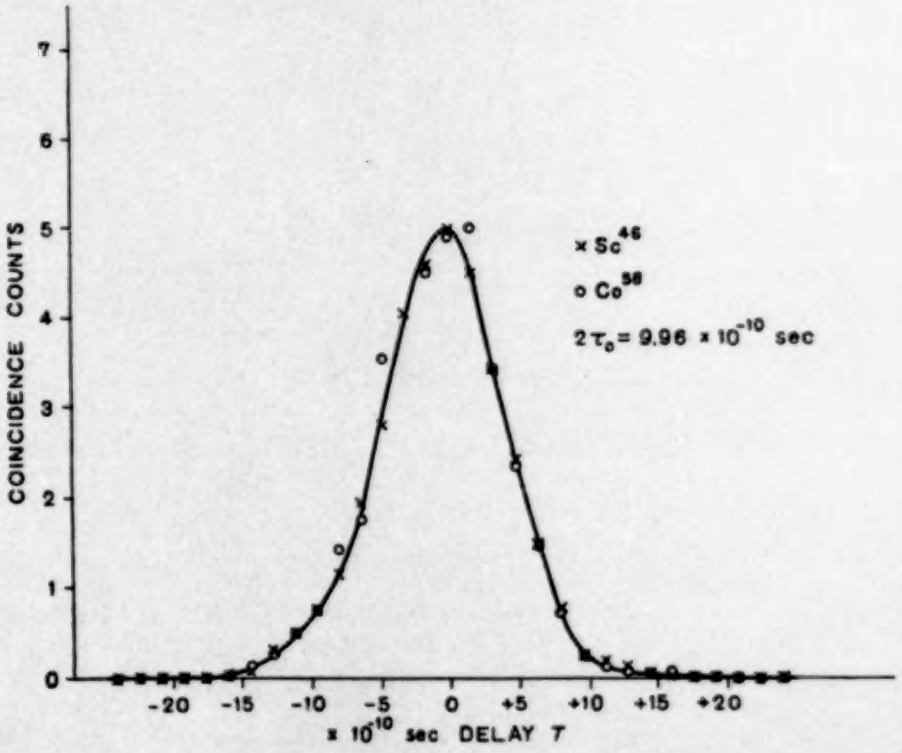

Fig. 2 γ-rays accepted symmetrically in the crystals A and B. Bias $\geqq$ 600 keV.

The second experiment determines the lifetime of the first excited state of Fe^{56} by comparing the γ-γ resolution curve with that of Ti^{46}. Sc^{46} has been preferred to Co^{60} as "prompt" source because the energies of gamma-rays of Ti^{46} (0.890 and 1.12 MeV) are nearly equal to gamma-rays energies (0.845 and 1.24 MeV) of Fe^{56}.

Fig. 1 and 2 give only one single run of the first and second experiment. A total of 10.000 coincidences has been performed. The curves in fig. 1 and 2 show no difference in their width. The average displacement of the centroids was about 10^{-11} sec.

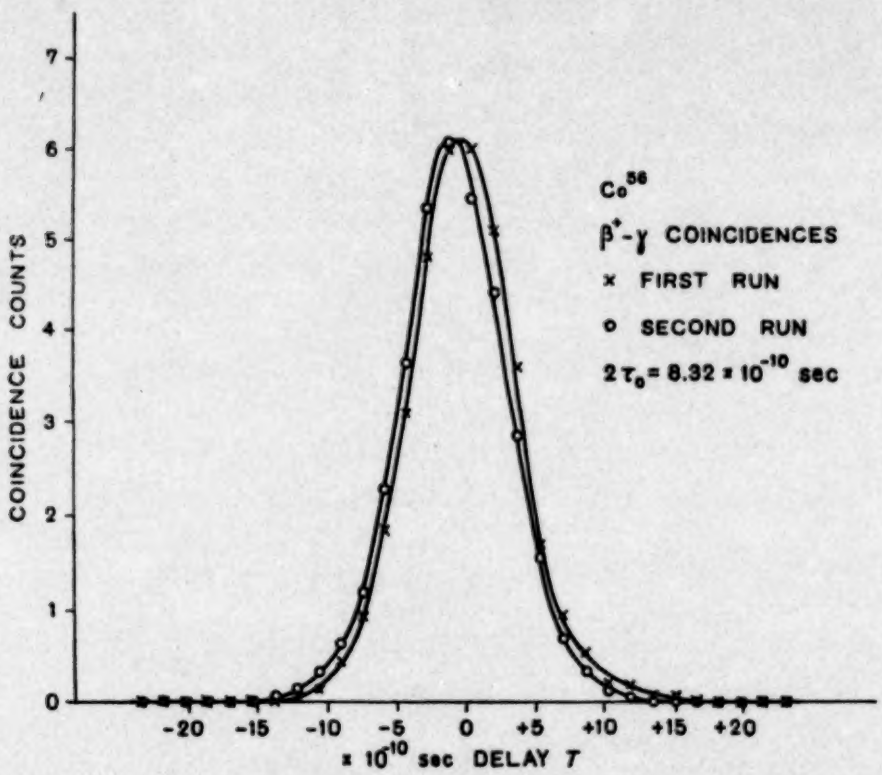

Fig. 3. First run: positons and γ-rays accepted in the crystal A, only γ-rays in the crystal B.
Second run: positons and γ-rays accepted in the crystal B, only γ-rays in the crystal A.
Bias $\geqq$ 600 keV.

To determine an upper limit for the lifetime of the 2.09 MeV level of Fe^{56} a "self-comparison" method was used. Let two crystals be called A and B. For the first run, with the polythene absorber between the source and the crystal A removed a composite coincidence curve $(\beta^+\text{-}\gamma_1+\beta^+-\gamma_2)+(\gamma_1-\gamma_2+\gamma_2-\gamma_1)$ was measured. For the second run, crystal B reveals the positons and A only the

gamma-rays. For the third run with the absorbers in place the "prompt" γ-γ coincidences were measured. The γ-γ coincidences were subtracted. Fig. 3 gives two single runs of this experiment. Four sets of these three runs corresponding to $\approx$ 30.000 coincidences were performed. The average displacement between the curves corresponding to the first and second run was about 2×10^{-11} sec. Errors due to coincidences resulting from back-scattering and (in the case of the Co^{56} source) from annihilation of positons have been eliminated by accepting in the slow coincidence (2×10^{-8} sec) of the time analyser only pulses corresponding to energies higher than 600 keV. This has been checked with a Na^{22} source. To calibrate the linearity and the sensibility of the time-analyser time-of-flight experiments were performed by varying the position of a source of Na^{22}(accepting in the slow coincidence pulses corresponding to 0.511 MeV annihilation quanta).

The results obtained confirm the E2 character of the 0.890 MeV gamma-ray of Ti^{46} and of the 0.845 and 1.24 MeV gamma-rays of Fe^{56}.

The author appreciates very much the hospitality of the C.I.S.E. Laboratories of Milan; he wishes to thank prof. G. Bolla, Director of the Institute, for his kind interest, prof. E. Gatti and Mr. C. Cottini for helpful informations on the time-analyser and Mr. Vaghi for his assistance in performing the experiments.

References

1) C. Cottini, E. Gatti and G. Giannelli, Nuovo Cimento **4** (1956) 156
2) T. Wood and P. S. Jastram, Phys. Rev. **98** (1955) 1187A
3) G. Bertolini, M. Bettoni and E. Lazzarini, Nuovo Cimento, to be published
4) Gallaher, Whittle, Been, Rittens, Garter and Steenland, Physica **21** (1955) 117
5) K. Jlakovac, Proc. Phys. Soc. A **67** (1954) 601
6) E. L. Brady and M. Deutsch, Phys. Rev. **78** (1950) 558
7) B. Novey, Phys. Rev. **78** (1950) 66
8) F. Metzger and M. Deutsch, Phys. Rev. **78** (1950) 551
9) R. E. Azuma, Phil. Mag. **46** (1955) 1031
10) G. Bertolini, M. Bettoni and E. Lazzarini, Nuovo Cimento **3** (1956) 800
11) V. F. Weisskopf, Phys. Rev. **83** (1951) 1073
12) Z. Bay, V. P. Henri and F. McLernon, Phys. Rev. **97** (1955) 561

Nuclear Physics **2** (1956/57) 664—679; *North-Holland Publishing Co., Amsterdam*

MEASUREMENT OF CIRCULARLY POLARIZED GAMMA-RADIATION FOLLOWING POLARIZED NEUTRON CAPTURE

GEORG TRUMPY

Joint Establishment for Nuclear Energy Research, Lillestrøm, Norway

Received 12 October 1956

Abstract: Circular polarization of the γ-rays emitted from nuclei capturing polarized neutrons was studied by means of the dependence of the Compton cross section upon the relative spin direction of the photon and the electron. Thermal neutrons polarized by transmission through magnetized iron fell on the (n, γ)-target, and the γ-rays were detected by two NaI(Tl)-crystals after passing through analyzers of iron magnetized in the direction of transmission. Measurements were carried out with the strongest neutron capture γ-rays from S, Ca, Ti, Cr, Fe, Ni, Zn and W. From the results, some of the spin-values of these nuclei could be derived. The degree of circular polarization was in accordance with theory.

1. Introduction

The study of reactions involving polarized particles has, during the last few years, become a very useful tool for the investigation of nuclear properties. So far, numerous experiments were carried out at medium and high energies. However, intense low-energy polarized neutron beams are easily produced. When polarized thermal neutrons are captured by unpolarized nuclei, partial alignment of the nuclear spins will be obtained. In the special case of capture by nuclei with spin zero, the resulting compound nuclei will be polarized to the same extent as the neutrons being captured. Tolhoek and Cox [1]) have shown that γ-radiation emitted from oriented systems will generally be anisotropic and polarized. However, the 2nd Polarization Theorem by Wolfenstein [2]) says that reactions induced by particles with angular momentum $l = 0$ and spin $s = \frac{1}{2}$ give isotropic distributions. Furthermore a theoretical investigation by Biedenharn *et al.* [3]) shows that the radiation is not linearly polarized.

Thus, circular polarization of the γ-rays is the only additional property obtained from the capture of polarized thermal neutrons. The present paper describes an attempt to demonstrate this effect,

as first mentioned by Halpern [4]), furthermore to investigate the possibility of using the degree of circular polarization for the determination of nuclear spins.

According to Wolfenstein's 3rd Polarization Theorem [2]), incident particles with spins aligned parallel to the axis of incidence, for example circularly polarized photons, have no effect upon the angular distribution of the emitted intensity. Therefore, in order to detect circular polarization of γ-rays we must let them interact with polarized matter. Gunst and Page [5]) studied the interaction at 2.62 MeV, using magnetized iron as the polarized matter. A γ-ray analyzer based on this principle has a rather small efficiency, mainly due to the fact that only about 2 out of the 26 electrons in the iron atom can be polarized by magnetization. The present investigation, therefore, requires measurements of very small effects, so that the accuracy of the results finally depends upon the counting time used to reduce the statistical errors.

In section 2 the main theoretical points concerned with the experiment are treated briefly. Sections 3 and 4 describe the apparatus employed for the measurements, and its use, and in section 5 the results of this investigation are quoted and discussed.

2. Theory

2.1. MAIN PRINCIPLES

The polarization of a particle beam is generally defined as the net alignment of the particle spins:

$$P = \frac{N^+ - N^-}{N^+ + N^-} \tag{1}$$

where P is the polarization and N^+ and N^- are intensities of particles with spins parallel and antiparallel to a certain axis of reference. This definition is also valid for circularly polarized γ-radiation. Left circular polarization means that the photon beam has excess spin in the direction of propagation.

Assuming capture of totally polarized thermal neutrons followed by a pure multipole transition, Biedenharn *et al.* [6]) found for the degree of left circular polarization of the γ-rays

$$P'_\gamma = R \cos \Theta \tag{2}$$

where

$$R = 2(J_c - J_i)\frac{L(L+1) + J_c(J_c+1) - J_f(J_f+1)}{L(L+1)(2J_i+1)} \tag{3}$$

and

Θ = angle between γ-ray propagation direction and neutron polarization vector (see figure 1),
J_1 = total angular momentum of target nucleus,
J_c = total angular momentum of compound nucleus, i.e. the state between neutron absorption and γ-ray transition,
J_f = total angular momentum of final nucleus,
L = multipole order of γ-ray transition.

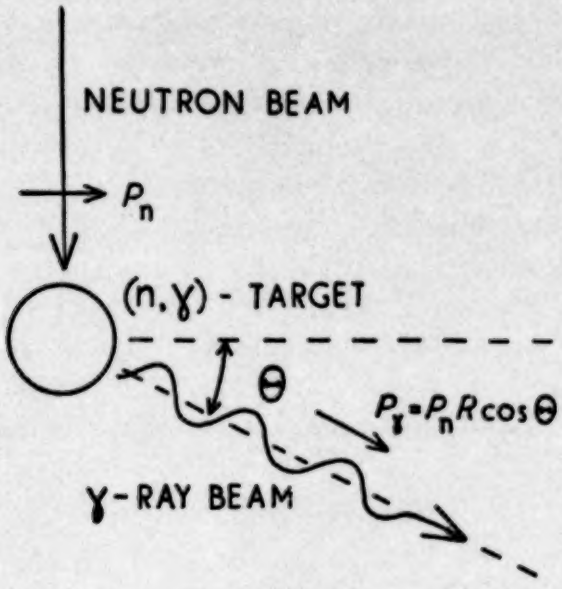

Fig. 1. Sketch of the (n, γ)-reaction.

The quantities of equation (3) satisfy the conditions

$$J_c = J_1 \pm \tfrac{1}{2}, \tag{4}$$

$$J_c + J_f \geqq L \geqq |J_c - J_f|, \tag{5}$$

$$1 \geqq R \geqq -\tfrac{1}{2}. \tag{6}$$

The degree of circular polarization is at maximum for $\cos\Theta = \pm 1$. Parallel and antiparallel spins of neutron and photon then correspond to R being positive and negative respectively.

It is clear from this that if R is measured, it will be possible to draw conclusions about the spin states involved in the transition. In the general case the spins cannot be determined unambiguously, but in most experiments J_1 will be known. Then, in certain cases information on the exact value of R can yield the other quantities in equation (3). If one of the spin values is known

from other experiments, the other two may be easily determined.

When the captured neutron beam is partially polarized, the γ-ray polarization is reduced accordingly:

$$P_\gamma = R \cdot P_n \tag{7}$$

where P_n and P_γ are neutron and circular γ-ray polarization respectively.

If a beam of particles is passing through two successive polarizing processes with polarizations P_1 and P_2, we get the asymmetry

$$P_1 P_2 = \frac{N'-N''}{N'+N''} \tag{8}$$

where N' and N'' are transmitted intensities measured for the two possible relative orientations of the polarizers, and $N' > N''$.

The analysis of the γ-ray beam with polarization P_γ is carried out by a process with polarization P_a. When N_a is the obtained γ-ray intensity, we get

$$P_\gamma P_a = R P_n P_a = \frac{N_a'-N_a''}{N_a'+N_a''}. \tag{9}$$

2.2 NEUTRON POLARIZATION

The total neutron cross section for iron is of the form

$$\sigma_t = \sigma_0 \pm \sigma_p \tag{10}$$

where σ_p is the spin-dependent part. The upper sign corresponds to neutron spin parallel to the magnetic field. σ_0 and σ_p are strongly varying with energy. These quantities were obtained partly from Cassels [7]) and from Stanford *et al.* [8]) and partly from calculations based on the neutron polarization theory by Halpern and Holstein [9]). A neutron beam transmitted through a block of magnetized iron obtains the polarization

$$P_n = \frac{\sigma_p x g}{1+\eta} \tag{11}$$

where

x = number of atoms per cm^2 of the beam,

g = a correction factor expressing the depolarization due to incomplete magnetic saturation (at saturation $g = 1$),

η = "single transmission effect", being the relative difference between transmission of the magnetized and the unmagnetized block of iron.

As σ_p is positive, the polarized beam contains predominantly neutrons with spin antiparallel to the magnetic field.

When the transmitted beam is not monoenergetic, the calculation of polarization requires integration over all neutron velocities. The thermal neutron spectrum from a reactor is a Maxwell distribution. Pelser [10]) studied the spectrum from JEEP.

The factor g is independent of energy, and can be obtained from a double transmission experiment in which the neutron beam passes successively through two identical polarizers. As the neutron spectrum alters by transmission through each iron block, the results must be compared with integrated quantities.

2.3. CIRCULAR POLARIZATION OF γ-RAYS

Lipps and Tolhoek [11]) calculated the general differential Compton cross section for a single electron

$$\frac{\mathrm{d}_e\tau(\vartheta,\varphi)}{\mathrm{d}\Omega} = r_0^2 \frac{k_1^2}{k_0^2} \Phi(\mathbf{k}_0\mathbf{k}_1\,\boldsymbol{\xi}^0\boldsymbol{\xi}^1\boldsymbol{\zeta}^0\boldsymbol{\zeta}^1) \tag{12}$$

where ϑ and φ are photon scattering angles, $r_0 = e^2/mc^2$, k is the photon momentum, $\boldsymbol{\xi}$ and $\boldsymbol{\zeta}$ are 3-dimensional polarization vectors for photon and electron respectively and the indices $_0$ and $_1$ denote the initial and final states. The magnitude of the component ξ_3 along the direction of propagation is equal to the degree of circular polarization.

In the case of circularly polarized γ-rays interacting with polarized electrons, one obtains after averaging over the final polarization directions $\boldsymbol{\xi}^1$ and $\boldsymbol{\zeta}^1$

$$8\Phi(\mathbf{k}_0\mathbf{k}_1\,\boldsymbol{\xi}^0\boldsymbol{\zeta}^0) = 1+\cos^2\vartheta+(k_0-k_1)(1-\cos\vartheta) \\ -\xi_3^0(1-\cos\vartheta)\,\boldsymbol{\zeta}^0\cdot(\mathbf{k}_0\cos\vartheta+\mathbf{k}_1). \tag{13}$$

For simplicity we have introduced the units $m = 1$, $c = 1$, $\hbar = 1$. If the electron is polarized parallel to the incident photon, $\boldsymbol{\zeta}^0 = \zeta_3^0\mathbf{k}_0/|\mathbf{k}_0|$, and

$$8\Phi = 1+\cos^2\vartheta+(k_0-k_1)(1-\cos\vartheta)-\xi_3^0\zeta_3^0(k_0+k_1)(1-\cos\vartheta)\cos\vartheta. \tag{14}$$

In this expression the last term which is due to polarization has nearly the same magnitude as the ordinary Compton cross section for certain scattering angles. The present experiment requires discrimination between various γ-ray energies. This is most easily carried out by measurement of the unscattered radiation transmitted through a

polarizer. Therefore the polarization dependence of the total cross section was applied. This is obtained by integration over the sphere:

$$\int\left(\frac{\mathrm{d}_e\tau}{\mathrm{d}\Omega}\right)\mathrm{d}\Omega \equiv {}_e\tau(k_0, \xi_3^0, \zeta_3^0) \equiv {}_e\tau_c + \xi_3^0 \cdot \zeta_3^0 \cdot {}_e\tau_p$$

$$= 2\pi r_0^2\left\{\frac{1+k_0}{k_0^2}\left[\frac{2(1+k_0)}{1+2k_0} - \frac{1}{k_0}\ln(1+2k_0)\right] + \frac{1}{2k_0}\ln(1+2k_0)\right.$$

$$\left. - \frac{1+3k_0}{(1+2k_0)^2} - \xi_3^0 \cdot \zeta_3^0 \cdot \left[\frac{1+k_0}{2k_0^2}\ln(1+2k_0) - \frac{1+4k_0+5k_0^2}{k_0(1+2k_e)^2}\right]\right\}. \quad (15)$$

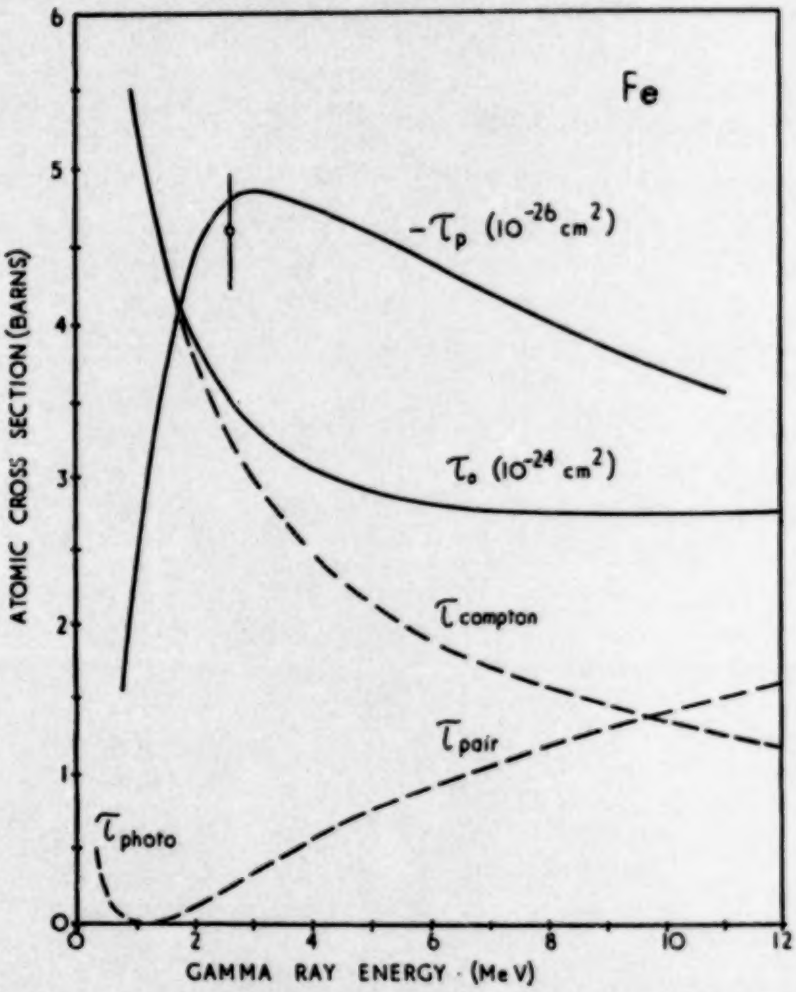

Fig. 2. γ-ray absorption cross sections for iron. Note that the polarization cross section τ_p is on a hundred times larger scale than the other quantities. The experimental value is taken from the work by Gunst and Page [5]).

Here ${}_e\tau_c$ is the ordinary total Compton cross section. One obtains the atomic cross section by multiplication with the number of

electrons:

$$_{a}\tau_{c} = Z\,{}_{e}\tau_{c}, \tag{16}$$

$$_{a}\tau_{p} = \nu_{eff} \cdot {}_{e}\tau_{p}. \tag{17}$$

where $Z = 26$ is the atomic number of iron and ν_{eff} is the effective number of polarized electrons in magnetized iron. Atomic cross sections for iron are shown in figure 2. τ_p is given at magnetic saturation when [12]) $\nu_{eff} = \nu_{sat} = 2.06$.

τ_p is negative for γ-energies above 0.65 MeV. The transmission is then greatest when ξ_3^0 and ζ_3^0 have the same sign, i.e. when the photon spin is parallel to the electron spin and antiparallel to the magnetic field.

3. Experimental Set-up

A schematical top view of the apparatus is shown in figure 3. A thermal neutron beam is emitted from the JEEP through a colli-

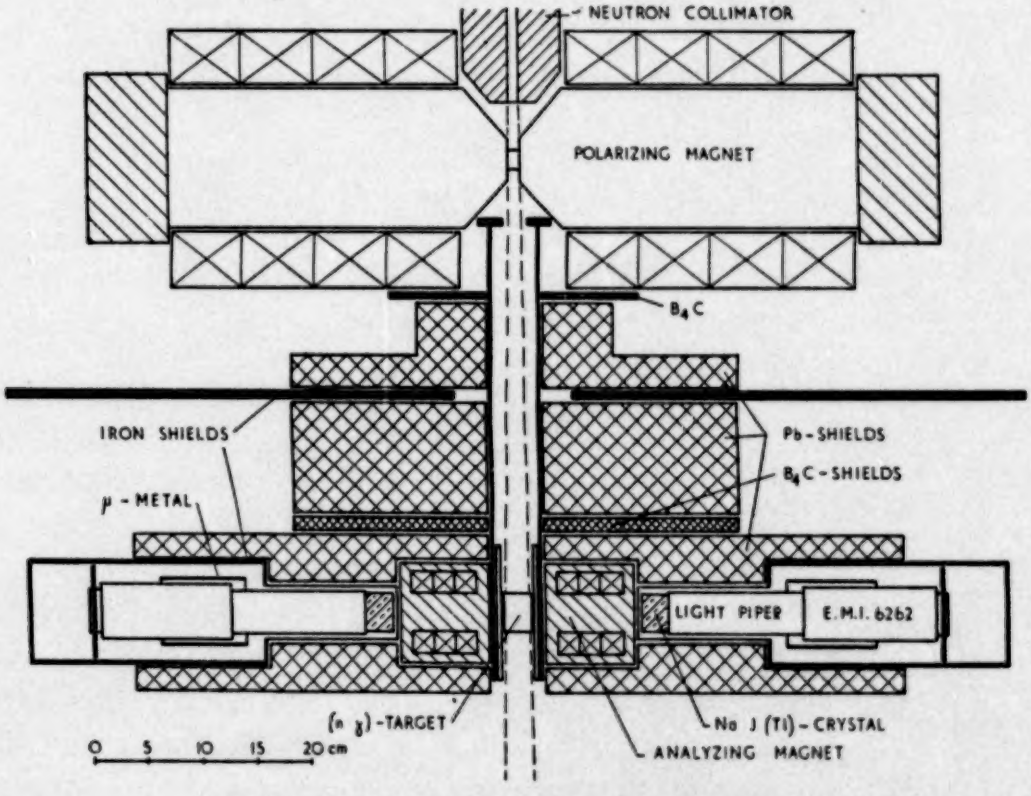

Fig. 3. Top view of the experimental set-up.

mator opening of 10×30 mm and the part passing through the polarizer falls on the (n, γ)-target. The neutron polarizer is a

$12 \times 18 \times 40$ mm block of iron, joined to the pole faces of a magnet by the 40×18 mm planes. The neutrons pass through 18 mm of iron. In the magnet gap is produced a field strength of 14900 Oersted. The block is cut from coldrolled iron in such a way that the magnetic field is applied in the direction of rolling. According to Hughes *et al.* [13]) this gives the highest degree of polarization. Between polarizer and target two parallel iron plates, which pick up part of the magnetic stray field, maintain approximately 100 gauss along the neutron beam. Thus the neutrons are not depolarized before they hit the target.

The target is a thin-walled aluminium cylinder containing the element to be studied. In a ferromagnetic material the neutrons may be depolarized before being captured. Nickel- and iron-targets therefore are made from non-ferro-magnetic salts.

The γ-rays of greatest circular polarization, being emitted parallel and antiparallel to the neutron polarization enter two identical analyzing and detecting systems. In each of these, the γ-rays are counted by a NaI(Tl)-crystal after having passed through an 8 cm long piece of iron magnetized in the direction of transmission. This compact core of the analyzing magnet has flat end pieces which are joined to an outer tube formed cylinder. The windings producing the magnetic field are placed between the core and the tube as shown in figure 3. Each detector consists of a cylindrical NaI(Tl)-crystal, 35 mm in diameter and 25 mm high, coupled to an EMI 6262 photomultiplier. Single channel discriminators were used for the selection of the γ-rays to be studied.

Systematic errors would arise if the photomultiplier pulse height was influenced by the inversion of the analyzing magnetic fields. Therefore, long light pipes are used to bring the photomultipliers away from the magnets, and the tubes are surrounded by μ-metal and soft iron shields. The EMI venetian blind photomultipliers employed are known to be less influenced by magnetic fields than other types [14]). Heavy shielding of lead and boron carbide serve to reduce the intense background radiation, which is largely due to neutron capture in the polarizing iron block.

4. Experimental Procedure

The neutron polarizer was studied by measurements of single and double transmission effects, using a BF_3 counter tube as detector. For the mean single transmission effect it was found $\bar{\eta} = 5.2\ \%$.

With the help of a second polarizing magnet the double transmission effect was measured, yielding $g = 0.66$. The polarization of the neutrons absorbed by the (n, γ)-targets was then calculated to $P_n = 19\ \%$. Integrations were performed graphically.

The magnetization of the analyzer cores was 86 % of saturation according to magnetic flux measurements. The polarization is then $P_a = 2.14\ \%$ at 7 MeV, and is slowly varying with energy above 3 MeV, as seen from figure 2.

These polarization values are inserted in equation (9):

$$\frac{N_a'-N_a'}{N_a'+N_a''} = RP_n P_a = 0.0041\ R. \tag{18}$$

It is seen that in order to determine the magnitude of R, which is between 0 and 1, extremely small relative variations of the counting rate N_a should be measured. Furthermore, the sensitivity of the method is considerably reduced by background and scattering.

P_n and P_a are the numerical, positive polarization values. Supposing R is positive, N_a' is the higher counting rate and it is observed for parallel polarizing and analyzing effects. As magnetization is antiparallel to polarization in both these processes, N_a' is the counting rate obtained when polarizing and analyzing magnetic fields are parallel. N_a'' is the counting rate when one of the fields is reversed.

Counts were recorded in periods of approximately 3 minutes, between which the analyzing field directions were changed. The two identical detecting channels were always so coupled that if channel number 1 would record N', channel number 2 would record N'' and vice versa. Thus, when the mean value of the asymmetry from the two channels was taken, effects due to voltage and reactor instability should be compensated. The number of counts in each period was so small that the fluctuations due to detector sensitivities would always be negligible compared to the statistical standard deviation. Those fluctuations would be random and would accordingly be negligible also after summation of all observations.

The most feared source of errors was the influence of the magnetic fields on the photomultipliers, because this effect could simulate polarization. The sensitivity to magnetic fields was increased and studied by lowering of the voltage between cathode and first dynode to 1/20 of the usual value. The observed correlation between counting

rate and magnetic field reversal was negligible. In table 1 are first given the results of a "symmetry control" experiment in which a titanium target was placed in the neutron beam 12 cm farther out than usual, so that the γ-rays passing from target to detector would not go through the analyzer core. The measurements showed the expected absence of asymmetry, but the statistical accuracy

TABLE 1

Data for the γ-rays studied

Emitting nucleus	γ-ray term	Energy E (MeV)	Experimental asymmetry Q (10^{-5})	Experimental value of $\Sigma\alpha_i R_i = \overline{R}_{exp}$	Derived value of R_x	Derived value of $\Sigma\alpha_i R_i = \overline{R}_{der}$
Ti	Symmetry Control Experiment		6 ±13			
S^{33}	G	5.44	−31 ±17	−0.44 ±0.24	−1/2	−0.37±0.13
Ca^{41}	C	6.42	−14 ±11	−0.26 ±0.20	−1/2	−0.43±0.07
Ti^{49}	F	6.75	− 9 ±7	−0.045±0.035	−1/2	−0.08±0.07
Ti^{49}	G	6.41	59 ±16	0.30 ±0.08	+1	0.18±0.07
Cr^{54}	A	9.72	−24 ±24	−0.09 ±0.09	−1/2	−0.25±0.02
Cr^{54}	B	8.88	34 ±13	0.16 ±0.06	+1/4	0.15±0.15
Fe^{57}	E	7.64	42 ±6.5	0.78 ±0.12	+1	0.90±0.10
Ni^{59}	A	9.00	−45 ±39	−0.25 ±0.22	−1/2	−0.37±0.13
Zn^{65}	E	7.88	−10.5±9	−0.21 ±0.18	−1/2	−0.32±0.18
					(−1/3)	(−0.19±0.14)
W^{183}	D	6.18	46 ±18	0.61 ±0.23	+1	0.85±0.15

is poor so that no decisive conclusion can be drawn from this experiment alone. In the polarization experiments a reversal of both polarizer and analyzer currents should give unchanged counting rate if no systematic errors are present. This means that a series of measurements with positive polarizer current should yield the same asymmetry as a series with negative current. An analysis of the measurements for all the targets failed to show any systematic effect.

For the experiment, it must be appreciated that N_a of equation (9) is the counting rate of γ-rays that are not scattered, produced by capture in the target by the incoming neutron beam plus the not depolarized part of the scattered neutrons. The actually observed asymmetry is

$$Q = \frac{N_t' - N_t''}{N_t' + N_t''} \tag{19}$$

where N_t is the total counting rate which consists of direct and

scattered γ-rays from the target and γ-rays due to neutrons scattered from the target as well as background. Equations (9) and (19) together with the abbreviation $N = \frac{1}{2}(N'+N'')$ gives

$$RP_n P_a = \frac{N_t}{N_a} Q. \tag{20}$$

If we define N_b = counting rate of γ-rays that are not scattered, produced by neutrons captured in the target after depolarizing scattering, N_a+N_b represents the direct γ-rays originating in the target. The correction factor $\beta = N_a/(N_a+N_b)$ due to multiple scattering and depolarization can be calculated. It seldom became smaller than 0.8. From measurements of the γ-ray intensities obtained with the analyzer removed one can calculate $\gamma = (N_a+N_b)/N_t$ which had values in the range 0.2 to 0.9. Usually, about half of this correction was due to background.

If several γ-rays are detected simultaneously, equation (20) must be modified:

$$\overline{RP_n P_a} = P_n \sum_i \alpha_i R_i P_{ai} = \beta\gamma Q \tag{21}$$

where α_i is the relative contribution of the i-th γ-ray, $\Sigma\alpha_i = 1$. As P_n is slowly varying with energy, a good approximation is

$$\overline{R} = \sum \alpha_i R_i = \frac{\beta\gamma Q}{P_n \bar{P}_a}. \tag{22}$$

Generally, R_i is unknown for all the γ-rays in the spectrum. If one of the γ-rays is predominant, i.e. it has a large α_i, the corresponding R_i may be determined from a measurement of $\Sigma\alpha_i R_i$ with the uncertainty that is due to the other R's being unknown.

By using discriminators, the γ-ray to be studied was separated as well as possible from the other ones. The resolving power of the experimental set-up was found by measurement of the spectra from titanium, iron, sulphur and aluminium. Figure 4 shows the results, where the dashed lines are the single γ-ray spectra, and the total calculated spectrum is given by the continuous line. The energies and relative intensities of the γ-rays from the various targets are obtained from Kinsey and Bartholomew [15]). Thus by decomposing the measured spectra, the relative contributions α_i of the single γ-rays at certain discriminator positions can be determined.

Suitable target materials have relatively high capture cross

section combined with emission of γ-rays that are strong compared to the rest of the spectrum. Most of the elements fulfilling these requirements are found in the region of atomic number 11 to 30.

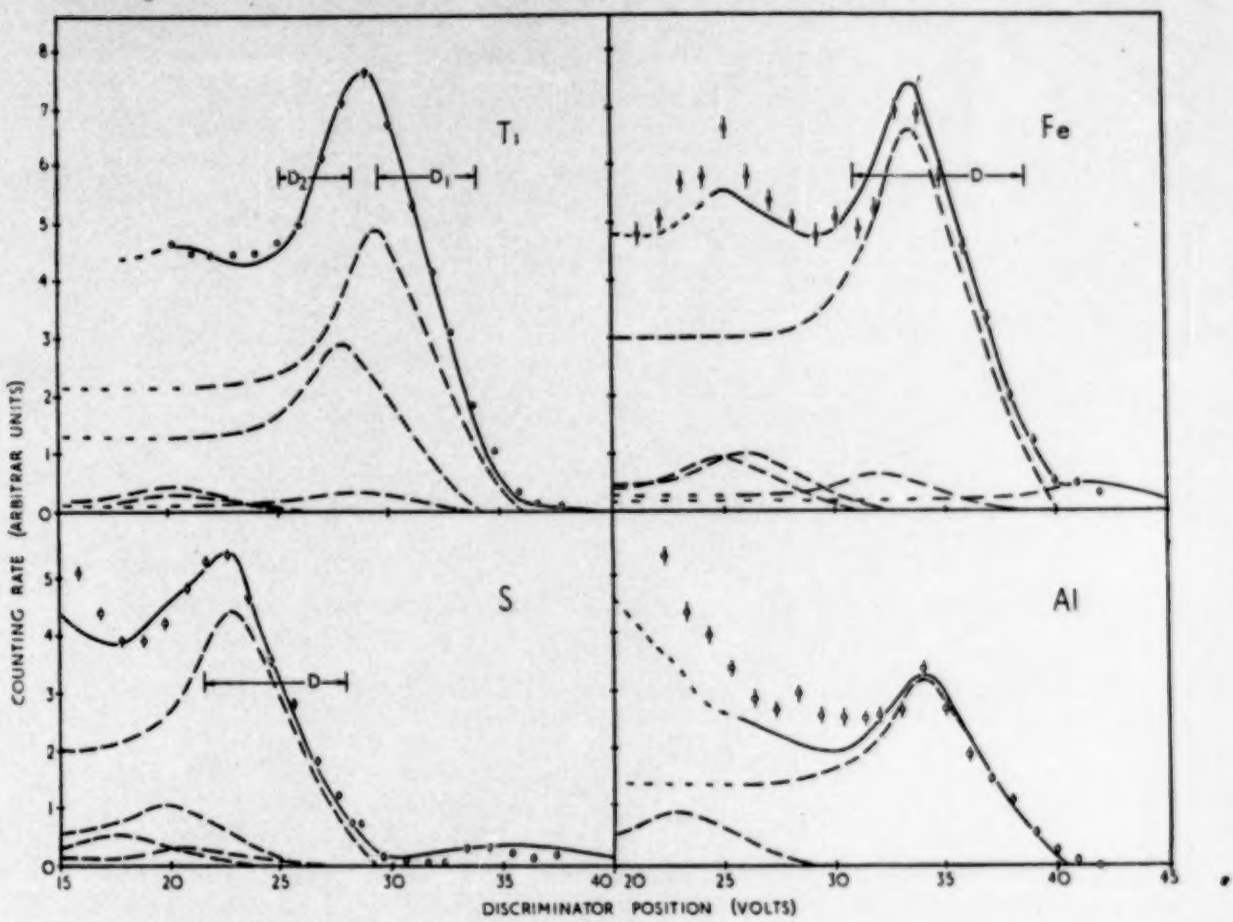

Fig. 4. γ-ray spectra as seen with the detectors employed. Discriminator positions used in the polarization measurements are shown.

With the JEEP running at 200 to 450 kW, a few times 10^7 neutrons per second were emitted from the collimator. The counting rates during the measurements were from 300 to 3000 counts per minute. To obtain standard deviations of Q as low as 10^{-4}, the time required for continuous measurements must be of the order of weeks or months.

5. Results

The γ-rays that were studied are listed in table 1, where the first column contains the nuclei in which the γ-transitions take place. Figures 5, 6 and 7 are the corresponding decay schemes. The γ-ray

terms, energies and intensities being quoted are taken from Kinsey and Bartholomew [15]). Column 4 of the table contains the uncorrected experimental asymmetry in units of 10^{-5}, together with the statistical standard deviation. Using equation (22) the experimental average value $\overline{R}_{exp}$ of the ratio between photon and neutron polarization

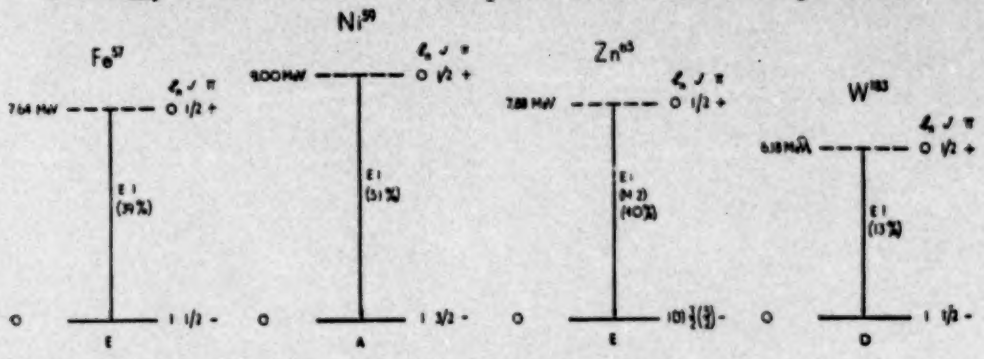

Fig. 5. Decay schemes for ground state neutron capture γ-rays. l_n and J are neutron and total angular momentum and π is parity.

was calculated and given in column 5 together with the standard deviation. R_x for the special γ-ray that was studied, was derived from $\overline{R}_{exp}$ with the help of previously known nuclear data, as discussed below. The last column of table I contains the most probable magnitude of $\overline{R} = \Sigma \alpha_i R_i$, calculated from R_x. Also given

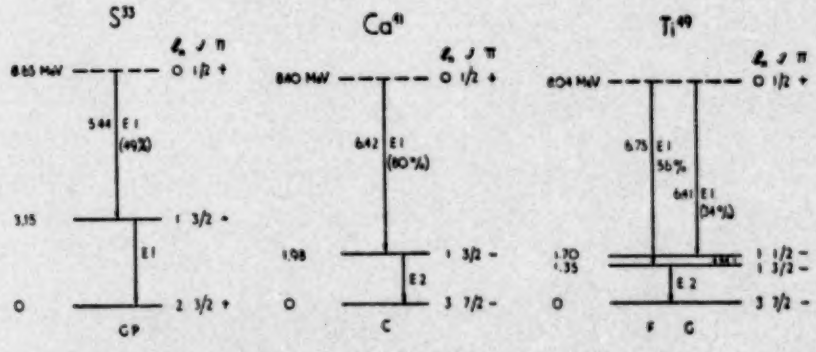

Fig. 6. Decay schemes for neutron capture γ-rays. Symbols are as in fig. 5.

is the total possible deviation which is due to the γ-rays for which R_i is unknown.

The simplest cases investigated were the ground state γ-rays resulting from capture in even nuclei. The compound state then has spin $\frac{1}{2}$ and even parity. In the case of dipole radiation, the ground state spin is $\frac{1}{2}$ or $\frac{3}{2}$, corresponding to $R = 1$ or $-\frac{1}{2}$ respectively. The ground state γ-rays in Fe^{57}, Ni^{59}, Zn^{65} and W^{183} are sketched in figure 5.

For W^{183} the ground state spin $J_f = \frac{1}{2}$ is given in the compilation by Walchli [16]). Spin $\frac{1}{2}$ and odd parity is also predicted by nuclear shell theory [17]). Therefore, the γ-ray D is known to be electric dipole (E1) with $R_D = 1$. For the discriminator used, this gave $\overline{R}_{der} = 0.85 \pm 0.15$ compared with $R_{exp} = 0.61 \pm 0.23$. This result verifies the theoretical prediction of the direction and the order of magnitude of the circular polarization.

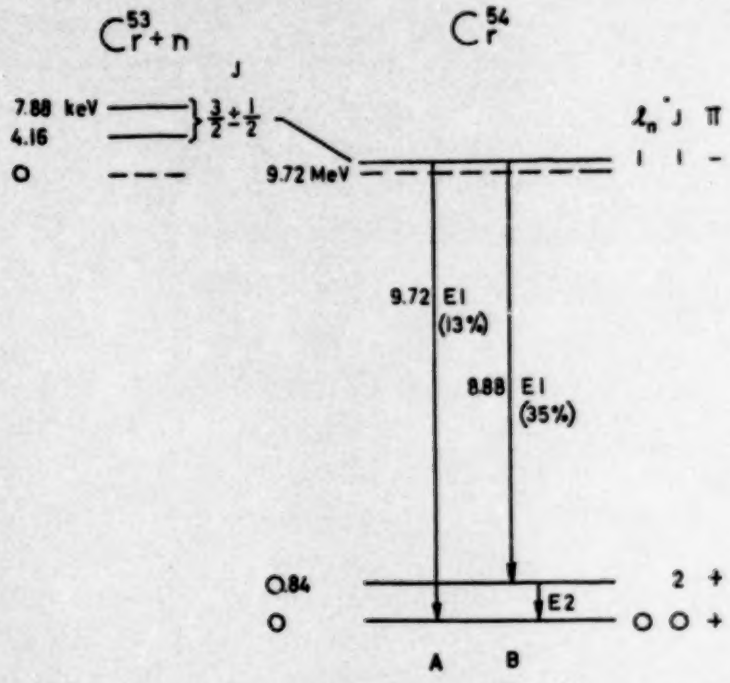

Fig. 7. Decay scheme for neutron capture γ-rays in Cr^{54}
Symbols are as in figure 5.

The ground state transitions of Fe^{57} and Ni^{59} are very similar, the only apparent difference between the two nuclei being the number of protons which is 26 and 28 respectively. Nuclear shell theory predicts a $p_{3/2}$-state for both. From studies of (d, p)-reactions [18]) it was found that Fe^{57} is in a p-state, and the polarization measurements show that the state is $p_{\frac{1}{2}}$, contradicting simple shell theory. The (d, p)-reaction on nickel [19]) shows that the spin of Ni^{59} is most probably 3/2, which is confirmed by our result. The nuclear shell theory prediction is perhaps more stringent in the case of Ni^{59} which has no unfilled proton shell.

Polarization measurements on the strong γ-ray E of Zn^{65} yielded $\overline{R}_{exp} = 0.21 \pm 0.18$ which is consistent with both the final spins 3/2 and 5/2, corresponding to $\overline{R}_{der} = -0.32$ and -0.19 respectively.

The high intensity of the γ-ray indicates that it is a dipole-transition. This would give $J_f = 3/2$ whereas the shell model predicts 5/2 for the ground state. It has, however, not been definitely established that the γ-ray is actually a ground state transition. It might be leading to the 0.052 MeV level found from measurements on the decay of Ga^{65} [20]).

The strongest high energy γ-rays of the nuclei S^{33}, Ca^{41} and Ti^{49} are transitions to levels that are known from (d, p)-reactions [21, 22]) to be p-states with odd parities. As the compound states, being due to neutron capture in even nuclei, have spin $\frac{1}{2}$ and even parity, the γ-rays are electric dipoles. The level spins 1/2 or 3/2 correspond to R = 1 or $-\frac{1}{2}$. The ground state spins and parities are given by Walchli [16]) and by the nuclear shell model [17]).

Polarization measurements give $J_f = 3/2$ for the 3.15 MeV level in S^{33}. The ground state spin is $3/2^+$, so that the γ-ray P in cascade with G is also electric dipole.

In Ca^{41} we find $J_f = 3/2$ for the 1.98 MeV level. With ground state spin $7/2^-$ the two γ-rays in cascade are electric dipole and quadrupole respectively.

For the two p-states in Ti^{49} at 1.70 and 1.35 MeV, 4 combinations of spins are possible. The polarization measurements are consistent with $J_f = 1/2$ and 3/2 respectively. The transition to the ground state, having spin 7/2–, will mainly consist of electric quadrupole radiation from the 1.35 MeV level.

Cr^{53} has ground state spin 3/2 according to Walchli [16]). When thermal neutrons are captured, the compound state will obtain spin 1 or 2 or both, dependent upon the spins of the neutron resonances that are responsible for the capture. However, spins and widths of those resonances are not known. Measurements of the angular correlation between the 8.88 MeV and the 0.84 MeV γ-rays[23]) showed that the cascade is 1(1)1(1)0 or 1(1)2(2)0. Then, for the first transition of the cascade the polarization ratio R_B equals $-\frac{1}{4}$ or $+\frac{1}{4}$ respectively. The experimental value agrees with the latter case. For the transition directly to the ground state one obtains $R_A = -\frac{1}{2}$, which means that this γ-ray also originates from $J_c = 1$ (see figure 7). Both A and B are then electric dipole transitions.

The most accurate measurement of $\overline{R}$ was performed for iron. The values $\overline{R}_{exp}$ and $\overline{R}_{der}$ agree well, but the added uncertainties are still 22 %.

In conclusion the present experiment demonstrates that circularly polarized γ-rays can be produced by the capture of polarized neutrons. The magnitude of the effect is in accordance with theory. In simple cases the accuracy with which we have measured is sufficient for the determination of spin values. However, for the study of more complicated cases, the statistical accuracy would have to be increased considerably.

References

1) H. A. Tolhoek and J. A. M. Cox, Physica **19** (1953) 101, 673
2) L. Wolfenstein, Phys. Rev. **75** (1949) 1664
3) L. C. Biedenharn, M. E. Rose and G. B. Arfken ORNL–986 (1951)
4) O. Halpern, Nature **168** (1951) 782, Phys. Rev. **82** (1951) 753
5) S. B. Gunst and L. A. Page, Phys. Rev. **92** (1953) 970
6) L. C. Biedenharn, M. E. Rose and G. B. Arfken, Phys. Rev. **83** (1951) 683
7) J. M. Cassels, in Progress in Nuclear Physics (ed. O. R. Frisch), vol. 1 (1950) p. 185
8) C. P. Stanford, T. E. Stephenson, L. W. Cochran and S. Bernstein, Phys. Rev. **94** (1954) 374
9) O. Halpern and T. Holstein, Phys. Rev. **59** (1941) 960
10) J. Pelser, Physica **21** (1954) 22
11) F. W. Lipps and H. A. Tolhoek, Physica **20** (1954) 85, 395
12) P. Argyres and C. Kittel, Acta Metallurgica **1** (1953) 241
13) D. J. Hughes, J. R. Wallace and R. H. Holtzmann, Phys, Rev. **73** (1948) 1277
14) J. Wardley, Transactions of the Instruments and Measurements Conference (Stockholm, 1952) p. 198
15) B. B. Kinsey and G. A. Bartholomew, Phys. Rev. **85** (1952) 1012, Phys. Rev. **89** (1953) 375, Can. Journ. Phys. **31** (1953) 1051
16) H. E. Walchli, ORNL-1469 (1953), with suppl. 1 and 2
17) M. G. Mayer and J. H. D. Jensen, Elementary Theory of Nuclear Shell Structure (Wiley, 1955)
18) C. F. Black, Phys. Rev. **90** (1953) 381
19) W. W. Pratt, Phys. Rev. **95** (1954) 1517
20) B. Crasemann, Phys. Rev. **93** (1954) 1034
21) J. R. Holt and T. N. Marsham, Proc. Phys. Soc. A **66** (1953) 467, 565
22) M. M. Bretscher, J. O. Alderman, A. Elwyn and F. B. Shull, Phys. Rev. **96** (1954) 103
23) G. Trumpy (to be published)

Nuclear Physics **2** (1956/57) 680—686; *North-Holland Publishing Co., Amsterdam*

DIRECTIONAL CORRELATION MEASUREMENTS IN Fe^{57}

TORSTEN LINDQVIST † and ERNST HEER
Swiss Federal Institute of Technology (ETH), Zürich

Received 25 September 1956

Abstract: The directional correlation of the 123 keV and 14 keV gamma lines in Fe^{57} has been investigated. The mother nucleus is the 270 day Co^{57}, decaying by K-capture to Fe^{57}. The influence of self absorption and scattering in the source as well as the influence of the chemical form of the source was investigated. In the correlation function $W(\theta) = 1 + A_2 P_2(\cos\theta) + A_4 P_4(\cos\theta)$ the coefficients A_2 and A_4 were determined as $A_2 = -0.024 \pm 0.003$, $A_4 = 0 \pm 0.01$. Mixing ratios of the gamma rays are discussed.

1. Decay of Co^{57}

The decay of 270 day Co^{57} has been investigated by many authors. References and results can be found in US-AEC report on Nuclear Level Schemes [1]). Co^{57} decays by K-capture to a 137 keV level in Fe^{57}. This level decays to the ground state through the 137 keV line with relative intensity of 7 % and through a cascade, 123 keV—14 keV, with a relative intensity of 93 %. The lifetime of the 14 keV level has been measured by Deutsch and Wright [2]) to be $\tau_{\frac{1}{2}} = 1.1 \times 10^{-7}$ s. Among various possibilities the spins and parities given in fig. 1 can be concluded from the facts given in table 1.

TABLE 1

Experiment	Conclusion	Ref.
1. Fe^{56} [d, p(θ)]	Fe^{57}-ground state spin 1/2 or 3/2 (shell model $p_{3/2}$)	[3])
2. Coulomb excitation of the 137 keV level	E2-excitation. 137 keV level same parity as g.s.	[4])
3. *ft*-value determination	$\Delta j \leqq 1$, no parity change (Co^{57} g.s. $j = 7/2-$, measured)	[5])
4. Conv. coeff. 14 keV and 123 keV lines	Mainly M1. All levels of same parity	[5, 6])
5. Coincidences 14 keV-X rays	No K-capture to 14 keV level; spin (14 keV level) $\neq 5/2$	[5])
6. Conv. coeff. 137 keV line	E2	[6])

† On leave from Institute of Physics, Uppsala, Sweden.

2. Source Preparation

The Co^{57} source was prepared by 7 MeV deuteron bombardment of spectroscopically pure iron in the Nobel Institute Cyclotron, Stockholm. The beam current was 100 μA and the bombardment

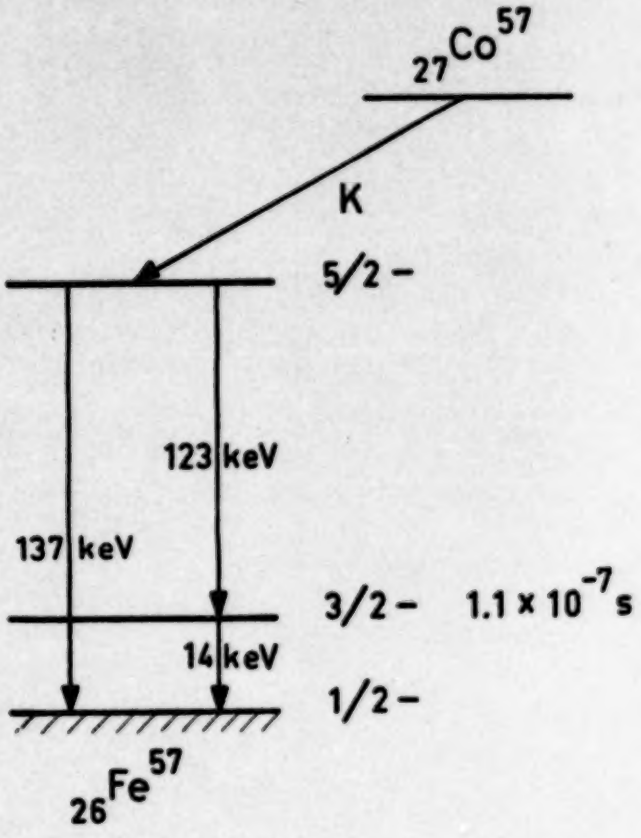

Fig. 1. Decay scheme of Co^{57}.

lasted 5 hours. Chemical separation of the cobalt activity from the target material was carried out by a method given by Maxwell *et al.* [7]). The radio-cobalt was obtained in the form of an aqueous solution of cobalt chloride.

3. Experiment

The counters were NaI crystals with DuMond 6292 multipliers. The fixed counter, which detected the 14 keV line, had a thin crystal, $\frac{1}{4}''$ thick and 1" diameter, covered with 0.001" Al foil and canned. In order to decrease the thermionic background the multiplier was held at a low temperature with dry ice. The movable counter, which detected the 123 keV line, had a $1'' \times 1''$ crystal. From the multipliers the pulses were fed through cathode followers,

linear amplifiers and differential pulse height analyzers. The single spectra of the two channels can be seen in fig. 2. The 123 keV channel was delayed about 0.1 μsec because of the lifetime of the 14 keV level. The two channels were fed into a coincidence unit with a resolving time of 2×10^{-7} s.

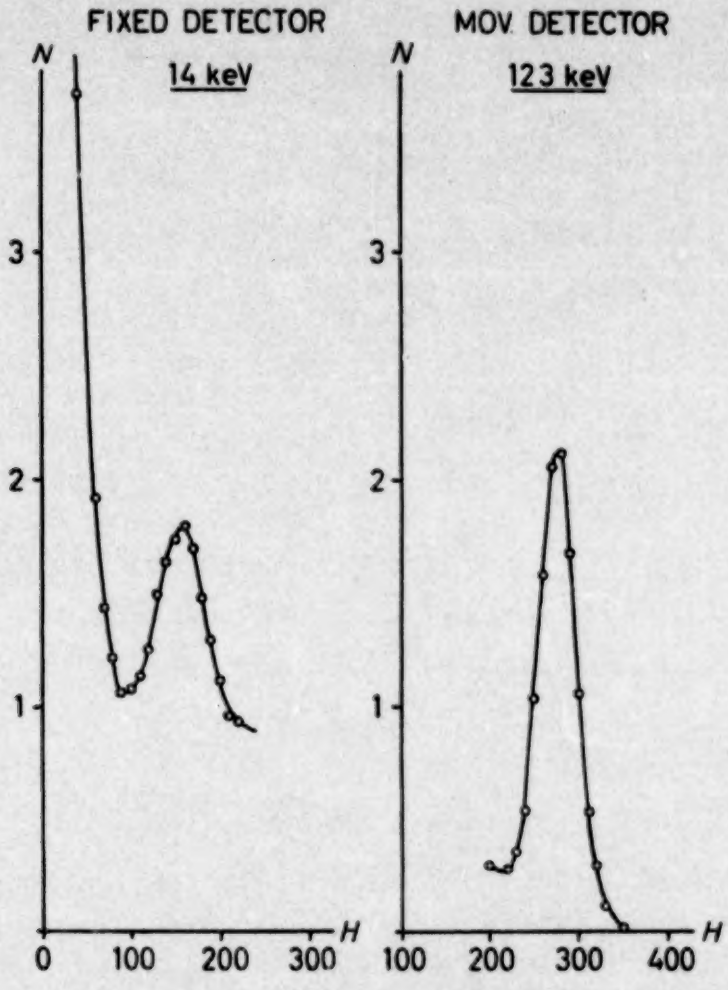

Fig. 2. Single spectra of 14 keV and 123 keV gamma lines.

The data were recorded automatically. The number of coincidences at 225°, 180°, 135° and 90° between the counters were registered, as well as the single counting rates at corresponding positions. The recording time at each position was 15 min or 30 min. The mean value of the coincidence rates at 225° and 135° was formed. After correcting for accidental coincidences the coefficients A_2 and A_4 in the correlation function $W(\theta) = 1+A_2P_2(\cos\theta)+A_4P_4(\cos\theta)$ were calculated according to Gimmi *et al.* [8]) (p. 159—160).

In order to obtain the true undisturbed correlation in this case one has to take two facts into consideration, namely the lifetime of the intermediate level, 1.1×10^{-7} s, and the low energy of one of the transitions, 14 keV. The first fact may introduce an attenuation of the anisotropy due to an interaction between the electric

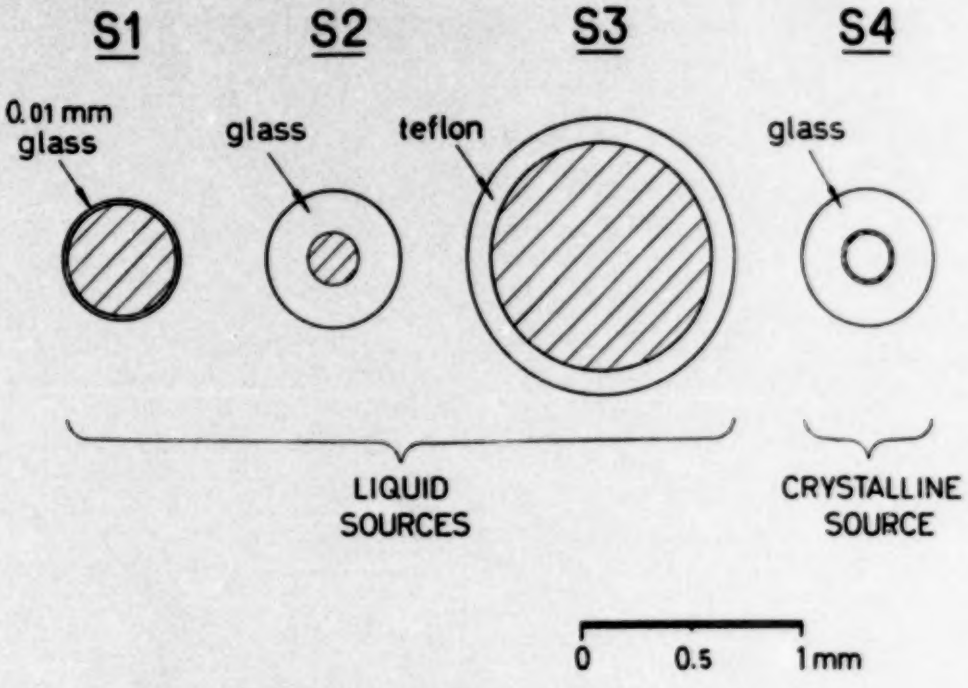

Fig. 3. Cross sections of the cylindrical sources.

quadrupole moment of the intermediate nuclear state and the gradient of the electric crystal field. The second fact may give rise to self-absorption and scattering in the source. Selfabsorption enhances the negative anisotropy and scattering attenuates the absolute value of the anisotropy.

Four different sources were used. Three of them were liquid sources. Cobalt chloride, aqueous solution, was put into small tubes of glass of various dimensions. The tubes were then sealed by melting. A fourth source was prepared by evaporating the solution in one of the tubes. A crystalline powder was then obtained on the inner wall of the tube. Fig. 3 shows the cross section dimensions of the four sources. All sources were of 7 mm height.

It is well known that a liquid source shows a minimum of electric quadrupole moment interaction because of the Brownian motion in the liquid cancelling on the average the electric field.

Further the quadrupole moment of the intermediate state of Fe^{57} is probably small, because all neighbour nuclei are known to have small electric quadrupole moments. It is therefore believed that the quadrupole interaction in this experiment is very small. A check on this assumption is done by measuring the crystalline source.

The problem of selfabsorption and scattering in the source was investigated by using different source diameters.

4. Results

The results of the measurements can be seen in table 2. Within the error limits the three first sources show the same value of A_2.

TABLE 2

Source No	A_2 % (± statistical error)	A_4 % (± statistical error)	Number of coinc.	Total measuring time
S1	-1.95 ± 0.20	$+0.18\pm0.32$	$8.1 \cdot 10^5$	110 h
S2	-1.97 ± 0.52	$+0.92\pm0.88$	$1.1 \cdot 10^5$	140 h
S3	-1.47 ± 0.60	-0.23 ± 1.00	$0.84 \cdot 10^5$	112 h
S4	-3.60 ± 0.76	-0.45 ± 1.25	$0.63 \cdot 10^5$	98 h

Note that A_2 and A_4 are not corrected for detector solid angle.

Table 2 shows that selfabsorption and scattering are negligible at least in the case of S1 and S2. The result of the strongest source, S1, will be taken as final result. The larger negative value in S4, the crystalline source, is probably due to self-absorption. Within error limits $A_4 = 0$ in agreement with the theory, since the spin of the intermediate level is 3/2.

When corrected for detector solid angle the correlation function for the 123 keV–14 keV gamma cascade in Fe^{57} is

$$W(\theta) = 1-[0.024\pm0.003]P_2(\cos\theta).$$

5. Discussion

As mentioned above the 123 keV and 14 keV transitions are mainly M1. Under the assumption that both transitions have a small admixture of E2 with mixing ratios δ_1^2 resp. δ_2^2, the measured correlation gives δ_2 as a function of δ_1. According to tables of Ferentz and Rosenzweig [9]) the A_2 term is a product of two coefficients

$$A_2 = A_2^{(1)} A_2^{(2)}$$

where

$$A_2^{(1)} = F_2(L_1 L_1 j_1 j) + 2\delta_1 F_2(L_1, L_1+1, j_1 j) + \delta_1^2 F_2(L_1+1, L_1+1, j_1 j);$$

$$A_2^{(2)} = F_2(L_2 L_2 j_2 j) + 2\delta_2 F_2(L_2, L_2+1, j_2 j) + \delta_2^2 F_2(L_2+1, L_2+1, j_2 j);$$

L_1 and L_2 are the multipolarities of the transitions and j_1, j, j_2 are resp. spins of levels. The F coefficients are tabulated in ref. [9]).

With A_2 known one can easily obtain the function

$$\delta_2 = \phi(\delta_1)$$

which is drawn in fig. 4. Only $|\delta| < 0.5$ is considered because both admixtures are small according to conversion coefficient experiments.

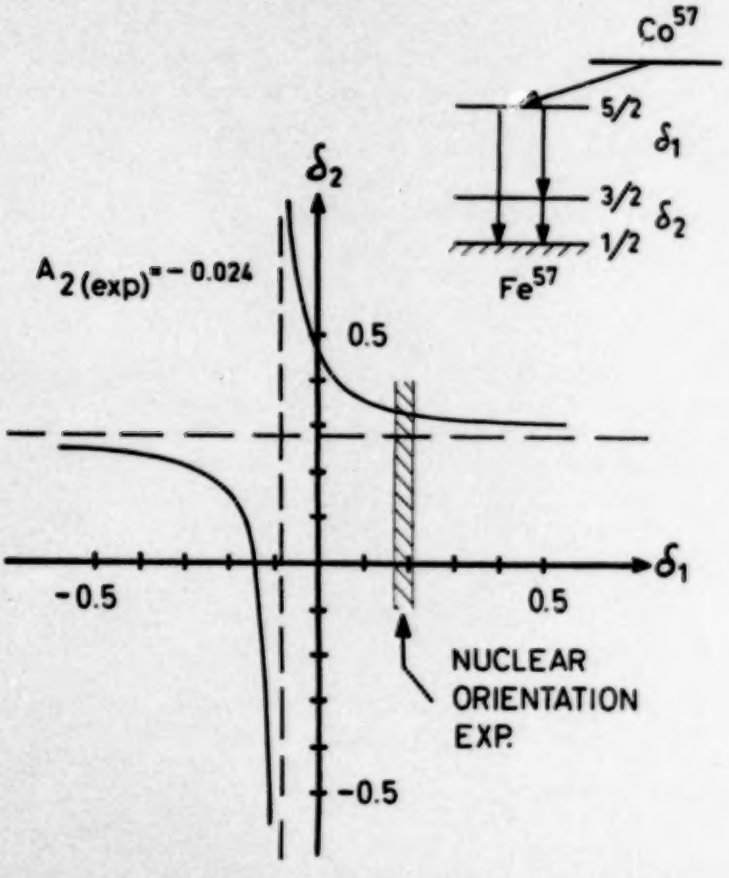

Fig. 4. Corresponding mixing ratios for $A_2 = -0.024$.

According to fig. 4 δ_2 is always $> +0.28$ for $\delta_1 > -0.08$, which means that the 14 keV transition has an admixture of more than 8 % E2. This is difficult to understand in the light of the measured life-time, 1.1×10^{-7} s, for the 14 keV level. One would therefore suggest that δ_1 is negative and in the region between -0.13 and

-0.30. Contradictory to these results is however a measurement by Bishop *et al.* [10]), who have determined $\delta_1 = +0.19 \pm 0.02$ by means of nuclear orientation. Their result is shown in fig. 4. It can be noted that the absolute value of δ_1 fits these directional correlation measurements.

The authors are indebted to Dr K. G. Malmfors, Stockholm, for the cyclotron bombardment and to Miss I.-B. Svensson, Uppsala, for making the chemical separation. One of the authors (T. L.) wishes to express his appreciation to Professor P. Scherrer, ETH, Zürich, for the opportunity of working in his laboratory and wishes also to acknowledge a grant from the Swedish Atomic Committee.

Note added in proof: Dr. M. A. Grace, Oxford, has kindly pointed out "that the discrepancy between the angular correlation experiment and the nuclear orientation measurements is more apparent than real". It turns out that the 123 keV line is a second member of a cascade in the nuclear orientation experiment. The change from second to first members of the cascade requires that δ_1 be reversed in sign. The value thus found for δ_2 is $+0.14$, not incompatible with the K-conversion coefficient of the 14 keV line, $\alpha_K = 14$, found by Lemner, Segaert and Grace [5]).

References

1) Nuclear Level Schemes, US-AEC Report TID-5300 (1955)
2) M. Deutsch and W. E. Wright, Phys. Rev. **77** (1950) 139
3) C. F. Black, Phys. Rev. **90** (1953) 381 A
4) G. M. Temner and N. P. Heydenburg, Phys. Rev. **96** (1954) 246
5) H. R. Lemner *et al.*, Proc. Phys. Soc. A **68** (1955) 701
6) D. E. Alburger and M. A. Grace, Proc. Phys. Soc. A **67** (1954) 280
7) R. D. Maxwell *et al.*, J. Chem. Phys. **17** (1949) 1340
8) F. Gimmi *et al.*, Helv. Phys. Acta, **29** (1956) 147
9) M. Ferentz and N. Rosenzweig, ANL—5324 (not published)
10) G. R. Bishop *et al.*, Phil. Mag. **46** (1955) 951

Nuclear Physics **2** (1956/57) 687—705; *North-Holland Publishing Co., Amsterdam*

DECAY SCHEME FOR Zr^{97} and Nb^{97}

N. N. DELYAGIN, A. A. SOROKIN, N. V. FORAFONTOV and V. S. SHPINEL

Moscow State University, Moscow

Received 4 October 1956

Abstract: The decay scheme for Zr^{97} and Nb^{97} has been investigated with a double-lens β-spectrometer connected in coincidence with a scintillation γ-spectrometer and also with a coincidence scintillation γ-spectrometer.

A partial β-spectrum has been separated which has an upper limit $E_\beta = 0.45$ MeV and can be assigned to Zr^{97}.

In addition to known intense γ-lines from Zr^{97}, weak γ-lines—1.35 (3—5 %); 1.62 ($\approx$ 1.5 %); 2.2 (1—2 %); 2.58 ($\leq$ 1 %) MeV—have been detected.

The existence of cascade γ-radiation has been established and a tentative decay scheme is proposed.

1. Introduction

The radioactive chain $Zr^{97} \rightarrow Nb^{97} \rightarrow Mo^{97}$ has been investigated by a number of authors. A summary of the results and list of references can be found in ref. [1]). It has apparently reliably been established that beta-decaying Zr^{97} produces a 0.747 MeV isomeric level in Nb^{97m} which then decays with a period of 60 sec and goes over to the Nb^{97} ground state. The Zr^{97} beta spectrum is a simple one and possesses a high energy end point $E_\beta = 1.91$ MeV. Nb^{97} subsequently undergoes beta decay with $E_\beta = 1.267$ MeV, accompanied by a γ-ray of $E_\gamma = 0.665$ MeV energy. In ref. [1]), in which a $Zr^{97}+Nb^{97}$ source was used, a soft β-spectrum with a high energy end point $E_\gamma = 0.48$ MeV and also a low intensity hard γ-radiation were detected. The results of β-γ and γ-γ coincidence studies of these nuclei were reported by us at the All-Union Conference on Nuclear Spectroscopy in 1955. The method applied in these investigations permitted us to separate the soft Zr^{97} β-spectrum from the gross $Zr^{97}+Nb^{97}$ β-spectrum; moreover, γ-γ-coincidences with an intensity of 10 % were detected with the same source. The energy of the cascade γ-quanta, as estimated by the absorption method, was found to be ≈ 0.7 MeV and > 1

MeV. In the present paper we report some refined data obtained by repeating our measurements with improved apparatus.

2. Source

The Zr^{97} radioactive source was obtained by irradiating zirconium with neutrons in a reactor during a period of 10 to 24 hours. The specific activity of the sources thus obtained was low due to low content of Zr^{96} in the natural isotopic mixture (2.6 %) and also due to the low value of the activation cross section (0.1—0.2 barn). This circumstance compels one to pay special attention to purity of the original raw material, especially if weak β or γ-transitions are being investigated. In most cases metallic Zr obtained by the iodide method was used instead of zirconium oxide, the raw material usually employed in earlier work. Small amounts of hafnium and titanium (1—2 %) which were present and also Zr^{95} which is formed during irradiation could not affect the results of the measurements since the decay periods of these isotopes are much greater than that of Zr^{97}.

Possible surface impurities (mainly sodium) were removed by rinsing in nitric acid after irradiation. In some check measurements ZrO_3 powder enriched 16 times in the Zr^{96} isotope was subjected to irradiation.

3. Gamma Spectrum

The $Zr^{97}+Nb^{97}$ gamma ray spectrum was measured with a single crystal scintillation spectrometer consisting of a NaI(Tl) crystal and a ФЭУ—19 photomultiplier tube. The sodium iodide crystal which was 12 mm thick, 30 mm in diameter and surrounded by a MgO reflector, was enclosed in an air tight aluminium container. Before striking the crystal the gamma rays traversed a 0.4 mm aluminium foil and a 1 mm layer of magnesium oxide. The measurements were conducted without beam collimation. Under these conditions the half-width of the Cs^{137} ($E_\gamma = 0.661$ MeV) photoelectric line was 12 %. By using lead collimators 3—7 mm in diameter and 40 mm in height the half-width could be reduced to 9—10 %. Linearity of the spectrometer energy scale was checked by using the radiation from Hg^{203}, Au^{198}, Cs^{137}, Zn^{65}, Co^{60}, ThC″ and Na^{24}.

To analyse the complex gamma spectrum measured with the scintillation spectrometer we resolved it into separate components,

using standard spectrum shapes obtained for well known gamma lines. These standard spectra reduced to equal height of full energy peaks (photopeaks) are represented in fig. 1. The energy expressed

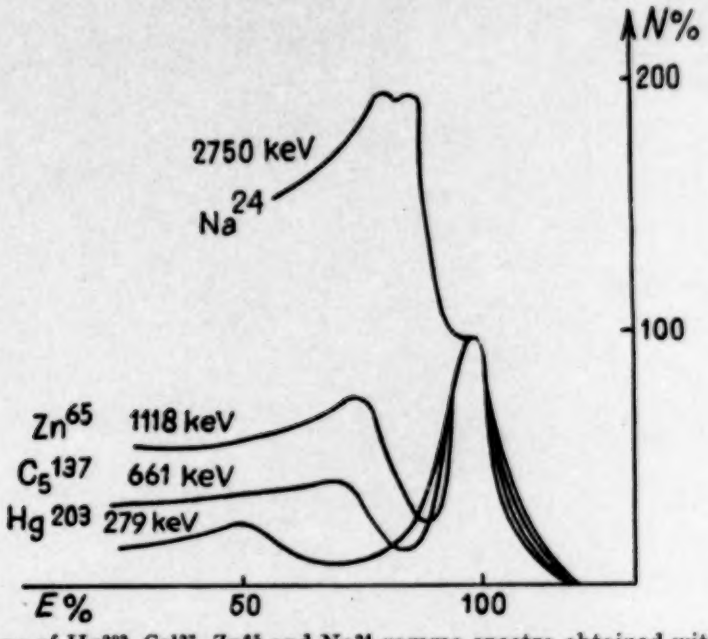

Fig. 1. Shape of Hg^{203}, Cs^{137}, Zn^{65} and Na^{24} gamma spectra obtained with a scintillation spectrometer.

in percentage of photopeak energy is plotted along the abscissa axis. The gamma line intensity was determined from the total energy peak by using the relative efficiency calibration curve for radiations of various energy (fig. 2). The method used to obtain the spectrometer efficiency curve was described in ref. [2]). Errors in spectrometer efficiency measurements were due mainly to inaccuracies in determination of absolute source activities (6 %) and in measurement of the photopeak areas (10—15 %).

The $Zr^{97}+Nb^{97}$ γ-spectrum for the enriched source mentioned above is shown in fig. 3. As can be seen from the figure, besides intense photopeaks attributable to the known 0.665 and 0.750 MeV gamma rays from Zr^{97} and Nb^{97} several maxima in the 1.0—2.6 MeV energy range are also evident. Measurement of attenuation of the hard component of the spectrum yielded a value of 17 ± 1 hours for the half-life which corresponds to the Zr^{97} decay period. The positions of the peaks correspond to the electron energies listed in column 1, table 1.

Assignment of each peak could be made by successively subtracting the standard spectrum shapes starting with the hard line.

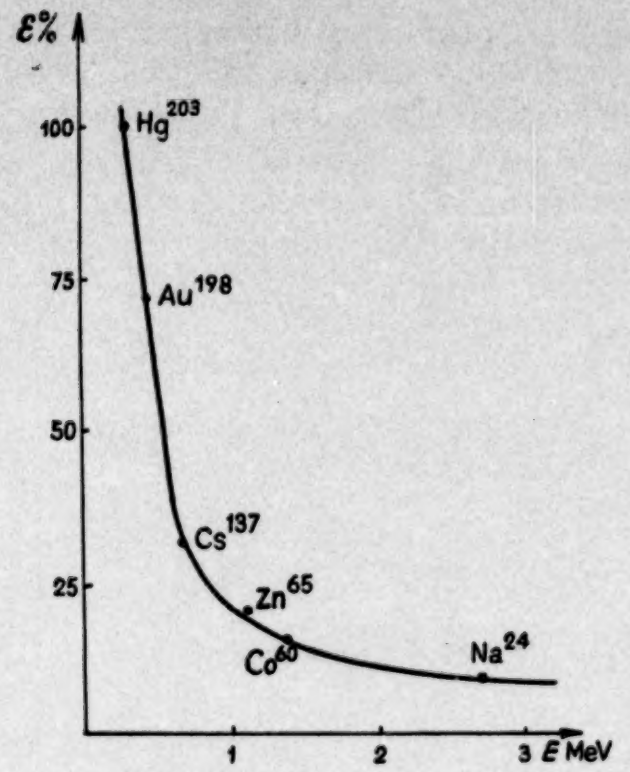

Fig. 2. γ-spectrometer efficiency curve.

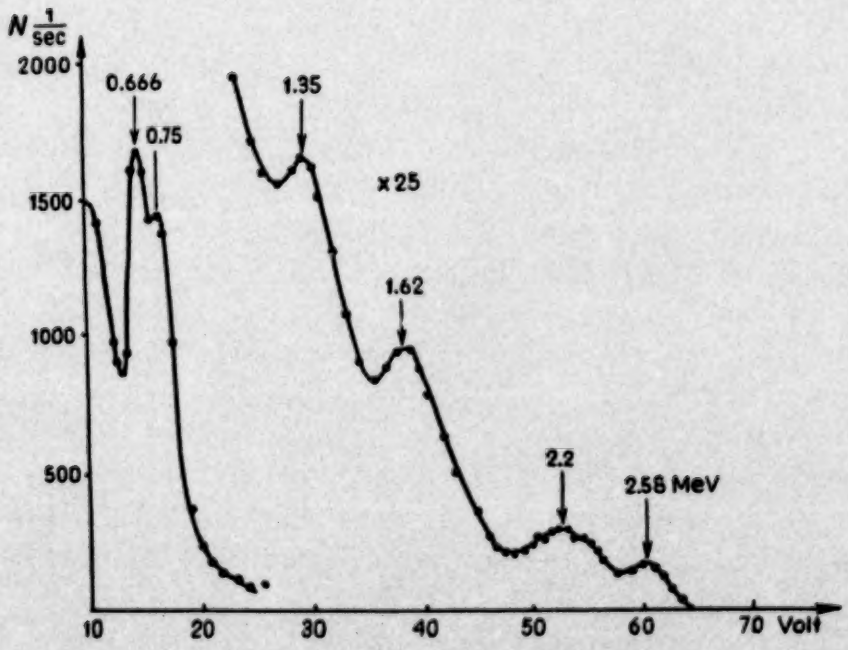

Fig. 3. $Zr^{97}+Nb^{97}$ gamma spectrum.

The results of the analysis which are presented in column 2 show that all peaks, excluding the hardest one, are due to superposition of pulse distributions of separate monochromatic γ-lines, the energy and intensities of which are indicated in columns 3 and 4. The intensities are expressed in percentage of total decay rate. It should be noted that, unfortunately, analysis of such a complex spectrum is not unique. To obtain additional information on the γ-radiation γ-γ coincidences were investigated.

TABLE 1

Position of peak MeV	Nature of peak	γ-line energy, MeV	Intensity of γ-line
2.58	P_1	2.58 ± 0.05	$\leqq 1\,\%$
2.3	C_1		
2.2	P_2	2.2 ± 0.05	$\approx 1-2\,\%$
2.1	π_1		
1.62	$P_3+\pi_1+\pi_2$	1.62 ± 0.03	$\approx 1.5\,\%$
1.35	P_4+C_2	1.35 ± 0.05	$3-5\,\%$
1.15	$C_4+\pi_3+\pi_3$		

P, C, π—photo, Compton and pair peaks, respectively.

4. Experimental Arrangement for Investigation of γ-γ Coincidence

Cascade γ-radiation was studied with a coincidence scintillation spectrometer. The fast-slow coincidence principle which permits one to combine short resolving time of the coincidence circuit ($\approx 10^{-8}$ sec) with pulse height analysis was utilized in the spectro-

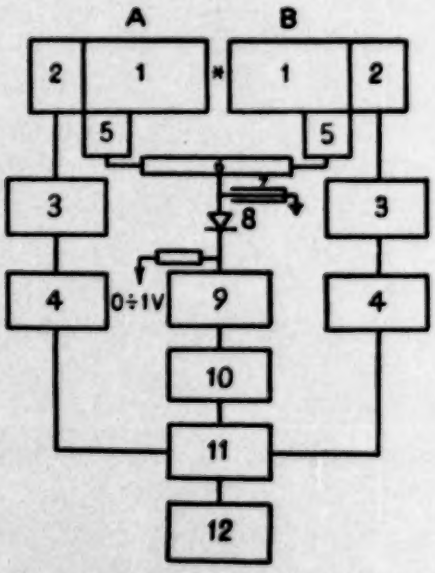

Fig. 4. Block diagram of arrangement for investigation of γ-γ coincidences.

meter. A block diagram of the spectrometer is shown in fig. 4. Commercial NaI(Tl) crystals 30 mm in diameter and 15 mm thick and ФЭУ —19 photomultipliers were used as detectors. The pulses from the photomultiplier anodes were fed into a fast coincidence circuit similar to those previously described in ref. [3, 4, 5]). These pulses were limited to cut-off pentodes 6Ж1П (5) and then fed into a variable delay line (6) which consisted of 50 cm segments of РК —50 cable ($\varrho = 150\Omega$) connected in series. Sliding contact with a ДГС —4 crystal diode (8) which selected coincidences was made at the points of connection of the cables. By moving the crystal carriage along the line one could either determine the position of the maximum true coincidence rate or the position corresponding to random coincidences. The resolving time of the coincident circuit was chiefly determined by the length of the shaping cable (7) (РК —1 cable, $\varrho = 77\Omega$) and, to a certain extent, by the diode bias (8). Coincidence pulses transmitted by the crystal were amplified (pass band of amplifier (9) 4 mc/sec, gain 1000), and fed into a discriminator (10) which reduced the amplifier noise and stopped single pulses which had leaked through the stray capacity of the crystal diode. For maximum coincidence counting efficiency the pulses from the photomultipliers should be as large as possible. The pulses from the multiplier anodes due to Co^{60} γ-rays were as high as 100 V when the multipliers selected in this work were operated by a voltage of 2200 V applied to a non-uniform voltage divider.

The pulses for amplitude analysis were taken from the ninth dynodes of the multipliers. They were then fed successively into a cathode follower (2), a linear amplifier (3) and single channel amplitude analyser (4); the amplifiers consisted of three-tube stages with negative feedback (6) and amplification factors of 100, 50 and 20; the circuit was linear for output voltages up to 100 V. Analysers (4) and the fast coincidence circuit discriminator (10) were connected to a triple coincidence circuit possessing a resolving time of 5×10^{-7} sec. Thus, scaler (12) recorded only coincidences between γ-rays of definite energy selected by the amplitude analysers.

The resolving time of the fast coincidence circuit, τ_0, was chosen to be $(2.5-3) \times 10^{-8}$ sec. A check on coincidences between 0.058 MeV X-rays and 0.345 MeV γ-quanta showed that even for such small energies the counting loss did not exceed several per cent.

Calibration of the spectrometer showed that its energy scale was linear up to 2.76 MeV (Na^{24}). The half-width of the Cs^{137} line was 13—14 % in both of the channels.

Performance of the apparatus was checked by carrying out measurements on coincidence spectra of a number of isotopes (Na^{24}, Co^{60}, $Hf^{175, 181}$). The results of measurements of $Hf^{175, 181}$ are given in fig. 5. Curve 1 (measured in channel A) is a section

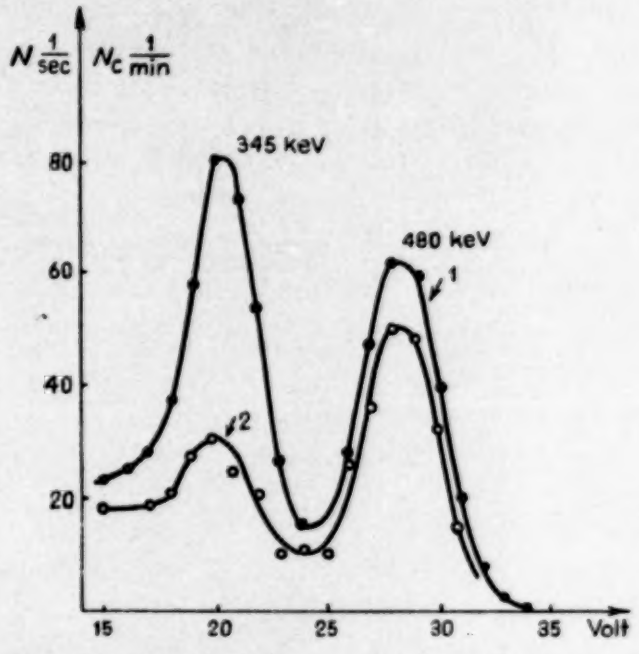

Fig. 5. 1) Segment of $Hf^{175, 181}$ gamma spectrum, including 0.345 and 0.480 MeV lines. 2) Spectrum of γ-quanta in coincidence with 0.132 and 0.135 MeV Hf^{181} γ-quanta.

of the γ-spectrum of this isotopic mixture and includes the 0.345 and 0.480 MeV. Most of the intense 0.345 MeV peak is due to the Hf^{175} γ-radiation as the intensity of the 0.345 MeV transition comprises only 15.7 % of the 0.480 MeV Hf^{181} transition [7]). Curve 2 is the spectrum of γ-rays in coincidence with the 0.132 and 0.135 MeV Hf^{181} γ-rays selected by the amplitude analyser in channel B. As can be seen from the graph, the intensity of the 0.345 MeV line is considerably reduced, this being a result of the fact that the Hf^{175} radiation which does not yield coincidence is not recorded. With account of the conversion coefficient for the 0.132 and 0.135 MeV transitions the intensity of this line relative to the 0.480 MeV line was estimated to be 15—20 %, a value which agrees with that cited above.

5. Measurement of γ-γ Coincidences in the $Zr^{97}+Nb^{97}$ Spectrum

The counter and source arrangement shown in fig. 6 was used in γ-γ-coincidence measurement of the $Zr^{97}+Nb^{97}$ spectrum. The

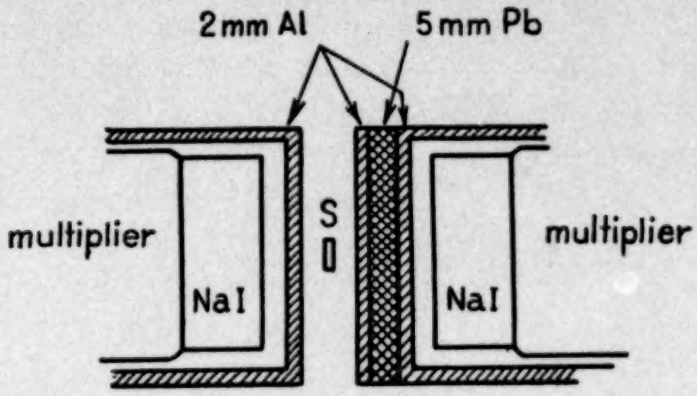

Fig. 6. Arrangement for investigation of γ-γ coincidences from $Zr^{97}+Nb^{97}$.

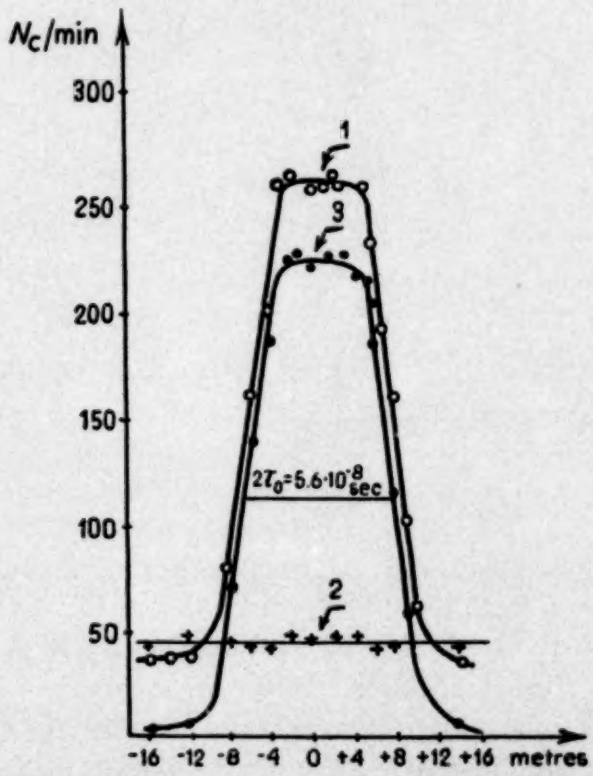

Fig. 7. Dependence of γ-γ coincidence rate on delay for sources: (1) $Zr^{97}+Nb^{97}$; (2) Nb^{97}; (3) Co^{60}.

5 mm lead filter in front of the crystal in channel B was used to suppress coincidences due to γ-rays scattered from one crystal to the other.

The existence of cascade γ-radiation in the investigated spectrum is evident from curve 1, fig. 7, which represents the dependence of the γ-γ coincidence rate recorded by the fast coincidence circuit on the delay time in the channels. For comparison, an analogous curve for Co^{60} (curve 3, fig. 7) is presented on the same graph; this curve characterizes the instrumental "resolving curve" of the experimental arrangement. The time decrease of the γ-γ coincidence counting rate was measured over a period of three days and yielded a lifetime of 17 hours which indicates that the cascade radiation can be attributed to either Zr^{97} or Nb^{97}. Similar experiments were performed with Nb^{97} chemically separated from zirconium to ascertain which of these nucleides was responsible for the coincidences. From the results (curve 2, fig. 7) thus obtained, it could be concluded that no γ-γ coincidences were present in this case. This compels one to assign the observed cascade radiation to Zr^{97}.

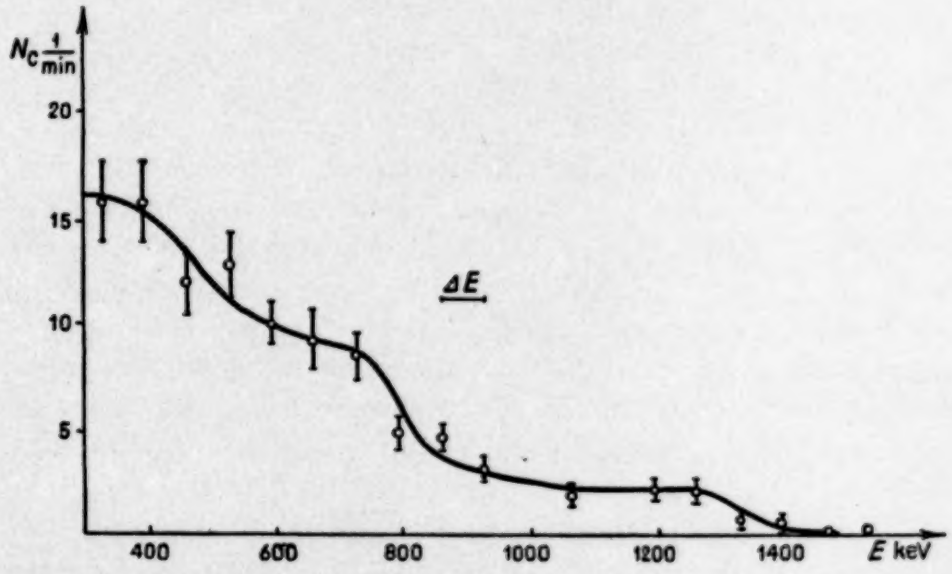

Fig. 8. Spectrum of γ-quanta in coincidence with $E_\gamma > 0.25$ MeV γ-rays for $Zr^{97}+Nb^{97}$.

Subsequently, the energy of the cascade γ-quanta was measured. The results are presented in fig. 8 and 9. Fig. 8 is the spectrum of quanta recorded in channel A in coincidence with γ-rays possessing

an energy > 0.250 MeV; these γ-rays were recorded in channel B in which an integral analyser output was utilized.

The spectrum shown in fig. 9 was obtained under conditions

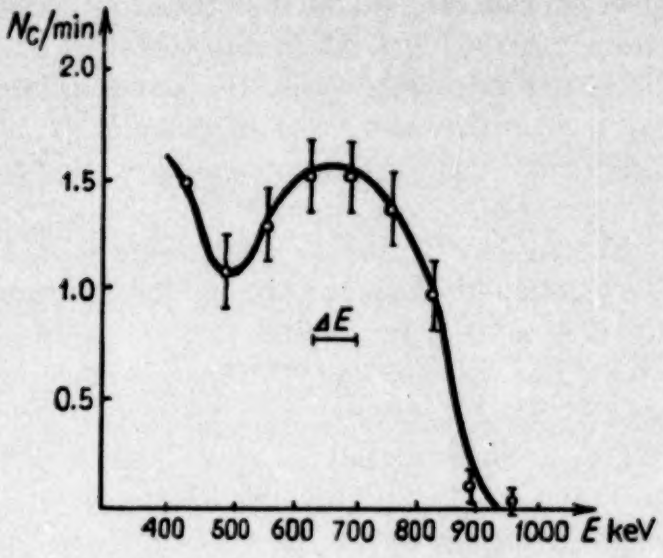

Fig. 9. Spectrum of γ-quanta in coincidence with $E_\gamma > 1$ MeV γ-rays for $Zr^{97}+Nb^{97}$.

when only γ-rays with $E_\gamma > 1$ MeV were recorded in channel B. The width of the analyser window in the channel was increased to 2 V (instead of the usual 1 V) and the points in the spectrum were measured at intervals of 2 V. A result of this was that the spectra were not measured with sufficient accuracy but this was inevitable in view of the necessity of reducing the measurement time.

The random coincidence background has been subtracted everywhere. In the soft part of the spectrum shown in fig. 8 it comprised 20—25 % of the true coincidence counting rate. In the hard part (> 1 MeV) of this spectrum and in the spectrum in fig. 9 it was considerably lower and could be neglected for all practical purposes.

The results of these measurements show that the energy of the most penetrating of the coincidence quanta lies in the 1.3—1.4 MeV range (fig. 8). The γ-rays whose spectrum is shown in fig. 9 are evidently in cascade with these quanta. The spectrum in fig. 9 contains a diffuse peak in the 0.6—0.8 MeV region which is broader than the photopeak which could be attributed to a single line. It may be assumed that this spectrum shape is due to the following causes:

1. In prolonged (10—12 hours) measurements instability of the apparatus becomes appreciable and this circumstance together with the large width of the analyser window leads to the result that, despite the existence of a single line, the photopeak in the spectrum becomes diffuse.

2. Two close lines exist which are not resolved by the spectrometer.

The following control experiment was performed to check these assumptions.

The NaI (Tl) crystal in channel B was replaced by a tolane crystal covered by only a thin (1.6 mg/cm^2) aluminium foil.

In this case besides γ-quanta the channel also recorded electrons of the 1.91 MeV Zr^{97} and 1.27 MeV Nb^{97} β-spectra. The β-γ coincidences should then be attributed to 1.27 MeV β-spectrum electrons

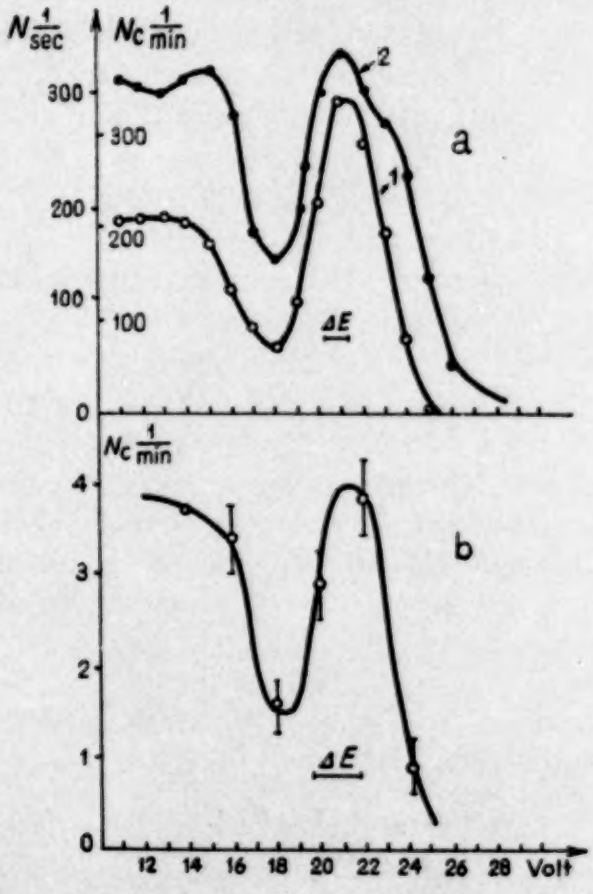

Fig. 10. a) Comparison of γ-spectrum in coincidence with β-particles (1) with the usual $Zr^{97}+Nb^{97}$ type of γ-spectrum (2).
b) Control γ-γ coincidence measurements yielding the same type of spectrum as that in 1(a).

and 0.665 MeV γ-rays of Nb^{97} (β-γ coincidences associated with the 0.45 MeV β-spectrum were suppressed by suitable selection of the discriminator threshold in channel B). Thus β-γ coincidence measurements of the γ-ray spectrum should single out the 0.665 MeV line from the gross γ-ray spectrum. Results of this type of measurements are presented in fig. 10a in which the coincidence γ-spectrum (1) is compared with the usual $Zr^{97}+Nb^{97}$ γ-spectrum (2).

The discriminator in channel B was then set so as to include the terminal region of the Nb^{97} β-spectrum. In this case most of the recorded β-particles could be attributed to the zirconium β-spectrum. The coincidence counting rate was about 100 times lower and equalled approximately several counts per minute. The analyser window in channel A was 2 V wide and the spectrum was measured at intervals of 2 V. Thus the conditions were similar to those which existed in the γ-γ coincidence spectrum measurements. As can be seen from the results of these measurements (fig. 10b) the 0.665 MeV line was quite distinctly separated. The spread of the spectrum in fig. 9 was apparently due to the second of the causes mentioned above.

The intensity of the cascade γ-radiation was assessed by comparing the γ-γ and β-γ coincidence counting rates. A tolane crystal in cnannel B was also used in these measurements, a lead filter being placed in front of crystal A.

The counter efficiency for Cs^{137} and Co^{60} γ-rays was approximately equalized by suitably adjusting the discriminator threshold. The γ-ray counter efficiency could then be considered to be the same for all γ-quanta contributing to the coincidences. Assuming that the efficiency of counters B for γ-rays from zirconium and niobium is the same and neglecting β-γ coincidences associated with the 0.45 MeV β-spectrum one may write the following: the β-γ coincidence counting rate

$$N_{\beta\gamma} = N_0 \, \varepsilon_\gamma^{\mathrm{A}} \, \varepsilon_\beta^{\mathrm{B}},$$

the γ-γ coincidence counting rate

$$N_{\gamma\gamma} = 2N_0 \, \varepsilon_\gamma^{\mathrm{A}} \, \varepsilon_\gamma^{\mathrm{B}} \, \delta.$$

The γ-quantum and β-particle counting rates in channel B are respectively

$$N_\gamma^{\mathrm{B}} = 2N_0 \, \varepsilon_\gamma^{\mathrm{B}}$$

$$N_\beta^{\mathrm{B}} = 2N_0 \, \varepsilon_\beta^{\mathrm{B}}.$$

(Here ε is the γ or β-ray efficiency of the respective counter with account of the solid angle, N_0 is the source activity and δ is the intensity of the cascade radiation). It is not difficult to verify that under the aforementioned assumptions one gets

$$\delta = \tfrac{1}{2} \frac{N_{\gamma\gamma}}{N_{\beta\gamma}} \frac{N_\beta^B}{N_\gamma^B}$$

and all involved quantities can be determined experimentally. The measurements yielded a value of δ lying between 7—10 %.

6. Experimental Arrangement for Measurement of Partial β-Spectra

The β-γ coincidence measurements were performed with an arrangement consisting of a 2 lens β-spectrometer [8]) and scintillation γ-spectrometer connected in coincidence. A block diagram of the arrangement is shown in fig. 11. Electrons emitted by the

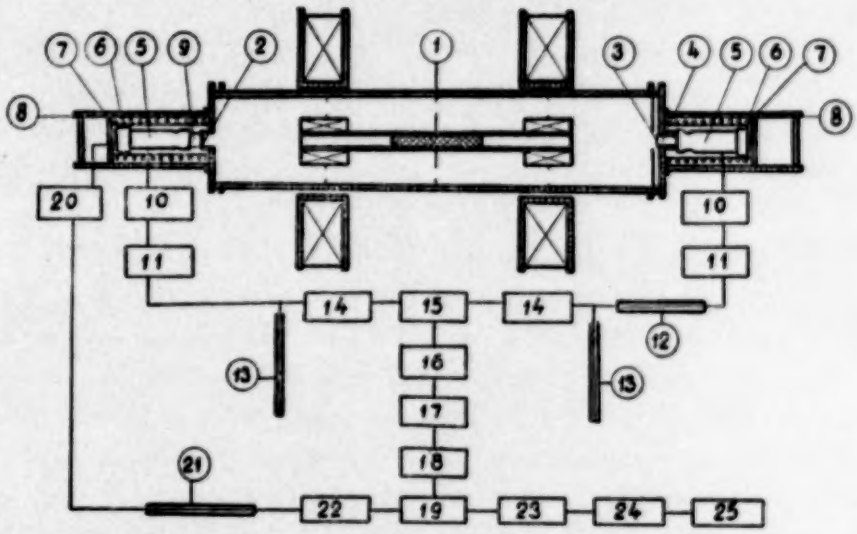

Fig. 11. Block diagram of arrangement for investigation of β-γ coincidences.

radioactive source (2) are selected by β-spectrometer (1) and recorded by a scintillation β-counter with an anthracene crystal (3), 3 mm thick and 10 mm in diameter; the crystal was covered by an aluminized celluloid film reflector whose thickness did not exceed 0.1 mg/cm^2. The crystal was coupled to the photocathode of a ФЭУ—19 multiplier by a plexiglas light pipe (4) 50 mm long.

The gamma radiation from the source impinged on a NaI(Tl) crystal (9) 15 mm thick and 30 mm in diameter enclosed in the

manner described above. The crystal was directly mounted on the ФЭУ—19 tube of the scintillation γ-spectrometer and arranged on the bottom of an aluminium glass in the centre of which the source was located. The solid angle subtended by the crystal with respect to the source centre was 15.2 % of 4π. The photomultipliers were enclosed in 3 mm thick permalloy cylinders (6), which shielded the magnetic field of the β-spectrometer. Solenoid-like compensating coils (7) were wound on the permalloy cylinders and together with the multipliers were enclosed in a cylindrical light-tight casing made of soft iron 10 mm thick. With this type of multiplier shielding the counting rate in the β and γ-channels did not change by more than 1.5 % when the spectrometer current varied from 0 to 9 amperes ($E \approx 1.4$ MeV).

The negative pulses from the photomultiplier anodes were fed to cathode followers (10), to preamplifiers (11) which possessed a gain of about 10 and after this were cut down to 2.5 V in the γ-channel and 1.7 V in the β-channel. The pulses were shaped by a $\approx$ 1.5 m short-circuited cable which reduced their amplitudes to about several hundredths of a volt. A delay line (12) consisting of a 10 m cable was introduced in the channel. The shaped pulses were subsequently amplified by wideband amplifiers (14) which had a pass band of 17 mc/sec and a gain of approximately 15 and were then fed into a bridge coincidence circuit (15) [9]) consisting of ДГЦ—9 germanium diodes. The coincidence circuit was followed by a differential amplifier(16) and a two stage amplifier with a cathode follower at the output (17). After the cathode follower the pulses were fed into a pulse height discriminator (18), a modified Schmitt circuit, which selected the coincidences. The coincidence pulses from the discriminator were 2μ sec wide and 25 V high and were applied to open the gating circuit (19). The gating circuit was designed by A. S. Melioransky and is featured by high stability, an amplification factor of about unity, a residual pedestal of 0.12 V and linearity up to 22 volts, the maximum magnitude of the leakage pulses being 0.7 V. For pulse height analysis in the γ-channel, positive pulses from the 11th multiplier dynode were fed into the gating circuit. After passing cathode follower (20) and a 0.6μ sec delay line (21) the pulses were preamplified by a non-overloaded amplifier (22) possessing a 8 mc/sec passband, a gain 10 and linearity for output pulses as large as 20 V. The pulses transmitted by the gating circuit were amplified by amplifier (23) which yielded

a maximum output of 100 V and were then fed into a single channel differential discriminator (24) and scaler ПС—64 (25). The load in the β and γ-channels was controlled during the measurements at each point, a 10000 decade scaler (not shown in the block diagram) being used for this purpose.

A check on the performance of the γ-spectrometer carried out with the aid of known γ-lines (Hg^{203}, Cs^{137}, Zn^{65}) showed that the gating circuit did not distort the shape of the obtained spectra of the linearity of the energy scale. With the geometrical arrangement described above the width of the Cs^{137} γ-line peak was 13 %. Operation of the β-spectrometer with the scintillation counter was verified with the aid of known β-spectra.

The resolving time of the coincidence circuit was determined from the β-γ-coincidence delay curve for a Co^{60} source. The measurements yielded $\tau = 4 \times 10^{-8}$ sec; the length of cable (12)corresponding to the curve maximum was 10 m and was independent of the discrimination setting in the γ-channel. Frequent measurements over prolonged periods showed that the delay curve and its position were sufficiently stable. The value obtained for τ satisfactorily agrees with measurements on the coincidence counting rate for two independent sources.

The correctness of measurements on the shape of β-spectra correlating with γ-rays was checked by directly measuring the Co^{60} β-spectrum with a single β-counter or by the β-γ coincidence method. In both cases the β-spectra were absolutely identical. On a straightened plot of this β-spectrum (fig. 12) the experimental points were found to lie on a straight line, starting from energies $\approx$ 0.1 MeV.

7. Partial β-Spectra

The source used in the β-spectrum investigations was a disk 8 mm in diameter cut from a metallic zirconium foil of 24 mg/cm^2 surface density. The straightened $Zr^{97}+Nb^{97}$ spectrum measured with our spectrometer containing a single β-counter is represented in fig. 13, curve 1. The shape of the spectrum is very similar to that obtained in ref. [1]). The β-spectra with upper limits 1.91 and 1.27 MeV belong respectively to Zr^{97} and Nb^{97}. The present type of experiments in which a thick source was utilized cannot be considered to reliably indicate the existence of a soft β-spectrum with an upper limit 0.48 MeV. To elucidate this point β-γ coincidence

measurements were carried out with the arrangement described in section 6. Two sets of measurements were performed with an integral discriminator output. In one case the discriminator

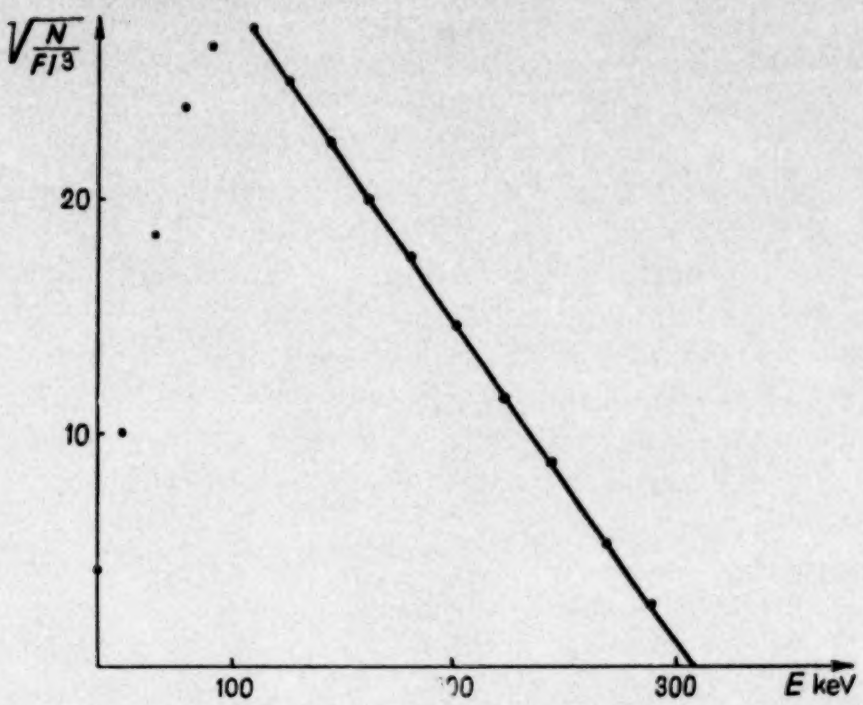

Fig. 12. Straightened plot of coincidence β-spectrum for Co^{60}.

threshold was adjusted so as to record coincidence with γ-quanta possessing $E_\gamma > 1$ MeV and in a second case the threshold was reduced to 0.8 MeV in order to increase the γ-counting efficiency. The β-γ coincidence rate was measured at various currents in the β-spectrometer. The results of these measurements are shown in the same fig. 13, curve 2 as a straightened spectrum plot. As can be seen from both plots a partial β-spectrum with an upper limit of 0.45 MeV could be isolated in both sets of measurements. Beyond the limits of the β-spectrum the counting rate was due to random coincidences.

The random coincidence rate at each point was checked by measuring the rate in the β and γ-channels and, in some cases, by introducing an auxiliary delay in the β-channel. For points lying in the soft region of the spectrum the random coincidence rate was about 1 count per hour, the true coincidence rate being about 30. The time decrease of the true coincidence counting rate measured for one of the spectrum points yielded a 17 hour decay period.

The γ-γ coincidence data also indicate that the soft spectrum should also correlate with a softer 0.6—0.8 MeV radiation which is in cascade with the hard γ-radiation. To check this possibility

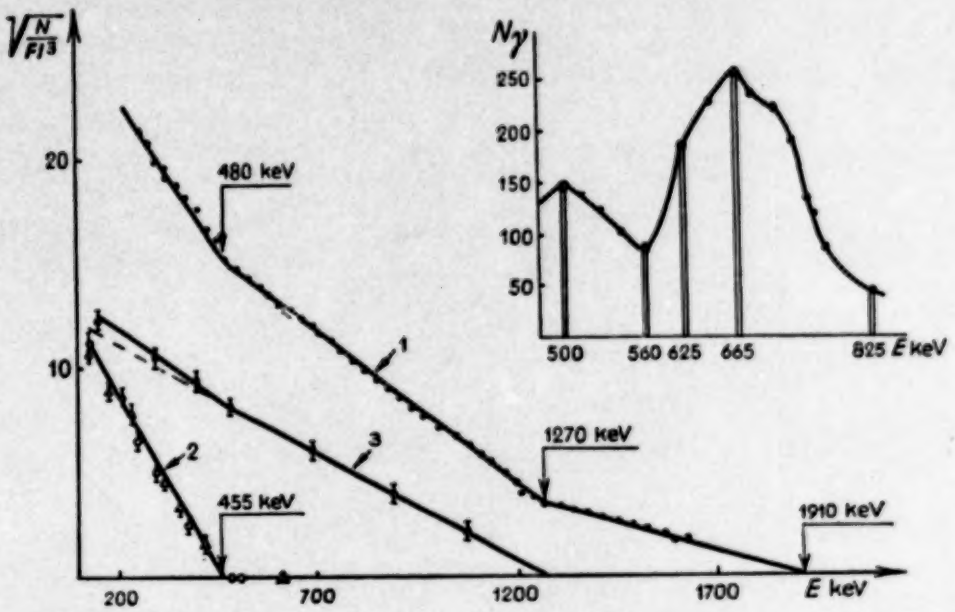

Fig. 13. Straightened plot of $Zr^{97}+Nb^{97}$ β-spectra 1) Measured with β-single-counter β-spectrometer.
2) Coincidence β-spectrum for $E_\gamma > 1$ MeV (○) and $E_\gamma > 0.8$ MeV (△).
3) Coincidence β-spectrum. Discriminator window set at maximum of photopeak ($E_\gamma = 0.665$ MeV).

β-γ coincidence measurements were carried out with a differential discriminator output possessing a window width of 2 V set at 5 various points in the γ-spectrum, from 0.5 to 0.82 MeV. The positions of the discriminator window are shown in the upper right hand corner in fig. 13. The results of this type of measurements for a window position corresponding to the peak of the 0.665 MeV photoelectron line are presented as a straightened β-spectrum plot in fig. 13, curve 3. The soft Zr^{97} β-spectrum and the Nb^{97} β-spectrum which correlates with the accompanying 0.66 MeV γ-rays are shown in the graph. If the soft β-spectrum were not in coincidence with γ-rays in the energy range under consideration (0.5—0.8 MeV) the ratio between the intensity of the soft β-spectrum and the intensity of the second β-spectrum would remain constant within the experimental errors. However, when the discriminator window was set in the vicinity of the photoelectron line the relative intensity of the soft β-spectrum was found to increase by several

times. This signifies that the soft β-spectrum yields coincidences with γ-rays lying in the vicinity of the intense Zr^{97} and Nb^{97} γ-lines.

8. Decay Scheme

A possible decay scheme for Zr^{97} and Nb^{97}, including the low intensity transitions, is depicted in fig. 14. This scheme contains

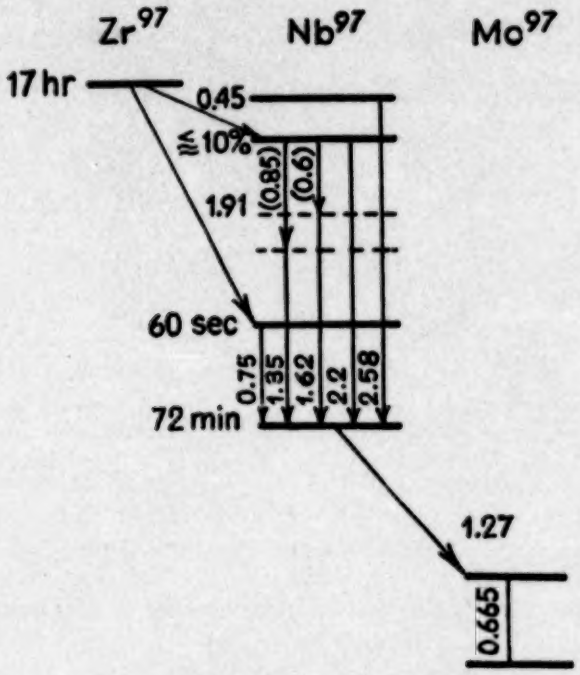

Fig. 14. Zr^{97} and Nb^{97} decay scheme.

some new levels for Nb^{97}. Proceeding from the value for the Zr^{97} decay energy, which is $1.91+0.75 = 2.66$ MeV, one obtains that the 0.45 MeV partial β-transition should excite a state with an energy of 2.2 MeV. Gamma rays of 1—2 % intensity and an energy which corresponds to a direct transition from this level to the ground state confirm the existence of this level. The discovery of cascade γ-radiation with a total cascade energy close to 2.2 MeV which yields coincidence with electrons of a soft spectrum indicates that the 2.2 MeV level can also be de-excited in cascade via an intermediate level. The position of this level cannot be exactly indicated in the scheme since the order of emission of the cascade γ-quanta is unknown.

The results of γ-γ coincidence measurements which indicate the existence in the 0.6—0.8 MeV energy range of two γ-quanta in coincidence with hard γ-rays and also the 1.62 and 1.35 MeV γ-

quanta detected with the scintillation spectrometer render probable the existence of two cascades.

The existence of the 2.58 MeV level was assumed by us only on basis of observation of γ-quanta emitted with this energy. However, we have not been able to detect in our experiments a corresponding β-transition to this level.

The authors are indebted to the students of the Physical Department of the Moscow State University, I. Astakhov and V. Gordeyev, for their help in carrying out the measurements, to G. A. Kuznetsova for the work on chemical separation of Nb^{97} and to A. S. Melioransky for valuable advice on the construction of electronic circuits.

References

1) V. S. Shpinel and G. A. Kuznetsova, JETP, **30** (1956) 231
2) N. N. Delyagin, graduate student investigation, Physics Dept. Moscow State University (1954)
3) P. Bell, R. Graham and H. Petch, Canad. Journ. Phys. **30** (1952) 35
4) H. de Waard, Physica **18** (1952) 1151
5) E. S. Berlovich, Izv. Akad. Nauk SSSR **19** (1955) 343
6) W. Jordan and P. Bell, Rev. Sci. Instr. **18** (1947) 703
7) F. K. McGowan, Phys. Rev. **93** (1954) 163
8) V. S. Shpinel, JETP **22** (1952) 255
9) A. Landby, Rev. Sci. Instr. **22** (1951) 324
10) R. Chase and W. Higginbotham, Rev. Sci. Instr **23** (1952) 34

Nuclear Physics **2** (1956/57) 706—722; *North-Holland Publishing Co., Amsterdam*

A MODEL OF AN UNSTABLE PARTICLE

V. GLASER

Institute Ruđer Bošković, Zagreb

and

G. KÄLLÉN

CERN Theoretical Study Division
at the Institute for Theoretical Physics,
University of Copenhagen

Received 5 September 1956

Abstract: The details of the Lee model are worked out when the mass of the so-called V-particle is larger than the sum of the masses of the N-particle and the θ-particle. In this case the V-particle is unstable and the corresponding eigenstate of the Hamiltonian does not exist. A wave-packet of states with N and θ-particles representing the unstable V-particle is explicitly constructed, and its decay is studied. Throughout this investigation a cut-off is used in the model and the renormalized coupling constant is assumed to be smaller than the corresponding critical value. In this way the complication with "negative probabilities" encountered earlier is avoided.

1. Introduction

The very interesting model of a field theory constructed some time ago by T. D. Lee [1]) has already been the subject of a large number of investigations. It has e.g. been shown that the point source limit of this model is not physically acceptable as an anomalous state appears in this limit and makes the S-matrix non-unitary [2]). Further, the eigenvalue equation of the model turns out to have complex roots in this limit [3]), a result which again emphasizes the pathological features of the point source case. In all investigations up to now it was assumed that the mass of the so-called V-particle in the model is either equal to the mass of the N-particle or at least so small that the decay process

$$\mathrm{V} \rightarrow \mathrm{N}+\theta \qquad (1)$$

is energetically forbidden. In the discussion below we are going to make this reaction energetically allowed and study the mathematical details of the resulting theory. This seems to us to be of some interest as it is the only case known to us where a theory with an unstable particle can be solved exactly. Especially we

want to study the behaviour of the particular state that corresponds to the V-particle. Below the threshold of (1) this state is an eigenstate of the Hamiltonian, but above the threshold this is not the case any more.

2. Basic Concepts of the Model

The Lee model contains three kinds of particles conventionally called V-particles, N-particles, and θ-particles. The model is defined by the following unrenormalized Hamiltonian †

$$H = H_0 + H_{\text{int}}, \tag{2}$$

$$H_0 = m_V \sum_{\vec{p}} \psi_V^*(\vec{p})\psi_V(\vec{p}) + m_N \sum_{\vec{p}} \psi_N^*(\vec{p})\psi_N(\vec{p}) + \sum_{\vec{k}} \omega(\vec{k}) a^*(\vec{k}) a(\vec{k});\ \omega(\vec{k}) = \sqrt{\vec{k}^2+\mu^2}, \tag{3}$$

$$H_{\text{int}} = -\frac{g_0}{\sqrt{V}} \sum_{\vec{p}=\vec{p}'+\vec{k}} \frac{f(\omega)}{\sqrt{2\omega}} \{\psi_V^*(\vec{p})\psi_N(\vec{p}')a(\vec{k}) + \psi_V(\vec{p})\psi_N^*(\vec{p}')a^*(\vec{k})\} \tag{4}$$

together with the commutation relations

$$[a(\vec{k}),\ a^*(\vec{k}')] = \delta_{\vec{k},\vec{k}'}, \tag{5a}$$

$$\{\psi_V(\vec{p}),\ \psi_V^*(\vec{p}')\} = \{\psi_N(\vec{p}),\ \psi_N^*(\vec{p}')\} = \delta_{\vec{p},\vec{p}'}. \tag{5b}$$

All other commutators between two θ-particle operators, between one θ-particle operator and one N or V-particle operator, or anticommutators between N or V-particle operators themselves vanish. As it is not to be expected that the unitary properties of the S-matrix will be influenced by the threshold (1), we are not particularly interested in the point source limit of the model. We therefore keep the cut-off function $f(\omega)$ in the calculation and assume that the renormalized coupling constant g is always smaller than the critical value g_{crit} [2]). All quantities appearing in the formalism are then well-defined, and there is no point in trying to express everything in terms of renormalized quantities only. We shall therefore use the unrenormalized fields, masses, and coupling constant in all calculations and only introduce the corresponding renormalized quantities in the final result. This is only a question of convenience and of no fundamental importance.

In the formulae (2)—(5) all field quantities are supposed to be enclosed in a finite box of volume V. This well-known but somewhat unphysical device is introduced to make the eigenvalue problem

† Except for the symbols m_V and m_N the notation is the same as in ref. [2]) We refer to that paper for a detailed explanation of all the symbols.

of the theory mathematically well-defined. In the following we shall ultimately be interested in the limit $V \to \infty$ and shall also discuss some of the mathematical details in connection with this limit.

For a finite value of V we can write all the eigenstates of the Hamiltonian in the special subspace spanned by the free particle states $|1_V, 0, 0\rangle$ and $|0, 1_N, 1_k\rangle$† in the following form

$$H|n\rangle = E_n|n\rangle, \tag{6a}$$

$$|n\rangle = \frac{1}{\sqrt{1+F'(E_n-m_N)}} \left[|1_V, 0, 0\rangle + \frac{g_0}{\sqrt{2V}} \sum_k \frac{f(\omega)}{\sqrt{\omega(m+\omega-E_n)}} |0,1_N, 1_k\rangle\right], \tag{6b}$$

$$F(x) = \frac{g_0^2}{2V} \sum_k \frac{f^2(\omega)}{\omega(\omega-x)}\,; \quad F'(x) = \frac{dF(x)}{dx}, \tag{6c}$$

$$m_V - E_n = F(E_n - m_N). \tag{6d}$$

The corresponding eigenvalues are the roots of eq. (6d) where the function $F(x)$ is defined in (6c). †† Eqs. (6), the derivation of which

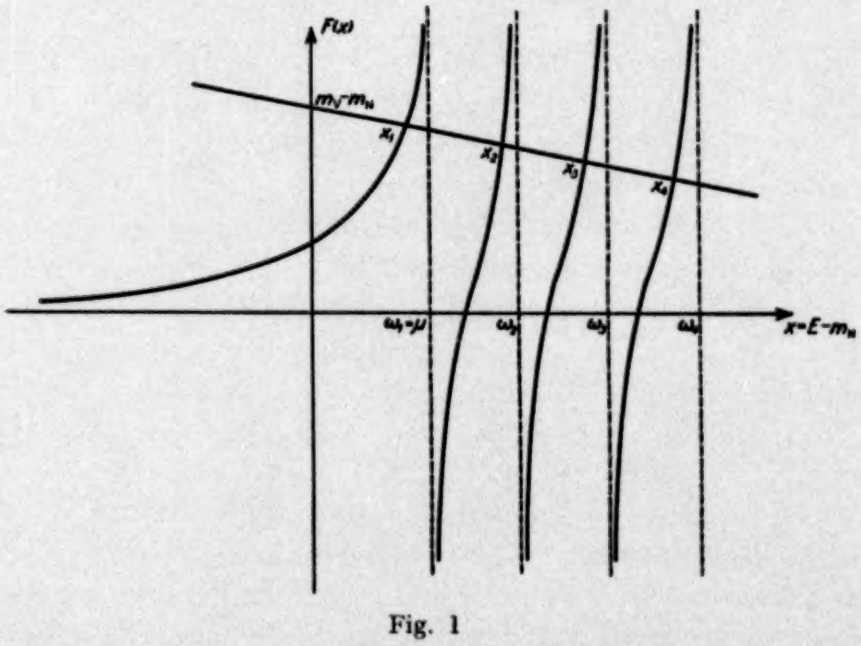

Fig. 1

† We refer again to ref. [2]) for an explanation of the notation.

†† This function is closely connected with $h(x)$ in eq. (36) in ref. [2]). The exact relation is

$$[1+F'(0)]h(x) = F(x) - F(0) + x.$$

The function $h(x)$ exists in the point source limit, but $F(x)$ does not. Cf. also eqs. (19) and (34.a) below.

is straight-forward, are quite general and no assumption is made so far about the magnitude of the masses. The quantity deciding whether or not the reaction (1) is energetically allowed is not the bare V-particle mass m_V appearing explicitly above but rather the mass of the physical V-particle corresponding to a root of eq. (6d). The positions of these roots are illustrated in fig. 1. We see from this diagram that however large the bare mass m_V is made there is always one root of the eigenvalue equation below the θ-particle mass μ.

It is therefore tempting to argue that the mass of the physical V-particle is always below the threshold of reaction (1) and that the model is not able to describe an unstable V-particle. However, this conclusion is incorrect. The mistake lies in the assumption implicitly made that the lowest root really corresponds to a state with a stable V-particle. That this is a non-trivial problem is immediately clear if we try to perform the limit $V \to \infty$. Below the point $x = \mu$ the function $F(x)$ goes over into the integral

$$\phi(x) = \gamma_0 \int_\mu^\infty \frac{f^2(\omega) k \, d\omega}{\omega - x}; \qquad \gamma_0 = \frac{g_0^2}{4\pi^2}, \tag{7}$$

but above this point the function does not tend to any well-defined

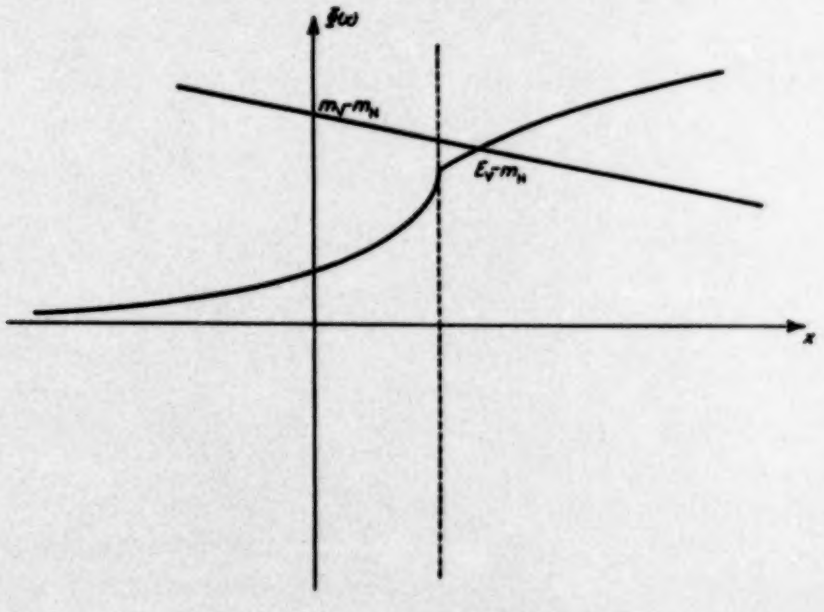

Fig. 2.

limit. However, it is natural to continue the function $\phi(x)$ above the point $x = \mu$ with the aid of the principal value of the integral

in (7). The resulting function is continuous at $x = \mu$ and has a certain value $\phi(\mu)$ there. The qualitative behaviour is shown in fig. 2. We now see that if m_V fulfils the inequality

$$m_V - m_N > \phi(\mu) + \mu \tag{8}$$

there is no root of the equation

$$m_V - E = \phi(E - m_N) \tag{9}$$

below the point $x = \mu$. On the other hand there is one root above this pount and the guess that this root corresponds to an unstable V-particle is very plausible. The argument here is hardly convincing as there is no immediate reason why this continuation of the function $\phi(x)$ should have anything to do with the eigenvalue problem of the theory. Nevertheless, this guess is correct and the rest of this paper is mainly concerned with a proof of that statement.

3. The Case of the Unstable V-Particle

As can be seen from an elementary argument all the roots of the eigenvalue equation (6d) are real. This is also an immediate consequence of the hermitian properties of the Hamiltonian. We now want to show that if the inequality (8) is fulfilled, it is possible to construct an approximate eigenstate of the Hamiltonian with an "eigenvalue" that is equal to the root of eq. (9). For this purpose we start from eq. (6b) and make the following "Ansatz":

$$|z\rangle = c\left[|1_V,\ 0,\ 0\rangle + \frac{g_0}{\sqrt{2V}} \sum_k \frac{f(\omega)}{\sqrt{\omega(m_N\omega - E - i\lambda)}} |0,\ 1_N,\ 1_k\rangle\right]. \tag{10}$$

The corresponding eigenvalue equation is

$$m_V - E - i\lambda = F(E + i\lambda - m_N). \tag{11}$$

Due to the complex value of the argument in the function $F(x)$ the limit $V \to \infty$ can be performed and yields

$$m_V - E - i\lambda = \phi(E + i\lambda - m_N). \tag{12}$$

If λ is small, the real part of this equation coincides with (9) and the root E_V appears in this way as an approximate eigenvalue. The imaginary part of (12) gives under the same assumption

$$-\lambda = \tfrac{1}{2}\Gamma_0(E_V - m_N)\frac{\lambda}{|\lambda|} + \lambda\phi'(E_V - m_V), \tag{13}$$

$$\Gamma_0(\omega) = 2\pi\gamma_0 f^2(\omega)\sqrt{\omega^2 - \mu^2}\,\theta(\omega - \mu). \tag{13a}$$

Eq. (13) can be "solved" and yields

$$|\lambda| = -\frac{1}{2}\frac{\Gamma_0(E_V - m_N)}{1+\phi'(E_V - m_N)}, \tag{14}$$

a result which can never be satisfied due to the minus sign on the right-hand side: This was only to be expected as a solution to this equation would have meant an exact eigenstate with a complex eigenvalue. The important point is rather that the quantity $\Gamma_0(E_V - m_N)$ is a measure of the deviation of the state (10) from an exact eigenstate of the Hamiltonian. If this quantity and λ both are small, we therefore have an "approximate eigenstate". The exact meaning of this statement is discussed in the next paragraph.

It is now reasonable to ask: How do the exact eigenstates of the Hamiltonian look in the case studied here and if the limit $V \to \infty$ is performed? A straight-forward calculation yields the following expression for the states describing the scattering of a θ-particle by a N-particle.

$$|N, \theta\rangle = |0, 1_N, 1_k\rangle + \sum_{\bar{k}'} \alpha(\bar{k}, \bar{k}')|0, 1_{N'}, 1_{k'}\rangle + \beta(\bar{k})|1_V, 0, 0\rangle, \tag{15}$$

$$\alpha(\bar{k}, \bar{k}') = \frac{g_0 f(\omega')}{\sqrt{2V\omega'}}\frac{\beta(\bar{k})}{\omega' - \omega - i\varepsilon}, \tag{16}$$

$$\beta(\bar{k}) = \frac{g_0 f(\omega)}{\sqrt{2V\omega}}\frac{1}{-m_N + m_V - \omega - \phi(\omega + i\varepsilon)}. \tag{17}$$

The only remaining question is then whether or not the states (15) form a complete set or if there are other eigenstates of the Hamiltonian in this subspace of the Hilbert space. To decide this point we compute the quantity $\sum_{\bar{k}} |N, \theta\rangle\langle\theta, N|$ and obtain

$$\begin{aligned}\sum_{\bar{k}} |N, \theta\rangle\langle\theta, N| &= \sum_{\bar{k}} |0, 1_N, 1_k\rangle\langle 1_k, 1_N, 0| + |1_V, 0, 0\rangle\langle 0, 0, 1_V| \sum_{\bar{k}} |\beta(\bar{k})|^2 \\ &+ |1_V, 0, 0\rangle \sum_{\bar{k}} A(\bar{k})\langle 1_k, 1_N, 0| + \sum_{\bar{k}} |0, 1_N, 1_k\rangle A^*(\bar{k})\langle 0, 0, 1_V| \\ &+ \sum_{\bar{k}, \bar{k}'} |0, 1_N, 1_k\rangle B(\bar{k}, \bar{k}')\langle 1_{k'}, 1_{N'}, 0|,\end{aligned} \tag{18}$$

with

$$A(\bar{k}) = \beta(\bar{k}) + \sum_{\bar{k}'} \beta(\bar{k}')\alpha^*(\bar{k}', \bar{k}) \tag{18a}$$

and

$$B(\bar{k}, \bar{k}') = \alpha(\bar{k}', \bar{k}) + \alpha^*(\bar{k}, \bar{k}') + \sum_{\bar{k}''} \alpha(\bar{k}'', \bar{k}')\alpha^*(\bar{k}'', \bar{k}'). \tag{18b}$$

The sums appearing in (18)—(18b) can be computed exactly with the aid of complex contour integration. Introducing a function $h_0(z)$ with the aid of

$$h_0(z) = z+\phi(z)-m_V+m_N = z+\phi(z)-\omega_0-\phi(\omega_0), \tag{19}$$

$$\omega_0 = E_V-m_N, \tag{19a}$$

we get e.g.

$$\sum|\beta(\bar{k})|^2 = \frac{g_0^2}{2V}\sum_{\bar{k}}\frac{f^2(\omega)}{\omega[h_0^2(\omega)+\frac{1}{4}\Gamma_0^2(\omega)]} = \frac{1}{2\pi}\int_\mu^\infty \frac{\Gamma_0(\omega)\mathrm{d}\omega}{h_0^2(\omega)+\frac{1}{4}\Gamma_0^2(\omega)}$$

$$= \frac{-1}{2\pi i}\int_C \frac{\mathrm{d}z}{h_0(z)}. \tag{20}$$

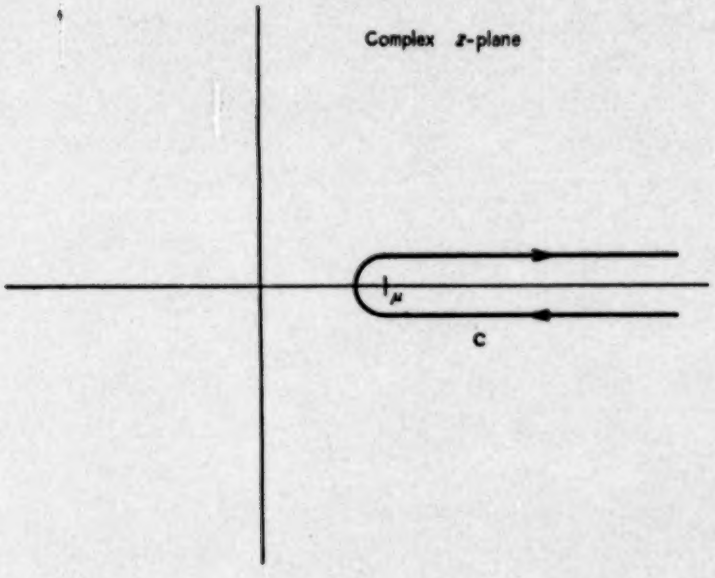

Fig. 3.

The contour C is illustrated in fig. 3 †. If the contour integration in (20) is closed with the aid of a very large circle, the integral over the closed contour is zero due to the absence of all singularities of $h(z)$ inside the contour. The integral over the circle is equal to 1, and we get

$$\sum_{\bar{k}}|\beta(\bar{k})|^2 = \frac{-1}{2\pi i}\int_C \frac{\mathrm{d}z}{h_0(z)} = 1. \tag{21}$$

In a similar way we obtain

† Cf. also appendix I of ref. [2])

$$\sum_{\bar{k}'}\beta(\bar{k}')\alpha^*(\bar{k}',\bar{k})=\frac{g_0 f(\omega)}{\sqrt{2V\omega}}\sum_{\bar{k}'}\frac{|\beta(\bar{k}')|^2}{\omega-\omega'+i\varepsilon}=\frac{g_0 f(\omega)}{\sqrt{2V\omega}}\frac{1}{2\pi i}\int_C \frac{dz}{h_0(z)}\frac{1}{z-\omega-i\varepsilon}$$

$$=\frac{g_0 f(\omega)}{\sqrt{2V\omega}}\frac{1}{h_0(\omega+i\varepsilon)}=-\beta(\bar{k}), \tag{22}$$

$$\sum_{\bar{k}'}\alpha(\bar{k}'',\bar{k}')\alpha^*(\bar{k}'',\bar{k}')=\frac{g_0^2}{2V}\frac{f(\omega)f(\omega')}{\sqrt{\omega\omega'}}\sum_{\bar{k}''}\frac{|\beta(\bar{k}'')^2}{(\omega-\omega''-i\varepsilon)(\omega'-\omega''+i\varepsilon)}$$

$$=\frac{g_0^2}{2V}\frac{f(\omega)f(\omega')}{\sqrt{\omega\omega'}}\frac{1}{2\pi i}\int_C \frac{dz}{h_0(z)}\frac{1}{(z-\omega+i\varepsilon)(z-\omega'-i\varepsilon)} \tag{22}$$

$$=\frac{g_0^2}{2V}\frac{f(\omega)f(\omega')}{\sqrt{\omega\omega'}}\left[\frac{1}{h_0(\omega-i\varepsilon)}\frac{1}{\omega-\omega'-2i\varepsilon}+\frac{1}{h_0(\omega'+i\varepsilon)}\frac{1}{\omega'-\omega+2i\varepsilon}\right]$$

$$=-\alpha(\bar{k}',\bar{k})-\alpha^*(\bar{k},\bar{k}').$$

Using (21)—(23) we can simplify (18) to

$$\sum_{\bar{k}}|\mathrm{N},0\rangle\langle 0,\mathrm{N}|=\sum_{\bar{k}}|0,1_N,1_k\rangle\langle 1_k,1_N,0|+|1_V,0,0\rangle\langle 0,0,1_V|, \tag{24}$$

which obviously is an expression for the completeness of the states (15). We therefore have the important result that *if the inequality* (8) *is fulfilled, the scattering states* $|\mathrm{N},0\rangle$ *form a complete set.* It therefore appears that the root below the point $x=\mu$ in fig. 1 also goes over into a scattering state (15) in the limit $V\to\infty$. The mathematical details in connection with this limit are discussed in the appendix.

4. The Lifetime of the Unstable V-Particle

This paragraph is devoted to a discussion of the statement made previously that if $\Gamma_0(\omega_0)$ and λ are small, the state (10) is an approximate eigenstate of the Hamiltonian. For this purpose we want to study the behaviour as a function of time of a state that at $t=0$ has the form (10). As the scattering states (15) form a complete set, we can write

$$|1_V,0,0\rangle=\sum|\mathrm{N},0\rangle\langle 0,\mathrm{N}|1_V,0,0\rangle=\sum_{\bar{k}}|\mathrm{N},0\rangle\beta^*(\bar{k}), \tag{25}$$

$$|0,1_N,1_k\rangle=\sum_{\bar{k}'}|\mathrm{N}_1\theta'\rangle[\delta_{\bar{k},\bar{k}'}+\alpha^*(\bar{k}',\bar{k})] \tag{26}$$

and hence

$$
\begin{aligned}
|z\rangle &= C\sum_{\bar{k}}|\mathrm{N},\theta\rangle\{\beta^*(\bar{k})+\frac{g_0}{\sqrt{2V}}\sum_{\bar{k}'}\frac{f(\omega')}{\sqrt{\omega'}}\,\frac{1}{\omega'-\omega_0-i\lambda}\,[\delta_{\bar{k},\bar{k}'}+\alpha^*(\bar{k},\bar{k}')]\}\\
&= C\,\frac{g_0}{\sqrt{2V}}\sum_{\bar{k}}|\mathrm{N},\theta\rangle\frac{f(\omega)}{\sqrt{\omega}}\Bigg[\frac{-1}{h_0(\omega-i\varepsilon)}+\frac{1}{\omega-\omega_0-i\lambda}\\
&\quad-\frac{1}{h_0(\omega-i\varepsilon)}\,\frac{1}{2\pi}\int_\mu^\infty\frac{\Gamma_0(\omega')\mathrm{d}\omega'}{(\omega'-\omega_0-i\lambda)(\omega'-\omega+i\varepsilon)}\Bigg] \qquad (27)\\
&= C\,\frac{g_0}{\sqrt{2V}}\sum_{\bar{k}}|\mathrm{N},\theta\rangle\frac{f(\omega)}{\sqrt{\omega}}\left[\frac{-1}{h_0(\omega-i\varepsilon)}+\frac{1}{\omega-\omega_0-i\lambda}-\frac{\phi(\omega-i\varepsilon)-\phi(\omega_0+i\lambda)}{(\omega-\omega_0-i\lambda)\,h_0(\omega-i\varepsilon)}\right]\\
&= C\,\frac{g_0}{\sqrt{2V}}\sum_{\bar{k}}|\mathrm{N},\theta\rangle\frac{f(\omega)}{\sqrt{\omega}}\,\frac{i\left(\lambda+\dfrac{\lambda}{|\lambda|}\,\dfrac{\Gamma(\omega_0)}{2}\right)(1+\phi'(\omega_0))}{h_0(\omega-i\varepsilon)(\omega-\omega_0-i\lambda)},
\end{aligned}
$$

with

$$
\Gamma(\omega)=\frac{\Gamma_0(\omega)}{1+\phi'(\omega_0)}. \qquad (27a)
$$

The wave-packet (27) represents the approximate eigenstate (10) written as a sum over physical scattering states. The constant C is easily determined from the normalization of the state (27)

$$
\begin{aligned}
C^{-2} &= \frac{g_0^2}{2V}\sum_{\bar{k}}\frac{f^2(\omega)}{\omega}\,\frac{\left[\lambda+\dfrac{1}{2}\,\dfrac{\lambda}{|\lambda|}\,\Gamma\right]^2(1+\phi')^2}{[h_0^2(\omega)+\frac{1}{4}\Gamma_0^2(\omega)]\,[(\omega-\omega_0)^2+\lambda^2]}\\
&= \left(\lambda+\frac{1}{2}\,\frac{\lambda}{|\lambda|}\,\Gamma\right)^2(1+\phi')^2\left(-\frac{1}{2\pi i}\right)\int_C\frac{\mathrm{d}z}{h_0(z)[(z-\omega_0)^2+\lambda^2]} \qquad (28)\\
&= \frac{1}{2i\lambda}\,(1+\phi'(\omega_0))^2\left[\lambda+\frac{1}{2}\,\frac{\lambda}{|\lambda|}\,\Gamma(\omega_0)\right]^2\left[\frac{1}{h_0(\omega_0-i\lambda)}-\frac{1}{h_0(\omega_0+i\lambda)}\right]\\
&= (1+\phi'(\omega_0))\left[1+\frac{1}{2}\,\frac{\Gamma(\omega_0)}{|\lambda|}\right],
\end{aligned}
$$

At a later time t we thus have

$$
|z,t\rangle = C\,\frac{g_0}{\sqrt{2V}}\sum_{\bar{k}}\frac{f(\omega)}{\sqrt{\omega}}\,\mathrm{e}^{-i(m_\mathrm{N}+\omega)t}|\mathrm{N},\theta\rangle\,\frac{i\left(\lambda+\dfrac{1}{2}\,\dfrac{\lambda}{|\lambda|}\,\Gamma(\omega_0)\right)(1+\phi'(\omega_0))}{h_0(\omega-i\varepsilon)(\omega-\omega_0-i\lambda)}. \qquad (29)
$$

A convenient measure of the change of the state $|z\rangle$ is the inner product

$$\langle z|z,t\rangle = C^2\lambda^2\left(1+\frac{\Gamma(\omega_0)}{2|\lambda|}\right)^2(1+\phi'(\omega_0))^2\frac{1}{2\pi}\int_\mu^\infty \frac{\Gamma_0(\omega)e^{-i(m_N+\omega)t}\,d\omega}{[h_0^2(\omega)+\frac{1}{4}\Gamma_0^2(\omega)][(\omega-\omega_0)^2+\lambda^2]}$$

$$= \left(1+\frac{\Gamma(\omega_0)}{2|\lambda|}\right)(1+\phi'(\omega_0))^2\frac{1}{2\pi}\int_\mu^\infty \frac{\Gamma(\omega)e^{-i(m_N+\omega)t}\,d\omega}{h_0^2(\omega)+\frac{1}{4}\Gamma_0^2(\omega)}\,\frac{\lambda^2}{(\omega-\omega_0)^2+\lambda^2} \qquad (30)$$

The integral in (30) cannot be evaluated with the aid of the previous technique as the exponential factor is very large on some parts of the circle closing the contour C in fig. 3. We therefore estimate the integral by observing that its main contribution comes from the neighbourhood of the point $\omega = \omega_0$. We therefore replace $h_0(\omega)$ by $(1+\phi'(\omega_0))(\omega-\omega_0)$ and extend the integral from $-\infty$ to $+\infty$. In this way we get

$$\langle z|z,t\rangle \approx \left(1+\frac{\Gamma(\omega_0)}{2|\lambda|}\right)\Gamma(\omega_0)e^{-iE_V t}\int_{-\infty}^{+\infty}\frac{dx e^{-ixt}\lambda^2}{[x^2+\frac{1}{4}\Gamma^2(\omega_0)](x^2+\lambda^2)}$$

$$= \frac{e^{-iE_V t}}{1-\dfrac{\Gamma(\omega_0)}{2|\lambda|}}\left[e^{-\frac{1}{2}\Gamma(\omega_0)t} - \frac{\Gamma(\omega_0)}{2|\lambda|}e^{-|\lambda|t}\right]. \qquad (31)$$

If we had built up a wave-packet of the form (10) around an arbitrary energy E' not satisfying (9), the life time of the packet would have been determined by the quantity λ. By making $|\lambda|$ very large the life time could have been made very small. Around the special energy E_V this is no longer possible. If $|\lambda| \gg \frac{1}{2}\Gamma(\omega_0)$ we find from (31)

$$|\langle z|z,t\rangle|^2 \approx e^{-\Gamma(\omega_0)t}. \qquad (32)$$

Quite independently of $|\lambda|$ the special state (10) therefore has a life time $1/\Gamma(\omega_0)$. This is the exact meaning of the statement that (10) is an approximate eigenstate of the theory. At the same time we find that the imaginary "deficit" in the eigenvalue equation (12) corresponds to the inverse of the life time of the state. The only diffrence between (13a) and the inverse life time is the factor $1+\phi'(\omega_0)$ in (27a). This factor can be understood as changing the coupling constant from its unrenormalized value g_0 to its renormalized value g determined from

$$\frac{\gamma_0}{\gamma} = \frac{g_0^2}{g^2} = 1+\phi'(\omega_0) = 1+\gamma_0\frac{\partial}{\partial\omega_0}P\int_\mu^\infty \frac{f^2(\omega)k\,d\omega}{\omega-\omega_0}. \qquad (33)$$

Eq. (32) is completely analogous to the renormalization of the coupling constant when the reaction (1) is energetically forbidden †.

† Ref. [2]), eqs. (16) and (33).

If the time t is much larger than the life time, the phases in the wave-packet (29) can be considered as random. In that case the only convenient description of the state is as a sum of independent states $|\mathrm{N}, \theta>$. We then obtain the decay spectrum of the unstable V-particle as

$$W(\omega)\mathrm{d}\omega = C^2 \frac{\Gamma_0(\omega)}{2\pi} \frac{(1+\phi'(\omega_0))^2 \lambda^2 \left(1+\dfrac{\Gamma(\omega_0)}{2|\lambda|}\right)^2}{[h_0^2(\omega)+\frac{1}{4}\Gamma_0^2(\omega)][(\omega-\omega_0)^2+\lambda^2]} \mathrm{d}\omega$$
$$= \frac{\lambda^2 \left(1+\dfrac{\Gamma(\omega_0)}{2|\lambda|}\right)}{(\omega-\omega_0)^2+\lambda^2} \frac{1}{2\pi} \frac{\Gamma(\omega)}{h^2(\omega)+\frac{1}{4}\Gamma^2(\omega)}, \tag{34}$$

$$h(\omega) = \frac{h_0(\omega)}{1+\phi'(\omega_0)}. \tag{34a}$$

For large values of $|\lambda|$ this simplifies to

$$W(\omega)\mathrm{d}\omega = \frac{1}{2\pi} \frac{\Gamma(\omega)\mathrm{d}\omega}{h^2(\omega)+\frac{1}{4}\Gamma^2(\omega)} \approx \frac{1}{2\pi} \frac{\Gamma(\omega_0)\mathrm{d}\omega}{(\omega-\omega_0)^2+\frac{1}{4}\Gamma^2(\omega_0)}, \tag{35}$$

which is exactly the expected line shape of the decay products from an unstable particle.

For completeness we also want to mention that the cross-section for the scattering of a θ-particle by an N-particle has a resonance at the energy ω_0 with a width determined by $\Gamma(\omega_0)$. This follows directly from the formulae (15)—(17) and is in complete accordance with what one would expect.

5. Anomalous States

Although we have not been particularly interested in the question of anomalous states with negative probabilities [2]) in this investigation, we want to show in this paragraph that the limit $f(\omega) \to 1$ cannot be taken in our case either without anomalous states of this kind appearing. To show this we rewrite the definition (33) as

$$\frac{\gamma}{\gamma_0} = 1-\gamma \frac{\partial}{\partial\omega_0} \mathrm{P}\int_\mu^\infty \frac{f^2(\omega)k\mathrm{d}\omega}{\omega-\omega_0}$$
$$= 1-\gamma\int_\mu^\infty \frac{f^2(\omega)k\mathrm{d}\omega}{\omega^2} - \gamma \frac{\partial}{\partial\omega_0}\left[\omega_0^2 \mathrm{P}\int_\mu^\infty \frac{f^2(\omega)k\mathrm{d}\omega}{\omega^2(\omega-\omega_0)}\right]. \tag{36}$$

The last integral stays finite in the limit while the first one diverges logarithmically. The (absolute) square (36) therefore becomes

negative if γ is larger than a certain critical value γ_{crit}, which is an indication of the appearance of a state with negative norm in the model. We shall not repeat the details here as they are completely analogous to the calculation in ref. [2]). In passing, we might remark that the critical value of the coupling constant is a function of the energy ω_0 and makes a jump when the threshold $\omega_0 = \mu$ is passed. When the threshold is approached from below, the critical coupling constant tends to zero, while it has a finite limit when the threshold is approached from above. Further, in the rather uninteresting case that the energy ω_0 is of the same order of magnitude as the cut-off energy, the derivative of the principal value of the integral in (36) might be negative. In that case, the square of the ratio of the coupling constants is always positive and larger than one. This would seem to violate the general theorem that the renormalized coupling constant is always smaller than the unrenormalized one. However, the general proof is based on the assumption that a stable one-particle state exists, and when that is not the case, no conclusion about the magnitude of the coupling constant renormalization factor can be drawn. The only property that must not be violated is its positive definiteness.

Appendix

In the discussion above we have made use of eigenstates belonging both to the continuous spectrum obtained in the limit $V \to \infty$ and the pseudocontinuous spectrum obtained for a finite value of V. In this appendix we want to discuss the connection between these two kinds of states and show that in spite of the rather different appearance of the states (6) and (15) they are nevertheless intimately connected. However, it is immediately clear that (15) cannot simply be considered as the limit of (6) as there can be no very simple relation between the standing waves in (6) and the incoming and outgoing waves in (15). To see the connection that really exists we have to build up wave-packets of the standing waves (6) and study their behaviour as a function of time. If we can show that such a wave-packet behaves approximately as a wave-packet built up of the continuum states (15) we have demonstrated the equivalence of the two kinds of solution. Although the considerations given here are certainly implicit in many papers, no detailed published discussion of this kind is known to us.

To study the behaviour of a general wave-packet we want to

investigate the time development of a state that for $t = 0$ is given by

$$|\psi(0)\rangle = \sum_{\bar{k}} a^{(0)}(\bar{k})\,|0,\ 1_N,\ 1_k\rangle + b^{(0)}\,|1_V,\ 0,\ 0\rangle. \tag{A.1}$$

At a later time t the packet is of the form

$$|\psi(t)\rangle = \sum_{\bar{k}} a(\bar{k}, t)\,|0,\ 1_N,\ 1_k\rangle + b(t)\,|1_V,\ 0,\ 0\rangle, \tag{A.2}$$

where the new coefficients are determined with the aid of the differential equation

$$H\,|\psi(t)\rangle = i\frac{\partial\,|\psi(t)\rangle}{\partial t}, \tag{A.3}$$

or

$$i\frac{\partial a(\bar{k}, t)}{\partial t} = (m_N+\omega)a(\bar{k}, t) - \frac{g_0 f(\omega)}{\sqrt{2V\omega}}\,b(t), \tag{A.4a}$$

$$i\frac{\partial b(t)}{\partial t} = m_V b(t) - \frac{g_0}{\sqrt{2V}}\sum_{\bar{k}}\frac{f(\omega)}{\sqrt{\omega}}\,a(\bar{k}, t). \tag{A.4b}$$

The solution of these equations can conveniently be expressed as complex integrals. For this purpose we introduce † the Laplace transforms of the functions $a(\bar{k}, t)$ and $b(t)$

$$a(\bar{k}, E) = \int_0^\infty \mathrm{e}^{-Et} a(\bar{k}, t)\mathrm{d}t, \tag{A.5a}$$

$$b(E) = \int_0^\infty \mathrm{e}^{-Et} b(t)\mathrm{d}t \tag{A.5b}$$

These integrals define analytic functions of E, regular everywhere in the half plane $\mathrm{Re}\,E > 0$. The Laplace transforms of the derivatives are given by

$$\int_0^\infty \mathrm{e}^{-Et}\frac{\partial a(\bar{k}, t)}{\partial t}\,\mathrm{d}t = \int_0^\infty \mathrm{e}^{-Et} a(\bar{k}, t) + Ea(\bar{k}, E) = Ea(\bar{k}, E) - a^{(0)}(\bar{k}), \tag{A.6a}$$

$$\int_0^\infty \mathrm{e}^{-Et}\frac{\partial b(t)}{\partial t}\,\mathrm{d}t = Eb(E) - b^{(0)}. \tag{A.6b}$$

With the aid of this well-known trick the differential equations (A.4) are transformed into a system of algebraic equations

$$Ea(\bar{k}, E) - a^{(0)}(\bar{k}) = -i(m_N+\omega)a(\bar{k}, E) + \frac{ig_0 f(\omega)}{\sqrt{2V\omega}}\,b(E), \tag{A.7a}$$

† This technique has earlier been used e.g. by W. Heitler and collaborators in connection with the theory of the radiation damping. A summary is given in ref. [4]).

$$Eb(E)-b^{(0)} = -im_{\mathrm{V}}b(E)+\frac{ig_0}{\sqrt{2V}}\sum_{\bar{k}}\frac{f(\omega)}{\sqrt{\omega}}a(\bar{k},E), \quad \text{(A.7b)}$$

with the solution

$$a(\bar{k},E) = \frac{1}{E+i(m_{\mathrm{N}}+\omega)}\left\{a^{(0)}(\bar{k})+\frac{ig_0 f(\omega)}{\sqrt{2V\omega}}\frac{b^{(0)}+G(iE-m_{\mathrm{N}})}{E+i(m_{\mathrm{V}}-F(iE-m_{\mathrm{N}}))}\right\}, \quad \text{(A. 8a)}$$

$$b(E) = \frac{b^{(0)}+G(iE-m_{\mathrm{N}})}{E+i(m_{\mathrm{V}}-F(iE-m_{\mathrm{N}}))}, \quad \text{(A.8b)}$$

$$G(z) = \frac{g_0}{\sqrt{2V}}\sum_{\bar{k}}\frac{f(\omega)}{\sqrt{\omega}}\frac{a^{(0)}(\bar{k})}{\omega-z}. \quad \text{(A.8c)}$$

The function $F(x)$ is defined in eq. (6.c). The well-known inversion formula for the Laplace transformation gives

$$a(\bar{k},t) = \frac{1}{2\pi i}\int_{\varepsilon-i\infty}^{\varepsilon+i\infty}\mathrm{e}^{Et}a(\bar{k},E)\mathrm{d}E = \frac{\mathrm{e}^{\varepsilon t}}{2\pi}\int_{-\infty}^{+\infty}\mathrm{e}^{-ixt}a(\bar{k},\varepsilon-ix)\mathrm{d}x \quad \text{(A.9a)}$$

$$= \frac{\mathrm{e}^{\varepsilon t}}{2\pi i}\int_{-\infty}^{+\infty}\frac{\mathrm{e}^{-ixt}\mathrm{d}x}{m_{\mathrm{N}}+\omega-x-i\varepsilon}\left\{a^{(0)}(\bar{k})+\frac{g_0 f(\omega)}{\sqrt{2V\omega}}\frac{b^{(0)}+G(x+i\varepsilon-m_{\mathrm{N}})}{m_{\mathrm{V}}-x-i\varepsilon-F(x-m_{\mathrm{N}}+i\varepsilon)}\right\},$$

$$b(t) = \frac{\mathrm{e}^{\varepsilon t}}{2\pi i}\int_{-\infty}^{+\infty}\mathrm{e}^{-ixt}\mathrm{d}x\,\frac{b^{(0)}+G(x+i\varepsilon-m_{\mathrm{N}})}{m_{\mathrm{V}}-x-i\varepsilon-F(x-m_{\mathrm{N}}+i\varepsilon)}. \quad \text{(A.9b)}$$

The quantity ε is real, positive, and of arbitrary magnitude. It is not necessarily infinitesimal. The two formulae (A.9) solve the most general initial value problem in the particular subspace of the Hilbert space that we are interested in. They are, in principle, exact. For our purpose they are also convenient in so far as they contain the function $F(x)$ with complex values of the argument and therefore permit the limit $V \to \infty$ to be performed. For this purpose we choose ε large compared with the distance between two poles of $F(x)$ but still so small that the function $\phi(x+i\varepsilon)$ can be replaced by its boundary value on the real axis. For sufficiently large values of V it is always possible † to find such a value of ε. We therefore get approximately

† Actually, one further condition is involved when this approximation is made under the integral sign in (A.9), viz. that the exponential factor must not change appreciably over a distance of the order of magnitude ε. This means that our approximation breaks down when the time t becomes too large. As the value of ε is only limited by the size of V, this is presumably connected with the reflection of the wave-packet at the walls of the box when the time is large enough. We shall not study that effect here.

$$a(\bar{k},t) \approx \frac{1}{2\pi i}\int_{-\infty}^{+\infty} \frac{e^{-ixt}dx}{m_N+\omega-x-i\varepsilon} \left\{a^{(0)}(\bar{k})+\frac{g_0 f(\omega)}{\sqrt{2V\omega}}\frac{b^{(0)}+G(x+i\varepsilon-m_N)}{-h_0(x-m_N)-\frac{1}{2}i\ \Gamma_0(x-m_N)}\right\}, \quad \text{(A.10a)}$$

$$b(t) \approx \frac{1}{2\pi i}\int_{-\infty}^{+\infty} e^{-ixt}dx \frac{b^{(0)}+G(x+i\varepsilon-m_N)}{-h_0(x-m_N)-\frac{1}{2}i\ \Gamma_0(x-m_N)}. \quad \text{(A.10b)}$$

As a preliminary step we specialize these formulae for the case $b^{(0)}=0$, $a^{(0)}(\bar{k})=\delta_{k,\bar{k}_0}$ and get (these $\bar{k}_0$ and ω_0 are *not* related to the ω_0 in (19a))

$$a(\bar{k},t)=\frac{g_0^2}{2V}\frac{f(\omega)f(\omega_0)}{\sqrt{\omega\omega_0}}\frac{-1}{2\pi i}\int_{-\infty}^{+\infty}\frac{e^{-ixt}dx}{m_N+\omega-x-i\varepsilon} \frac{1}{m_N+\omega_0-x-i\varepsilon}\frac{1}{h_0(x-m_N+\frac{1}{2}i\ \Gamma_0(x-m_N)}, \quad \text{(A.11a)}$$

$$b(t)=\frac{g_0 f(\omega_0)}{\sqrt{2V\omega_0}}\frac{-1}{2\pi i}\int_{-\infty}^{+\infty}\frac{e^{-ixt}dx}{m_N+\omega_0-x-i\varepsilon}\frac{1}{h_0(x-m_N)+\frac{1}{2}i\ \Gamma_0(x-m_N)}. \quad \text{(A.11b)}$$

We approximate these integrals in a way similar to the approximation made after eq. (30). If the time t is much larger than the life time of the instable V-particle the contribution from the zero of $h_0(x-m_N)$ can be neglected and we obtain from (A.11b)

$$b(t) \approx \frac{g_0 f(\omega_0)}{\sqrt{2V\omega_0}}\frac{-1}{h_0(\omega_0)+\frac{1}{2}i\ \Gamma_0(\omega_0)}\int_{-\infty}^{+\infty}\frac{e^{-ixt}dx}{m_N+\omega_0-x-i\varepsilon} = \beta(\omega_0)e^{-i(m_N+\omega_0)t} \quad \text{(A.12)}$$

The evaluation of (A.11a) is a little more complicated as we there have two factors involving $i\varepsilon$. It can be done in the following way:

$$\begin{aligned}
&\frac{1}{2\pi i}\int_{-\infty}^{+\infty}\frac{e^{-ixt}dx f(x)}{(\omega-x-i\varepsilon)(\omega_0-x-i\varepsilon)} \\
&=\frac{f(\omega)}{2\pi i}\int_{-\infty}^{+\infty}\frac{e^{-ixt}dx}{(\omega-x-i\varepsilon)(\omega_0-x-i\varepsilon)}+\frac{1}{2\pi i}\int_{-\infty}^{+\infty}\frac{e^{-ixt}dx}{\omega_0-x-i\varepsilon}\frac{f(x)-f(\omega)}{\omega-x-i\varepsilon} \\
&\approx\frac{f(\omega)}{2\pi i}\int_{-\infty}^{+\infty}\frac{e^{-ixt}dx}{(\omega-x-i\varepsilon)(\omega_0-x-i\varepsilon)}+\frac{f(\omega_0)-f(\omega)}{\omega_0-\omega}\frac{1}{2\pi i}\int_{-\infty}^{+\infty}\frac{e^{-ixt}dx}{\omega_0-x-i\varepsilon} \\
&=\frac{f(\omega_0)e^{-i\omega_0 t}-f(\omega)e^{-i\omega t}}{\omega-\omega_0}.
\end{aligned} \quad \text{(A.13)}$$

It follows

$$a(\bar{k},t)=\frac{g_0^2}{2V}\frac{f(\omega)f(\omega_0)}{\sqrt{\omega\omega_0}}\frac{e^{-im_N t}}{\omega_0-\omega}\left[\frac{e^{-i\omega_0 t}}{h_0(\omega_0)+\frac{1}{2}i\,\Gamma_0(\omega_0)}-\frac{e^{i\omega t}}{h_0(\omega)+\frac{1}{2}i\,\Gamma_0(\omega)}\right]. \tag{A.14}$$

The right-hand side of (A.14) is regular also for $\omega=\omega_0$ and no prescription for the treatment of the denominator is necessary. We can, however, arbitrarily add $+i\varepsilon$ and write

$$a(\bar{k}_1,t)=\alpha(\bar{k}_0,\bar{k})e^{-i(m_N+\omega_0)t}+\frac{g_0}{\sqrt{2V}}\frac{f(\omega_0)}{\sqrt{\omega_0}}\beta(\omega)\frac{e^{-i(m_N+\omega)t}}{\omega_0-\omega+i\varepsilon} \tag{A.15}$$

For the special case we have studied here we thus have

$$|\psi(t)\rangle=e^{-i(m_N+\omega_0)t}|N,\theta_0\rangle+\frac{g_0}{\sqrt{2V}}\frac{f(\omega_0)}{\sqrt{\omega_0}}\sum_{\bar{k}}\frac{\beta(\omega)e^{-i(m_N+\omega)t}}{\omega_0-\omega+i\varepsilon}|0,1_N,1_k\rangle. \tag{A.16}$$

We then start with a wave-packet of the following shape

$$a^{(0)}(\bar{k})=\delta_{k_x,0}\,\delta_{k_y,0}\,\lambda(k_z-k_0)e^{-ik_z z_0}, \tag{A.17}$$

$$\lambda(k)=\frac{1}{2\pi}\int e^{-ikx}A(x)dx. \tag{A.17a}$$

If the function $A(x)$ is different from zero only in some region of the order L around the origin, this wave-packet represents a N-particle at the origin and a packet of plane waves of θ-particles centered around the point z_0 and moving along the z-axis with approximate momentum k_0. In this case the last term in (A.16) gives

$$\begin{aligned}&\frac{g_0}{\sqrt{2V}}\sum_{\bar{k},\bar{k}'}a^{(0)}(\bar{k}')\frac{f(\omega')}{\sqrt{\omega'}}\frac{\beta(\omega)e^{-i(m_N+\omega)t}}{\omega'-\omega+i\varepsilon}|0,1_N,1_k\rangle\\&\quad=\sum_{k'_z}\lambda(k'_z-k_0)\frac{f(\omega')}{\sqrt{\omega'}}e^{-ik'_z z_0}\left(-\frac{g_0^2}{2V}\right)\sum_{\bar{k}}\frac{f(\omega)}{\sqrt{\omega}}\frac{e^{-i(m_N+\omega)t}}{\omega'-\omega+i\varepsilon}\\&\quad\times\frac{1}{h_0(\omega)+\frac{1}{2}i\,\Gamma_0(\omega)}|0,1_N,1_k\rangle.\end{aligned} \tag{A.18}$$

The corresponding wave-function in x-space is given by

$$
\begin{aligned}
&e^{-im_N t}\int dk_z'\,\lambda(k_z'-k_0)\frac{f(\omega')}{\sqrt{\omega'}}\left(\frac{-g_0^2}{2(2\pi)^3}\right)\int\frac{d^3k e^{i(\bar{k}\bar{x}-\omega t)}f(\omega)}{\sqrt{\bar{\omega}}(\omega'-\omega+i\varepsilon)[h_0(\omega)+\frac{1}{2}i\,\Gamma_0(\omega)]}\\
&\approx\frac{-g_0^2}{16\pi^3}e^{-im_N t}\frac{f^2(\omega_0)}{\omega_0}\frac{1}{h_0(\omega_0)+\frac{1}{2}i\,\Gamma_0(\omega_0)}\int dk_z'\,\lambda(k_z'-k_0)e^{-ik'z_0}\int\frac{d^3k e^{i(\bar{k}\bar{x}-\omega t)}}{\sqrt{k_2'^2+\mu^2}-\omega+i\varepsilon}\qquad\text{(A.19)}\\
&=\frac{\gamma_0 f^2(\omega_0)}{r}\frac{e^{-im_N t}}{h_0(\omega_0)+\frac{1}{2}i\,\Gamma_0(\omega_0)}\int dk_z'\,\lambda(k_z'-k_0)e^{-ik_z'z_0+i|\bar{k}_z'|r-i\omega' t}\;\theta(r-t)\\
&\approx\frac{\gamma_0 f^2(\omega_0)}{r}\frac{e^{-im_N t}\theta(r-t)}{h_0(\omega_0)+\frac{1}{2}i\,\Gamma_0(\omega_0)}\,\Lambda\left(\frac{k_0}{|k_0|}\left(r-\frac{|k_0|}{\omega}t\right)-z_0\right)e^{i|k|r-i\omega_0 t-ik_0 z}.
\end{aligned}
$$

If the product $k_0 z_0 < 0$, the simultaneous appearance of $\theta(r-t)$ and the function Λ in (A.19) makes the expression vanish. The last condition means that the motion of the initial wave-packet is directed towards the scatterer at the origin. We then have found that for a wave-packet of the form (A.17) the last term in (A.16) gives no contribution due to destructive interference of the terms for all values of $\bar{x}$. The only non-vanishing contribution comes from the first term in (A.16) and this demonstrates the equivalence of the two solutions.

References

1) T. D. Lee, Phys. Rev. **95** (1954) 1329
2) G. Källén and W. Pauli, Dan. Mat. Fys. Medd. **30** (1955) No. 7
3) S. Weinberg, Phys. Rev. **102** (1956) 285
4) W. Heitler, The Quantum Theory of Radiation, third edition (Clarendon Press, Oxford, 1954) esp. chapter IV, § 16

Nuclear Physics **2** (1956/57) 723—735; *North-Holland Publishing Co., Amsterdam*

ON THE INFORMATION ABOUT β-INTERACTION AND NUCLEAR LEVELS DERIVED FROM THE POLARIZATION OF X-RAY QUANTA

A. Z. DOLGINOV

Physico-Technical Institute of the USSR Academy of Sciences, Leningrad

Received 4 October 1956

Abstract: It is shown that the sign and magnitude of the ratio of the scalar and tensor β-interaction constants can be determined by observing the polarization of X-ray quanta emitted when the vacancy in the atomic shell is filled after allowed K-capture. It is suggested for this purpose that the correlation between circular polarization of the X-ray quanta and the direction of predominant orientation of nuclear spins in an external field be studied. If there is no external field but the nucleus undergoes a radiative transition after K-capture it should be feasible to investigate the correlation between the circular polarizations of the X-ray and nuclear quanta. If the atomic shell vacancy is due to a conversion transition, information on nuclear level moments and parities can be obtained by observing polarization correlation of the X-ray quanta. The polarization of β-electrons and γ-quanta in a complex cascade transition is also considered.

1. Polarization of K-capture X-ray Quanta

At present it can apparently be considered that tensor and scalar interactions predominate in β-decay processes. The role of pseudoscalar interaction is not clear but for allowed transitions its contribution is certainly not large. A more or less crude estimate of the contribution from S and T interactions has been made by studying the character of the β-spectra and the angular distribution of β-decay recoil nuclei [1]). The question as to the relative sign of the interaction constants g_T/g_S remains open. The sign of g_T/g_S can be found by studying the angular correlation between the β-particle and the γ-quantum in forbidden β-transitions [2]). Interpretation of the experiments in this case, however, is very difficult. The theoretical formulae contain several unknown ratios of nuclear matrix elements which must either be roughly estimated or else be considered as empirical quantities. An important advantage of studying allowed transitions is that only one unknown quantity $g_T\int\sigma/g_S\int 1$ enters the theoretical formula. $\int\sigma/\int 1$ is the ratio of the nuclear matrix elements and in some cases the sign of this

quantity can be reliably established on basis of existing conceptions relating to the structure of the nucleus. Known methods [3, 4]) in which it has been proposed that allowed transitions be used to determine g_T/g_S require that one investigates the correlation between the polarization of the β-electron and nucleus or cascade nuclear γ-quantum. This is an intricate and hitherto unsolved problem. A study of circular photon polarization is a simpler problem. It will be shown in the present paper that definite information on the sign of $g_T\int\boldsymbol{\sigma}/g_S\int 1$ can be obtained by investigating the correlation between circular polarization of X-ray quanta emitted when the shell vacancy appearing after K-capture is filled up and the polarization of the nucleus or cascade nuclear γ-quantum.

Let us first assume that prior to K-capture the nucleus was polarized and let a_{μ_0} be the probability that μ_0 is the projection of the nuclear moment j_0 on the quantization axis z (which may be, for example, the direction of an external magnetic field). The bispinor wave function of the shell electron possessing a total moment j and orbital angular momentum $l = j+\lambda$, $\lambda = \pm\frac{1}{2}$ can be written in the form

$$\psi_{j\mu\lambda}(\mathbf{r}) = \left(iF_{j\lambda}(r)\hat{Y}^{-\lambda}_{j\mu}(\vartheta\varphi),\ G_{j\lambda}(r)\hat{Y}^{\lambda}_{j\mu}(\vartheta\varphi)\right) \tag{1}$$

where $G_{j\lambda}(r)$ is the large, and $F_{j\lambda}(r)$ the small, radial component of the electron wave function in the nuclear Coulomb field; $\hat{Y}^{\lambda}_{j\mu}(\vartheta\varphi)$ is a spherical spinor whose components are

$$[\hat{Y}^{\lambda}_{j\mu}(\vartheta\varphi)]_\sigma = (-1)^{\sigma-\frac{1}{2}} C^{j\mu}_{l m \frac{1}{2}-\sigma} Y_{lm}(\vartheta\varphi), \qquad \sigma = \mp\tfrac{1}{2};$$

the $C^{jm}_{j_1 m_1 j_2 m_2}$ are Clebsch-Gordan coefficients.

The wave function of a neutrino possessing a momentum $\mathbf{q}(q, \theta_2, \phi_2)$ can be represented as a superposition of wave functions $\psi_{inv}(\mathbf{r})$ which differ from (1) only in that their radial parts are the solution of the free particle equation

$$\psi_{\mathbf{q}}(\mathbf{r}) = \sum_{inv} i^{i-\nu-1} \varphi^{*}_{inv}(\theta_2\phi_2)\,\psi_{inv}(\mathbf{r}); \tag{2}$$

$$\varphi_{inv}(\theta_2\phi_2) = \sum_{\chi m_2} C^{in}_{l_2 m_2 \frac{1}{2}\chi} v_\chi(\xi) Y_{lm}(\theta_2\varphi_2) \tag{3}$$

where $l_2 = i+\nu$; ν, χ and $\xi = \pm\frac{1}{2}$; $v_\chi(\xi)$ is a spinor which determines the polarization of the neutrino.

The matrix element for allowed K-capture can be written in the form †

$$H_K = g_S \int (\psi^*_{j_1\mu_1}\beta\psi_{j_0\mu_0})(\psi^*_q\beta\psi_{j\mu\lambda})d\mathbf{r} + g_T \int (\psi^*_{j_1\mu_1}\beta\boldsymbol{\sigma}\psi_{j_0\mu_0})(\psi^*_q\beta\boldsymbol{\sigma}\psi_{j\mu\lambda})d\mathbf{r} \tag{4}$$

where $\psi_{j_k\mu_k}$ are wave functions of the nucleus in a state with a moment j_k and its projections μ_k, β and $\boldsymbol{\sigma}$ are four-row Dirac matrices.

To compute (4) we use (2) and the following relations

$$(\hat{Y}^{\lambda *}_{j\mu}\hat{Y}^{\nu}_{in}) = \sum_J \alpha^J_{\lambda\nu} C^{j\mu}_{JMin} Y^*_{JM},$$
$$\alpha^J_{\lambda\nu} = \sqrt{(2J+1)(2i+1)(2l_2+1)}\, Y_{00} C^{l_1 0}_{l_2 0 j 0} W(Jjl_2\tfrac{1}{2};\ il_1); \tag{5}$$

$l_1 = j+\lambda$, $l_2 = i+\nu$; $W(abcd;\ ef)$ are Racah functions [6]);

$$(\hat{Y}^{\lambda *}_{j\mu}\boldsymbol{\sigma}\hat{Y}^{\nu}_{in}) = \sum_{J,\tau} \beta^{J\tau}_{\lambda\nu} C^{j\mu}_{JMin} \mathbf{Y}^{\tau *}_{JM},$$
$$\beta^{J\tau}_{\lambda\nu} = (-1)^{J+j+i+1}\sqrt{6(2J+1)(2i+1)(2l_2+1)(2l+1)}\, Y_{00} C^{l_1 0}_{l_2 0 1 0} \times \sum_s (2S+1) W(\tfrac{1}{2}l_2 Jj;\ iS) W(ll_1 Sj;\ l_2\tfrac{1}{2}) W(JS1\tfrac{1}{2};\ \tfrac{1}{2}l). \tag{6}$$

It would be noted that the definition of spherical function y_{lm} used here is the same as that in ref. [7]) and differs by the factor $(-1)^m$ from the expression given, say, in ref. [8]). Correspondingly, the cyclic components of a vector $\mathbf{a}$ are defined by the relations $a_0 = a_z$, $a_{\pm 1} = \pm\sqrt{\tfrac{1}{2}}\,(a_x \pm i a_y)$, and in particular the components of the spherical vector [5]) are ($\sigma = 0,\ \pm 1$):

$$[\mathbf{Y}^{\tau}_{JM}]_\sigma = (-1)^{\sigma+1} C^{JM}_{lm1-\sigma} Y_{lm}, \qquad \begin{matrix} l = J+\tau, \\ \tau = 0,\ \pm 1. \end{matrix}$$

We now write (4) as follows:

$$H_K = \sum_{inrJ\tau} i^{\nu-i+1} \varphi_{inr}(\theta_2\phi_2) C^{in}_{JMj\mu} C^{j_0\mu_0}_{JMj_1\mu_1} B^{J\tau}_{\nu\lambda}, \tag{7}$$

$$B^{J\tau}_{\nu\lambda} = \alpha^J_{-\nu-\lambda} K_1 - \alpha^J_{\nu\lambda} K_2 + \beta^{J\tau}_{-\nu-\lambda} K_3 - \beta^{J\tau}_{\nu\lambda} K_4,$$
$$K_1 C^{j_0\mu_0}_{JMj_1\mu_1} = g_S \int (\psi^*_{j_1\mu_1}\beta\psi_{j_0\mu_0}) Y^*_{JM} F^*_{i\nu} F_{j\lambda}\, d\mathbf{r}, \tag{8}$$
$$K_3 C^{j_0\mu_0}_{JMj_1\mu_1} = g_T \int (\psi^*_{j_1\mu_1}\beta\boldsymbol{\sigma}\psi_{j_0\mu_0}) \mathbf{Y}^{\tau *}_{JM} F^*_{i\nu} F_{j\lambda}\, d\mathbf{r};$$

K_2 and K_4 differ respectively from K_1 and K_3 in that $F^*_{i\nu}(r)F_{j\lambda}(r)$ is replaced by $G^*_{i\nu}(r)G_{j\lambda}(r)$.

† For a linear combination of vector and tensor interaction matrix β in the first integral in (4) should be replaced by 1. This leads to a similar substitution in integrals K_1 and K_2 in formula (8) and to a change in the sign of K_2.

If $\psi_{l\omega\varepsilon}(\mathbf{r})$ is the wave function of an electron which goes to the vacant $(j\mu\lambda)$ atomic level the matrix element for the radiative transition will have the form

$$H_{\mathrm{X}} = \int \psi^*_{j\mu\lambda} \boldsymbol{\alpha} \mathbf{A} \psi_{l\omega\varepsilon} \, \mathrm{d}\mathbf{r}. \tag{9}$$

The transition vector potential can be expanded in a series of multipole potentials

$$\begin{aligned} \mathbf{A} = \boldsymbol{\epsilon} \mathrm{e}^{i\mathbf{k}\cdot\mathbf{r}} = \sum_{L\Lambda l\sigma} \sqrt{4\pi(2l+1)}\, i^{l+2} f_l(kr) \varepsilon_\sigma(0) \\ \times D^L_{\Lambda\sigma}(\phi\theta 0) C^{L\sigma}_{l01\sigma} \mathbf{Y}^{\tau *}_{L\Lambda}(\vartheta\varphi) \end{aligned} \tag{10}$$

where

$$f_l(kr) = \sqrt{\pi/2kr}\, J_{l+\frac{1}{2}}(kr);$$

$J_{l+\frac{1}{2}}(kr)$ are Bessel functions, $D^L_{\Lambda\sigma}(\phi\theta 0)$ is a component of the matrix of the irreducible $(2L+1)$ dimensional representation of the rotation group [9]). $\varepsilon_\sigma(0)$ is the component of the polarization vector of the quantum in a coordinate system in which $\mathbf{k}(k, \theta, \phi)$ is the polar axis and the X axis lies in the $(\mathbf{k}z)$ plane:

$$\varepsilon_0(0) = 0, \qquad \varepsilon_{\pm 1}(0) = \pm\sqrt{\tfrac{1}{2}}\, \mathrm{e}^{\pm i\alpha}; \tag{11}$$

α is the angle of the vector $\boldsymbol{\epsilon}$ with respect to the axis x in a plane $\perp \mathbf{k}$.

Inserting (10) into (9) and utilizing (6) we obtain

$$\begin{aligned} H_{\mathrm{X}} &= \sum_{L\Lambda l\sigma} (-1)^{L+\Lambda} C^{L\sigma}_{l01\sigma} C^{j\mu}_{L-\Lambda l\omega} \varepsilon_\sigma(0) D^L_{\Lambda\sigma}(\phi\theta 0) R^I_{Ll}, \\ R^I_{Ll} &= \sqrt{4\pi(2l+1)}\, i^{-l-1} \{\beta^{L\tau}_{-\lambda\varepsilon} K_5 - \beta^{L\tau}_{\lambda-\varepsilon} K_6\}, \\ K_5 &= \int f_l F^*_{j\lambda} G_{l\varepsilon} r^2 \mathrm{d}r, \qquad K_6 = \int f_l F_{l\varepsilon} G^*_{j\lambda} r^2 \mathrm{d}r. \end{aligned} \tag{12}$$

For X-ray transitions it is sufficient to consider only dipole electric radiation and hence in (12) we put $l = 0$, $L = 1$, $\tau = -1$.

In order to find the correlation between the polarization of the X-ray quantum and the direction of the nuclear spin the quantity $\langle |H_{\mathrm{K}} H_{\mathrm{X}}|^2 \rangle$ should be computed, $\langle\,\rangle$ denoting summation over all states of the neutrino spin and integration over the angles of vector $\mathbf{q}$. The following relationships were used in the calculations:

$$\sum_{\alpha\beta\gamma} C^{c\gamma}_{a\alpha b\beta} C^{ee}_{d\delta b\beta} C^{d\delta}_{a\alpha f\varphi} = \sqrt{(2c+1)(2d+1)}\, W(cbfd;\, ae), \tag{13}$$

$$D^{L_1 *}_{\Lambda_1\sigma_1} D^L_{\Lambda\sigma} = \sum_F [(2F+1)/(2L+1)] C^{L\Lambda}_{L_1\Lambda_1 F\varphi} C^{L\sigma}_{L_1\sigma_1 F\varphi} D^F_{\varphi\psi}. \tag{14}$$

The following expression is then obtained for the correlation.

$$W(\theta) = \Sigma(2F+1)(2i+1)\sqrt{(2j+1)(2j'+1)}W(1IFj;\ j'1)$$
$$\times W(j'iFJ;\ J'j)W(J'j_1Fj_0;\ j_0J)\varepsilon_\sigma(0)\varepsilon^*_{\sigma'}(0)a_{\mu_0} \qquad (15)$$
$$\times C^{j_0\mu_0}_{j_0\mu_0 F_0}C^{1\sigma}_{1\sigma' F\varphi}D^F_{0\varphi}(\phi\theta 0)B^{J\tau}_{\nu\lambda}B^{J'\tau'*}_{\nu\lambda'}.$$

Summation here is carried out over all permissible values of $F,\ J,\ J',\ \tau,\ \tau',\ j,\ j',\ \lambda,\ \lambda',\ i,\ \mu_0$.

Expression (15) is valid for transitions of any order of forbiddenness but now $B^{J\tau}_{\nu\lambda}$ is not defined by formula (8). It is not difficult to find $B^{J\tau}_{\nu\lambda}$ for first order forbidden transitions by comparing (7) and the corresponding expression for the β-transition matrix element given in ref. [2]). For reasons considered above we confine our attention to allowed transitions. In this case $j = j' = i = \frac{1}{2};\ \lambda = \lambda' = \nu = -\frac{1}{2};\ \sigma = \sigma' = \pm 1;\ \varphi = 0;\ F = 0$ or 1; J and $J' = 0$ or 1; $J+\tau = J'+\tau' = 0;\ I = \frac{1}{2}$ or $3/2$. Using the explicit form of the radial part of (2) and taking into account that the neutrino wave length is much larger than the nuclear dimensions we get

$$B^{0,0}_{-\frac{1}{2},-\frac{1}{2}} = K_2, \qquad B^{1,-1}_{-\frac{1}{2},-\frac{1}{2}} = \sqrt{3}\,K_4.$$

If the X-ray quantum is emitted in a transition to the K-level from a level whose moment was $I = \frac{1}{2}$ (e.g., a L_{II} level) formula (15) may be written as follows:

$$W(\theta) = 1+X^2+\sigma\varrho\left\{1-2X\sqrt{j_0(j_0+1)}\right\}\cos\theta, \qquad (16)$$

$\sigma = \pm 1$ depending on whether the quantum is circulary polarized in the right or left hand direction: $\varrho = \sum_{\mu_0} a_{\mu_0}\mu_0/j_0(j_0+1)$ determines the degree of polarization of the nuclear spins, $\sum_{\mu_0} a_{\mu_0} = 1$. Formula (16) refers to the most interesting case when $j_1 = j_0$ since only in this case the selection rules for allowed K-capture permit scalar and tensor interaction to exist simultaneously. The quantity $X = K_2/K_4$ is real because the condition of invariancy on inversion of time leads to a phase shift between K_2 and K_4 which is equal to either 0 or π. On computing K_2 and K_4 we shall fit the electron wave function in the Coulomb field outside the nucleus onto the wave function inside the nucleus. Using the results obtained in ref. [10 11]) it is easy to show that to an accuracy of small terms of the order of $(\alpha Z)^2$ compared with 1 one gets

$$X = g_S K_\beta/g_T K_\sigma; \qquad K_\beta = \int \psi^*_{j_0\mu_0}\beta\psi_{j_0\mu_0}\,\mathrm{d}\mathbf{r},$$
$$K_\sigma C^{j_0\mu_0}_{1M j_0\mu_0} = \int \psi^*_{j_0\mu_0}\beta\boldsymbol{\sigma}\psi_{j_0\mu_0}\,\mathbf{Y}^{-1*}_{1M}\,\mathrm{d}\mathbf{r}. \qquad (17)$$

For a transition from a level with a moment $I = 3/2$ (e.g., a L_{III}-level) equation (16) is still valid if the factor $(-\frac{1}{2})$ is written before the braces. Since the transition probability from a level with $I = 3/2$ is twice that for a transition from a level with $I = \frac{1}{2}$ no overall correlation should exist. Thus it is necessary to determine the polarization of the quanta emitted from levels with $I = 3/2$ and $I = \frac{1}{2}$ and employ energy discrimination. For sufficiently heavy nuclei the difference between frequencies of the K_{α_1} and K_{α_2} lines permits one to perform this separation.

It should be kept in mind that magnetic fields acting on the atom may change the mutual distances and the order of the atomic levels. For various concrete cases it is not difficult to establish experimentally or theoretically the nature of these changes.

Since $|X| \approx 1$, $\varrho > 0$ and quanta of a definite circular polarization are chosen, in order to find the sign of X it is sufficient to find the sign of the whole expression in front of $\cos\theta$. Because of this structure of formula (16) a rough estimation of ϱ is quite sufficient. One must merely be sure that ϱ is not very small.

It should be noted that in atoms with unfilled $p_{3/2}$ shells the polarization of quanta emitted from $p_{\frac{1}{2}}$ levels is not completely compensated by oppositely polarized quanta from $p_{3/2}$ levels and hence energy discrimination is not obligatory. In this case it is better to use very light atoms with unfilled L-shells. If the $p_{3/2}$ level, say in the N-shell, is unfilled, a large background due to quanta in transitions from M or L-shells to the K-level will be added to the observed effect. As a rule, light nuclei which experience K-capture possess a short life time and it is thus difficult to utilize them for experiments involving polarization of nuclear spins. However, if a nuclear γ-quantum is emitted after K-capture the sign of g_T/g_S can be found by studying the correlation between circular polarization of the X-ray and γ-quanta.

In order to find this correlation the quantity $\langle |H_\gamma H_K H_X|^2 \rangle$ must be computed, H_γ being the matrix element of the γ-transition:

$$H_\gamma = \sum_{L\Lambda\sigma l} i^l \varepsilon_\sigma(0) D^L_{\Lambda\sigma}(\phi\theta 0) C^{L\sigma}_{l01\sigma} C^{j_1\mu_1}_{L\Lambda j_2\mu_2} R_{Ll},$$
$$R_{Ll} C^{j_1\mu_1}_{L\Lambda j_2\mu_2} = \sqrt{4\pi(2l+1)} \int \psi^*_{j_2\mu_2} f_l(kr)\,(\hat{\mathbf{J}}\mathbf{Y}^{\tau *}_{L\Lambda})\psi_{j_1\mu_1}\,d\mathbf{r}, \tag{18}$$

where j_1 and j_2 are the moments of the nuclear levels between which the γ-transition takes place; $\hat{\mathbf{J}}$ is a current density transition

operator; L is the multipole order of the quantum, $l = L$ for magnetic and $l = L-1$ for electric radiation.

Performing calculations similar to those which were carried out to get (15) we obtain the correlation expression in the form

$$\begin{aligned} W(\eta) &= \sum (-1)^F [(2F+1)/\sqrt{2L+1}] i^{l-l'} (-1)^{L+L'} C^{1\sigma_1}_{1\sigma_1 F_0} \\ &\times C^{L\sigma}_{l01\sigma} C^{L'\sigma}_{l'01\sigma} C^{L\sigma}_{L'\sigma F0} W(1lF\tfrac{1}{2};\ \tfrac{1}{2}1) W(L' j_2 F j_1;\ j_1 L) \\ &\times W(FJ\tfrac{1}{2}\tfrac{1};\ J'\tfrac{1}{2}) W(j_1 j_0 FJ;\ J' j_1) B^J B^{J'*} R_{Ll} R^*_{L'l'} P_F(\cos\eta). \end{aligned} \tag{19}$$

Here η is the angle between the directions of the quanta, $\sigma = \pm 1$ determines the polarization of the γ, and $\sigma_1 = \pm 1$, the polarization of the X-ray radiation. The only terms in sum (19) which do not vanish are those for which F, J and J' are 0 or 1. For pure γ-radiation of 2^L multipole order we get $L = L'$ and $l = l'$ and moreover $l = L$ or $L-1$. For mixed magnetic and electric radiation of multipole order 2^L and 2^{L+1} one must put $L = l = l'$ and $L' = L+1$.

If the X-ray quantum is emitted in a transition of the electron from a level with a moment $I = \frac{1}{2}$ to the K-shell and the multipole order of the γ-quantum is 2^L, formula (19) assumes the simple form ($j_0 = j_1$)

$$\begin{aligned} W(\eta) &= 1+X^2-\sigma_1\sigma\sqrt{(2L+1)(2j_0+1)/L(L+1)j_0(j_0+1)} \\ &\times W(Lj_2 1j_0;\ j_0 L)\{1+2X\sqrt{j_0(j_0+1)}\}\cos\eta. \end{aligned} \tag{20}$$

If the electron leaves a level with $I = 3/2$ the factor $(-\frac{1}{2})$ should be written before the braces in (20). For a mixed γ-transition we obtain instead of (20)

$$\begin{aligned} W(\eta) &= (1+X^2)(1+b^2)-\sigma_1\sigma\{1+2X\sqrt{j_0(j_0+1)}\} \\ &\times\sqrt{(2L+1)(2j_0+1)/L(L+1)j_0(j_0+1)}\{W(Lj_2 1j_0;\ j_0 L) \\ &+b^2\sqrt{L(2L+3)/(L+2)(2L+1)}\, W(L+1,\ j_2 1j_0;\ j_0,\ L+1) \\ &-2b\sqrt{(L+2)/(2L+1)}\, L W(L+1,\ j_2 1j_0;\ j_0 L)\}\cos\eta; \end{aligned} \tag{21}$$

b^2 is the ratio of the electric and magnetic radiation intensities:

$$b = \pm|b| = \sqrt{(L+2)/(2L+3)}\,[R_{L+1,L}/R_{L,L}]. \tag{22}$$

If a γ-quantum is not emitted directly after K-capture and one or several quanta are emitted between them in the same cascade the following factor should be added [12]) before the braces in (20) or (21):

$$\prod_{k=1}^{N-1} \sqrt{(2j_k+1)(2j_{k+1}+1)}\, W(j_{k+1} L_k 1 j_k;\ j_k j_{k+1})$$

where L_k determines the multipole order of the intermediate quanta $j_0(\mathrm{K})j_0(\gamma_1)j_2(\gamma_2)\ldots j_N(\gamma)j_{N+1}$. Experimentally only the polarization of those γ-quanta which are radiated in a $j_N(\gamma)j_{N+1}$ transition are studied. If one of the intermediate γ-transitions is mixed one should add the expressions for the magnetic and electric transitions whose weights are equal to their intensities. On integration over the γ-quantum angles the interference terms drop out.

2. Polarization of β-electrons and Cascade Transition γ-quanta

The sign of g_T/g_S can be determined by studying the correlation between the polarization of allowed β-transition electrons and the direction of the nuclear spin or the polarization of the subsequent nuclear γ-quantum. This was suggested by Tolhoek and de Groot [3]) and Zeldovich [4]). However, none of the formulae obtained in these investigations refer to correlation between polarization of the β-particle and the subsequent γ-quantum. The relevant formulae have been obtained in the present paper for a complex cascade transition with account of Coulomb interaction between the β-particle and nucleus.

The wave function for an electron in the Coulomb field of a nucleus with momentum $\mathbf{p}(p,\ \theta_1,\ \phi_1)$ at infinity can be written as follows:

$$\psi_{\mathbf{p}} = \sum_{j\mu\lambda} i^{j-\lambda-1} \varphi^*_{j\mu\lambda}(\theta_1 \phi_1)\psi_{j\mu\lambda}(\mathbf{r})\mathrm{e}^{-i\delta_{j\lambda}}; \tag{23}$$

$\delta_{j\lambda}$ is the phase shift in the Coulomb field [5]), an expression similar to (3) is valid for $\varphi_{j\mu\lambda}$, the spinor $v_\mu(\xi)$ determining the electron polarization.

The β-decay matrix element differs from (4) only in that $\psi_{j\mu\lambda}$ is substituted for $\psi_{\mathbf{p}}$. After transformations which are similar to those applied to deduce (7) we get

$$\begin{aligned} H_\beta = \sum_{j\mu\lambda i n\nu} & i^{j\lambda-\nu+i-j}\, \mathrm{e}^{i\delta_{j\lambda}}\, \varphi_{j\mu\lambda}(\theta_1\phi_1) \\ & \times \varphi^*_{in\nu}(\theta_2\phi_2) C^{j\mu}_{JMin} C^{j_0\mu_0}_{JMj_1\mu_1} B^{J\tau}_{\lambda\nu}. \end{aligned} \tag{24}$$

The integrals involved in $B^{J\tau}_{\lambda\nu}$ are computed in a manner similar to that employed in section 1. For allowed β-transitions $J = 0$, $\tau = 0$ or $J = 1$, $\tau = -1$ and $j = i = \frac{1}{2}$, $\lambda = \nu = \pm\frac{1}{2}$.

Denoting $B^{Jr}_{\lambda\mu}$ by B^{J}_{λ} and utilizing the explicit form [10]) of $F_{j\lambda}$ (r) and $G_{j\lambda}$ (r) we obtain

$$B^{(0)}_{\pm\frac{1}{2}} = n_{\pm} A_{\frac{1}{2}\mp\frac{1}{2}} K_{\beta}, \qquad B^{(1)}_{\pm\frac{1}{2}} = \sqrt{3}\, n_{\pm} A_{\frac{1}{2}\mp\frac{1}{2}} K_{\sigma}; \tag{25}$$

$n_{\lambda} A_{j\lambda}$ are matching coefficients for the radial part of the electron wave function at the nuclear boundary. Their explicit form and numerical values are presented in ref. [10, 13]). With an accuracy of terms $(\alpha Z)^2$ we get

$$n_{\pm} A_{\frac{1}{2}\mp\frac{1}{2}} / n_{\mp} A_{\frac{1}{2}\mp\frac{1}{2}} = \sqrt{(E+1)/(E-1)}, \tag{26}$$

where E is the total β-electron energy in mc^2 units. Only the ratio (26) of the $n_{\lambda} A_{j\lambda}$, and not these quantities themselves, enters the formulae for polarization $\beta-\gamma$ correlation. Thus for allowed β-transitions the correlation will not depend on the Coulomb interaction between the β-particles and nucleus.

The quantity $\langle |H_{\beta} H_{\gamma}|^2 \rangle$ must be evaluated in order to determine the correlation. Using (18) and (24) and performing the relevant summations over the magnetic quantum numbers we obtain the following expression for correlation between the electron polarization and circular polarization of the subsequent γ-quantum:

$$\begin{aligned} W(\theta_1, \theta) &= 1+X^2-\sigma E^{-1}\sqrt{(2L+1)(2j_0+1)/L(L+1)\, j_0(j_0+1)} \\ &\times W(Lj_2 1 j_0;\ j_0 L)\{1+2X\sqrt{j_0(j_0+1)}\}\{E(v_{\frac{1}{2}} v^*_{\frac{1}{2}} \\ &-v_{-\frac{1}{2}} v^*_{-\frac{1}{2}}) \cos\theta_1 + (v_{\frac{1}{2}} v^*_{-\frac{1}{2}} + v_{-\frac{1}{2}} v^*_{\frac{1}{2}}) \sin\theta_1\} \cos\theta. \end{aligned} \tag{27}$$

Here L is the multipole order, $\sigma = \pm 1$ is the γ-quantum polarization, θ_1 and θ are the angles of emission of the electron and γ-quantum, $j_0 = j_1$. The factor $v_{\frac{1}{2}} v^*_{\frac{1}{2}} + v_{-\frac{1}{2}} v^*_{\frac{1}{2}} = \zeta_{\perp}$ determines the transverse electron polarization and vanishes if the quantization axis is chosen along $\mathbf{p}(p, \theta_1, \phi_1)$. The factor $v_{\frac{1}{2}} v^*_{\frac{1}{2}} - v_{-\frac{1}{2}} v^*_{-\frac{1}{2}} = \zeta_{\parallel}$, determines the longitudinal polarization. $\boldsymbol{\zeta} = E\boldsymbol{\zeta}_{\parallel} + \boldsymbol{\zeta}_{\perp}$ is the polarization vector [14]). The possibility of experimental investigation of electron polarization has been considered in a number of papers [15, 16]). A generalization of formula (27) for the case when a complex cascade transition folllows β-decay can be carried just as in section 1 and does not require additional explanation.

Formula (27) also describes the polarization of β-electrons emitted by polarized nuclei if the factor in front of the first braces is replaced by $-\varrho E^{-1}$; ϱ being defined in section 1. This result is identical with that obtained in ref. [3]).

Cox and Tolhoek [17]) have shown that the relative contribution

of tensor and scalar interactions can be found by studying the angular distribution of γ-quanta emitted after β-transitions in a nucleus whose spin is polarized in an external field. In order to find the quantity $X^2 \propto (g_S/g_T)^2$ from experiment one must have sufficiently accurate data on the degree of nuclear polarization (i.e., on the values of a_{μ_0}). It may not always be possible to simultaneously determine X^2 and all the a_{μ_0} if only γ-quantum angular distribution experiments are used. Let us find the expression for the polarization of γ-quanta emitted in a complex cascade after a β-transition in the polarized nucleus. This will yield an auxiliary equation for X^2 and a_{μ_0}. Consider the cascade $j_0(\beta)j_0(\gamma_1)j_2 \ldots j_N(\gamma_N)j_{N+1}$ and let α be the angle of the polarization vector (11) of the quantum γ_N and 2^L be its multipole order. Computing $\langle |H_\beta H_{\gamma_1} \ldots H_{\gamma N}|^2 \rangle$ with help of (18) and (24) we obtain

$$W(\theta,\alpha) = \sum_{F,\mu_0} (2F+1) W(L j_{N+1} F j_N;\ j_N\ L) \times \{1 + yF(F+1)/2j_0(j_0+1)\} \prod_{k=1}^{N-1} \sqrt{(2j_k+1)(2j_{k+1}+1)}\, W(j_{k+1} L_k F j_k;\ j_k j_{k+1}) \times \{C^{L1}_{L1F0} P_F(\cos\theta) - \xi\sqrt{4\pi/(2F+1)}\, C^{L1}_{L-1F2} \cos 2\alpha\, Y_{F2}(\theta 0)\} a_{\mu_0} C^{j_0 \mu_0}_{j_0 \mu_0 F0}; \tag{28}$$

F assumes all even values in the interval from 0 to the lowest of the values of $2L$ or $2j_k$; $y = 1/(1+X^2)$. Extension to the case of mixed γ-transitions is performed as in (20), (21). $\xi = 1$ or -1 for electric or magnetic transitions, respectively.

The angular distribution of γ-quanta emitted by a polarized Co^{58} nucleus after K-capture has been calculated in ref. [18]). We give here the explicit expression for the polarization of these quanta. Expressing (28) in the form $W(\theta,\alpha) = \sum_{\mu_0} a_{\mu_0} W_{\mu_0}$ and denoting $\beta = \cos\theta$ we obtain

$$W_0 = 6\beta^2(1-\beta^2) + y(1 - 9\beta^2 + 10\beta^4) + (1-\beta^2)\{6\beta^2 + y(1-10\beta^2)\}\cos 2\alpha,$$

$$W_{\pm 1} = 1 - 3\beta^2 + 4\beta^4 - (y/2)[1 - 11\beta^2 + (40/3)\beta^4] + (1-\beta^2)\{1 - 4\beta^2 - (y/6)(7 - 40\beta^2)\}\cos 2\alpha,$$

$$W_{\pm 2} = 1 - \beta^4 - y\beta^2[1 - (5/3)\beta^2] - (1-\beta^2)\{(1-\beta^2) + y[1 - (5/3)(1-\beta^2)]\}\cos 2\alpha.$$

3. Polarization of X-ray Quanta Emitted after Internal Conversion

If the nuclear transition is accompanied by internal conversion and the conversion coefficient is large one can determine the spins

and parities of the nuclear levels by studying the angular correlation between the conversion electron and ensuing (or preceding) γ-quantum [19, 20]). In some cases it is difficult to observe this correlation because of electron scattering which makes it difficult to determine the direction of the electrons. It is also difficult to observe the correlation under experimental conditions in which the source is located in a magnetic field which strongly deflects the electrons.

We shall now show that polarization correlation of X-ray quanta emitted after a conversion transition yields the same information on the properties of nuclear levels as can be obtained from conversion electron angular correlation studies.

The matrix element of an electric conversion transition of multipole order 2^L can be written in the form [20])

$$H_e^{el} = C^{j_0\mu_0}_{LAj_0\mu_1} R^{el}_{Lj_0j_1} \int \psi^*_{\mathbf{p}} \{ iF_L(kr) Y_{LA}(\vartheta\varphi) - \sqrt{(2L+1)/L}\, F_{L-1}(kr) \boldsymbol{\alpha} \mathbf{Y}^{-1}_{LA}(\vartheta\varphi) \} \psi_{J_0 M_0 \lambda_0} \mathrm{d}\mathbf{r}, \tag{29}$$

where $R^{el}_{Lj_0j_1}$ is the reduced nuclear transition matrix element and $F_L(kr) = \sqrt{\pi/2kr}\, H^{(1)}_{L+\frac{1}{2}}(kr)$, $J_0 = l_0 - \lambda_0$ is the total angular momentum of the initial and $J = l - \lambda$ the total angular momentum of the final conversion electron state.

For a magnetic conversion transition

$$H_e^{mg} = C^{j_0\mu_0}_{LAj_1\mu_1} R^{mg}_{Lj_0j_1} \int \psi^*_{\mathbf{p}} F_L(kr) \boldsymbol{\alpha} \mathbf{Y}^0_{LA}(\vartheta\varphi) \psi_{J_0 M_0 \lambda_0} \mathrm{d}\mathbf{r}. \tag{30}$$

Using (1), (5), (6) and (24) we obtain

$$H_e = \sum_{Jm\lambda} i^{\lambda - J} \varphi_{JM\lambda} e^{i\delta_{J\lambda}} C^{j_0\mu_0}_{LAj_1\mu_1} C^{JM}_{LAJ_0M_0} B^L_{J\lambda}, \tag{31}$$

where for an electric transition

$$B^L_{J\lambda} = \int_0^\infty r^2 \mathrm{d}r \{ \alpha^L_{-\lambda-\lambda_0} F^*_{J\lambda} F_{J_0\lambda_0} F_L + \alpha^L_{\lambda\lambda_0} G^*_{J\lambda} G_{J_0\lambda_0} F_L + \sqrt{(2L+1)/L}\, [\beta^{L,-1}_{-\lambda,\lambda_0} F_{L-1} F^*_{J\lambda} G_{J_0\lambda_0} - \beta^{L,-1}_{\lambda,-\lambda_0} F_{L-1} G^*_{J\lambda} F_{J_0\lambda_0}] \} \tag{32}$$

and for a magnetic transition

$$B^L_{J\lambda} = \int_0^\infty r^2 \mathrm{d}r \{ \beta^{L,0}_{-\lambda,\lambda_0} F^*_{J\lambda} G_{J_0\lambda_0} - \beta^{L,0}_{\lambda,-\lambda_0} G^*_{J\lambda} F_{J_0\lambda_0} \} F_L. \tag{33}$$

After a conversion transition in the atomic shell an empty level appears. An X-ray quantum is emitted when the vacancy is filled up. A correlation exists between the polarization of these quanta and the direction of the nuclear spin prior to the conversion transition. The correlation expression can be found by calculating

$\langle|H_e H_X|^2\rangle$ with the help of (12) and (31):

$$W_{eX}(\theta) = \sum_{F, J, \lambda, \mu_0} (2F+1)(2J+1) W(1IFj_0;\ j_0 1) W(Lj_1 Fj_0;\ j_0 L) \times W(j_0 JFL;\ Lj_0) |B^L_{J\lambda}|^2 C^{1\sigma}_{1\sigma F0} a_{\mu_0} C^{j_0\mu_0}_{j_0\mu_0 F0} P_F(\cos\theta). \quad (34)$$

This expression is valid for conversion in any atomic shell. The $B^L_{J\lambda}$ contain radial integrals which are usually encountered in internal conversion theory. In ref. [21, 22]) they have been evaluated by numerical integration.

In the case of K-shell conversion formula (34) can be simplified. If the K-shell is filled by an electron which was on the $p_{\frac{1}{2}}$ level ($I = \frac{1}{2}$), one obtains

$$W_{eX}(\theta) = 1+\sigma\varrho[j_0(j_0+1)-j_1(j_1+1)+L(L+1)]Q_L \cos\theta, \quad (35)$$

$$Q_L = [\sum_J (-1)^{L-J-\frac{1}{2}} |B^L_{J\lambda}|^2] / [\sum_J (2J+1)|B^L_{J\lambda}|^2]; \quad (36)$$

$\lambda = L-J$ for electric and $\lambda = J-L$ for magnetic transitions. The quantities $\alpha^L_{\lambda_1\lambda_2}$ and $\beta^{L\tau}_{\lambda_1\lambda_2}$ involved in the calculations of $B^L_{J\lambda}$ which enters (36) are equal to

$$\alpha^{L,\,J=L+\frac{1}{2}}_{\lambda_1,\lambda_2} = \delta_{\lambda_1,\lambda_2}, \qquad \alpha^{L,\,J=L-\frac{1}{2}}_{\lambda_1,\lambda_2} = \delta_{\lambda_1,-\lambda_2},$$

$$\beta^{L,-1}_{\lambda_1,\lambda_2} = \sqrt{1/L(2L+1)}\,\{L-2\lambda_2-\lambda_1(2J+1)\}\,\alpha^L_{-\lambda_1,\lambda_2},$$

$$\beta^{L,0}_{\lambda_1,\lambda_2} = \sqrt{1/L(L+1)}\,\{\lambda_1(2J+1)-2\lambda_2\}\,\alpha^L_{\lambda_1,\lambda_2}.$$

In the case when $I = 3/2$ a factor $(-\frac{1}{2})$ must be written in front of σ in (35). All considerations presented in section 1 concerning the necessity of energy discrimination of quanta emitted from $p_{\frac{1}{2}}$ and $p_{3/2}$ levels therefore remain valid.

If the nuclear spin is not oriented and a radiative nuclear transition takes place after (or before) the conversion transition there will be a correlation between the circular polarization of X-ray and γ-quanta. This correlation can be found by computing $\langle|H_\gamma H_e H_X|^2\rangle$ with the help of (12), (18), (31). If the conversion takes place in the K-shell and a γ-quantum of $2^{L\gamma}$ multipole order is then emitted one gets

$$W_{\gamma eX}(\vartheta) = 1-\sqrt{(2L+1)(2j_1+1)/L(L+1)j_1(j_1+1)}\,\{j_1(j_1+1) - j_0(j_0+1)+L(L+1)\}\,W(L_\gamma j_2 1 j_1;\ j_1 L_\gamma) Q_L \sigma_X \sigma_\gamma \cos\theta \quad (37)$$

where θ is the angle between the direction of the X-ray and γ-quanta; $\sigma_X = \pm 1$ and $\sigma_\gamma = \pm 1$ are their circular polarizations respectively. Generalization of (37) for the case of a mixed type of γ-transition or of several consecutive γ-quanta is performed in exactly the same way as in section 1.

Moments of the nuclear levels and multipole orders of the transitions enter formula (37) and hence they can be determined from experiment. If the level moments are known one may determine the ϱ degree of nuclear polarization from formula (35).

References

1) Beta- and Gamma-Ray Spectroscopy, edited by K. Siegbahn (Amsterdam, 1955)
2) A. Z. Dolginov and I. N. Toptigin, Nuclear Physics **2** (1956/1957) 147
3) H. A. Tolhoek and S. R. de Groot, Physica **17** (1951) 81
4) Ya. B. Zeldovich, Izvestia Akad. Nauk SSSR, ser. fyz. **18** (1954) 243
5) V. B. Berestetsky, A. Z. Dolginov and K. A. Ter-Martirosyan, JETP **20** (1950) 527
6) G. Racah, Phys. Rev. **62** (1942) 438
7) H. Bethe, Quantum Mechanics of Simplest Systems (1935) (Russian edition)
8) F. Condon and G. Shortley, Theory of Atomic Spectra (1949)
9) F. Wigner, Gruppentheorie und ihre Anwendung auf die Quantenmechanik der Atmospektren (Braunschweig, 1931)
10) A. Z. Dolginov, JETP **22** (1952) 658
11) A. Z. Dolginov, JETP **22** (1952) 668
12) A. Z. Dolginov, JETP **23** (1952) 493
13) L. A. Sliv and B. A. Volchok, Tables of Coulomb Phases and Amplitudes with Account of Finite Nuclear Dimensions (in press)
14) H. A. Tolhoek and S. R. de Groot, Physica **17** (1951) 1
15) A. I. Akhiezer and V. B. Berestetsky, Quantum Electrodynamics (Moscow, 1953)
16) H. A. Tolhoek and S. R. de Groot, Physica **17** (1951) 17
17) I. A. M. Cox and H. A. Tolhoek, Physica **19** (1953) 673
18) I. A. M. Cox and S. R. de Groot, Physica **19** (1953) 1119
19) V. B. Berestetsky, JETP **18** (1948) 1070
20) A. Z. Dolginov, Izv. Akad. Nauk., ser. fyz. **16** (1952) 322
21) M. F. Rose, G. H. Goertzel and B. I. Spinrad, Phys. Rev. **83** (1951) 79
22) L. A. Sliv and I. M. Band, Tables of Gamma-Ray Internal Conversion Coefficients (in press)

Nuclear Physics **2** (1956/57) **736**; *North-Holland Publishing Co., Amsterdam*

NOTE ON THE ISOTOPIC EFFECT IN THE FRACTIONAL DECOMPOSITION OF POTASSIUM FLUOBORATE

MAURICE D'HONT and ANDRÉ DE LATTRE
C.E.A.N., Mol, Belgium

Received 4 October 1956

It has been established by Shuittse [1]) that in the thermal decomposition of KBF_4 the first fractions of BF_3 are enriched in the heavy isotope B^{11}. The author points out that this is contrary to what would be expected from kinetic considerations.

It may be interesting to note that in a preliminary study of the problem of chemical separation of boron isotopes we were led in June 1954 to calculate from spectroscopic data the equilibrium constant of the exchange reaction

$$B^{10}F_3 + B^{11}F_4^- = B^{11}F_3 + B^{10}F_4^- .$$

Using the vibration frequencies given by Goubeau and Bues [2]), it is easily shown that

$$\frac{(B^{11}F_3)}{(B^{10}F_3)} = K\frac{(B^{11}F_4^-)}{(B^{10}F_4^-)}, \qquad \text{with } K = 1.05.$$

The effect reported by Shuittse therefore appears to be in conformity with theoretical predictions if we assume rapid exchange between boron trifluoride and the fluoborate from which it originates The deviation of K from unity is practically entirely due to the zero-point energy effect.

References

1) Shuittse, JETP (American edition) **2** (1956) 402
2) Goubeau and Bues, Zeitschrift für anorganische Chemie **268** (1952) 221

BOOK REVIEW

DAVID H. GURINSKY and GEORGE J. DIENES, *Nuclear fuels* (D. Van Nostrand Company Inc., Princeton 1956. xvi—364 p. $ 7.50).

This volume represents an attempt to rewrite some of the information presented at the Geneva Conference on the peaceful uses of Atomic Energy as an introductory treatment of materials for nuclear fuel elements suitable for metallurgists and, perhaps, engineers. It should be said at once that the volume under review is a credit to the editors and publisher.

The separate papers presented at the Conference involved a good deal of overlapping, as for instance in the repeated presentation by successive authors of the same Al—U equilibrium diagram printed, however, on different scales. Much of this sort of duplication has been removed in the preparation of the present volume, although minor discrepancies remain, as in the choice of transformation temperatures for U, where slightly different values are given on pages 22 and 69 without any indication of which values are to be preferred. An interesting addition to the terminology of science is to be found in fig. 19, where SPECIMAN is presented as a singular version of specimen. Fig. 19, like many others, has been specially redrawn for the present publication and the singularity has arisen as a result of this redrafting. Taken by and large, however, the diagrams are excellent and often an improvement on the original Conference versions.

The general theme of the book is symbolized by the frontispiece, which is a photograph of the display panel prepared to illustrate the fabrication of a Geneva Reactor fuel element from its components. In pursuing the theme fabrication and use a certain amount of more academic metallurgy has been discarded from the original Conference material. The volume itself is in three parts.

Part I — The Metallurgy of Uranium and Thorium reviews in some detail American practice in the preparation of these two metals from their ores and outlines British practice. The physical properties of the two elements are reported and their response to deformation processes and to heat treatment discussed in some detail. The influence of alloying additions is outlined and correlated with the metallography of the alloy systems. In considering fabrication processes, attention is given to casting processes for U and powder metallurgy processes for Th. Some account is also given of the corrosion behaviour of these materials. The treatment in Part I is strictly metallurgical and gives a very satisfactory account of the fundamental properties of the two metals and their alloys, thus preparing the reader for Part II.

Part II — Radiation Effects contains also a mass of information on the response of Uranium metal to thermal cycling, which is not strictly a radiation effect. Other editors might have been tempted to discuss thermal cycling in Part I as a fairly straightforward metallographic consequence of the anisotropic thermal expansion of metallic U. Radiation effects proper are considered from three points of view. Firstly a short account is given of the basic theory. Secondly a fairly detailed account is given of the observed effects of radiation upon such metallic and non-metallic structural materials as may be associated with a nuclear reactor—particular attention being given to graphite. Thirdly there is an extensive account of radiation effects in such fissile materials as solid uranium, uranium rich alloys, dispersion type fuel elements in which the fissile material is dispersed in a matrix of non-fissile material, ceramic fuels and liquids.

Part III — Solid and Fluid Fuels contains a detailed account of the fabrication of selected fuel element assemblies, particular attention being given to the canning of uranium slugs and the preparation of dispersion type fuel elements using an aluminium matrix.

There is no doubt that the editors have achieved a most valuable integration of the Conference transcript as it relates to Nuclear Fuels.

H. J. Axon

AUTHOR INDEX

ALKHAZOV, D. G., D. S. ANDREYEV, A. P. GREENBERG and I. KH. LEMBERG, Investigation of Coulomb excitation of nuclei by nitrogen ions 65
ANDREYEV, D. S., *see* Alkhazov
ATTERLING, H., J. BEYDON, M. CRUT et J. OLKOWSKY, Transmutation du cuivre par le carbone, l'oxygène et le néon 619
ATTERLING, H., *see* Crut
BARTHOLOMEW, G. A., *see* Gove
BELENKY, S. Z. Connection between scattering and multiple production of particles 259
BELL, J. S., R. J. EDEN and T. H. R. SKYRME, Magnetic moments of nuclei and the nuclear many-body problem 586
BERGSTRÖM, I., *see* Schmorak
BERTOLINI, G., Upper limit for the lifetimes of excited states of Fe^{56} and Ti^{46} 660
BEYDON, J., R. CHAMINADE, M. CRUT, H. FARAGGI, J. OLKOWSKY et A. PAPINEAU, Étude de la transmutation du cuivre par l'azote et l'oxygène 593
BEYDON, J., *see* Atterling
BISWAS, S. N. and H. S. GREEN, Radially symmetric solutions of Bethe-Salpeter equation 177
BLANK, V. Z. and D. V. SHIRKOV, Improvement of quantum electrodynamics perturbation theory with help of the renormalization group 356
BLIN-STOYLE, R. J., Collective nuclear motion and the effective mass of a nucleon. 169
CERINEO, M., Energy levels of C^{11} and angular distributions of some neutron groups from the B^{10} (d, n) reaction . . . 113
CHAMINADE, R., M. CROS, I. GRATOT et M. LE PAPE, Mise en évidence d'un isotope léger de rubidium 634
CHAMINADE, R., *see* BEYDON
CHUMIN, V. G., *see* Dzhelepov
CORINALDESI, E., Causality and dispersion relations in wave mechanics 420
CROS, M., *see* Chaminade
CRUT, M., H. FARAGGI, J. OLKOWSKY et L. ATTERLING, Comparaison des réactions $^{59}Co+^{20}Ne$ et $^{63}Cu+^{16}O$. . . 624

CRUT, M., *see* Atterling
CRUT, M., *see* Beydon
DE HEMPTINNE, M., *see* Macq
D'HONT, M. and A. DE LATTRE, Note on the isotopic effect in the fractional decomposition of potassium fluoborate . 736
DE LATTRE, A., *see* D'hont
DELYAGIN, N. N., A. A. SOROKIN, N. V. FORAFONTOV and V. S. SHPINEL, Decay scheme for Zr^{97} and Nb^{97} 687
DOLGINOV, A. Z., On the information about β-interaction and nuclear levels derived from the polarization of X-ray quanta 723
DOLGINOV, A. Z. and I. N. TOPTIGIN, Effect of distribution of nuclear charge on angular correlation in beta decay . . 147
DZHELEPOV, B. S., N. N. ZHUKOVSKY, V. G. NEDOVESOV, I. F. UCHEVATKIN and V. G. CHUMIN, The gamma spectrum of Sb^{124} 408
EDGE, R. D., The (γ, n) reaction in Be^{9} at intermediate energies 485
EDEN, R. J., *see* Bell
ERIKSSON, T., Polarization of fast protons scattered by nuclei with inclusion of the electro-magnetic spin-orbit coupling 91
ERÖ, J. and L. KESZTHELYI, Cross section of the $I^{127}(\gamma, n)I^{126}$ reaction 371
FARAGGI, H., *see* Beydon
FARAGGI, H., *see* Crut
FORAFONTOV, N. V., *see* Delyagin
GERHOLM, T. R., *see* Schmorak
GLASER, V., and G. KÄLLÉN, A model of an unstable particle 706
GOVE, H. E., G. A. BARTHOLOMEV, E. B. PAUL and A. E. LITHERLAND, Properties of low lying levels in Mg^{25} 132
GRATOT, I., *see* Chaminade
GREEN, H. S., *see* Biswas
GREENBERG, A. P., *see* Alkhazov
GUREVICH, I. I. and M. I. PEVSNER, Repulsion of nuclear levels 575
GYÖRGYI, G., Ladungskonjugation und verwandte Transformationen in Nukleonenfeld 267
HANSTEEN, J. M. and S. MESSELT, Characteristic X-rays produced by protons of 0.2 to 1.6 MeV energy 526
HEER, E., *see* Lindqvist
IOFFE, B., L. OKUN and I. POMERANCHUK, Concerning the

number of different types of K-mesons 277
KÄLLÉN, G., *see* Glaser
KELMAN, V. M., V. A. ROMANOV, R. YA. METSKHVARISHVILI and V. A. KOLYUNOV, Investigation of internal conversion lines in the β-spectrum of a mixture of Eu^{152} and Eu^{154} isotopes 395
KESZTHELYI, L., *see* Erö
KLEMA, E. D., *see* Osborn
KOFOED-HANSEN, O., Shell effects in nuclear Coulomb energy differences 441
KOLYUNOV, V. A., *see* Kelman
LEMBERG, I. KH., *see* Alkhazov
LE PAPE, M., *see* Chaminade
LINDQVIST, T., and E. HEER, Directional correlation measurements in Fe^{57} 680
LITHERLAND, A. E., *see* Gove
MA, S. T., Contact and core interactions according to Dirac's relativistic theory of the electron 347
MACQ, P. C. et M. DE HEMPTINNE, Interprétations des résultats expérimentaux de corrélation angulaire 160
MATTHEWS, P. T. and A. SALAM, The coupling constants of strong interactions. 582
MC DONELL, J. A., *see* Schmorak
MESSELT, S., *see* Hansteen
METSKHVARISHVILI, R. YA., *see* Kelman
MITRA, A. N., Burst production by spin-3/2 particles . . . 283
NATAF, R. S., Sur les mouvements collectifs de rotation des noyaux. 497
NATHAN, O. and M. A. WAGGONER, Decay of Eu^{152} and Eu^{152m} 548
NAUTA, H., Differential elastic scattering of 14 MeV neutrons in lead, mercury and zinc 124
NEDOVESOV, V. G., *see* Dzhelepov
NIELSEN, K. O., O. B. NIELSEN and M. A. WAGGONER, Internal conversion coefficients for M1 transitions in $_{83}Bi^{214}$, $_{84}Po^{214}$ and $_{83}Bi^{212}$ 476
NIELSEN, O. B., *see* Nielsen
OKUN, L., *see* Ioffe
OLKOWSKY, J., *see* Atterling
OLKOWSKY, J., *see* BEYDON
OLKOWSKY, J., *see* Crut

OSBORN, R. K. and E. D. KLEMA, Analysis of nuclear quadrupole moments on the basis of a kinematical model . . . 454
PAPINEAU, A., *see* BEYDON
PAUL, E., *see* Gove
PEVSNER, M. I., *see* Gurevich
POMERANCHUK, I., Note on the number of different types of K-mesons 281
POMERANCHUK, I., *see* Ioffe
PRYCE, M. H. L., The energy levels of Pb^{205} 226
RIAZUDDIN, On the charge independence of nuclear forces 188
RIVIÈRE, A. C., The formation of He^5 by the deuteron bombardment of Li^7 81
ROBL, H., Kern-Anregung durch Elektronen 641
ROMÁN, P., On the isocovariance properties of leptons . . 651
ROMANOV, V. A., *see* Kelman
ROSENFELD, L., Remarks on the charge distribution in nuclei 450
SALAM, A., The interaction lagrangian for fundamental particles 173
SALAM, A., *see* Matthews
SCHMORAK, M., R. STOCKENDAL, J. A. MC DONELL, I. BERGSTRÖM and T. R. GERHOLM, Energy levels in Pb^{205} from the decay of Bi^{205} 193
SHELINE, R. K., The possible existence of rotational levels in Al^{28} 382
SHIRKOV, D. V., *see* Blank
SHPINEL, V. S., *see* Delyagin
SIEKMAN, J. G., Lifetime measurement by time to pulse height conversion, applied to the 517 keV level of ^{85}Rb. . . . 254
SKYRME, T. H. R., *see* Bell
SOROKIN, A. A., *see* Delyagin
STOCKENDAL, R., *see* SCHMORAK
THIEBERGER, R., Calculations in nuclear spectroscopy with the harmonic oscillator shell model 533
TIDMAN, D. A., A quantum theory of refractive index, Čerenkov radiation and the energy loss of a fast charged particle. 289
TOPTIGIN, I. N., *see* Dolginov
TREACY, P. B., Magnetic properties of F^{19} in the 197 keV nuclear level 239
TRUMPY, G., Measurement of circularly polarized gamma

radiation following polarized neutron capture 664
UCHEVATKIN, I. F., *see* Dzhelepov
VOTRUBA, V., Isobaric spin and description of antiparticles 98
WAGGONER, M. A., *see* Nielsen
WAGGONER, M. A., *see* Nathan
ZELDES, N., The competition between nuclear shells in Mayer's model 1
ZHUKOVSKY, N. N., *see* Dzhelepov

INDEX BOOK REVIEWS

BETHE, H. A. and P. MORRISON, Elementary nuclear theory (L. R.). 109
EVANS, R., The atomic nucleus (L. R.) 109
GURINSKY, D. H. and G. J. DIENES, Nuclear fuels (H. J. Axon) 737
Interscience tracts on physics and astronomy (L. R.) . . . 109
MURPHY, G. M. (Editor), Production of heavy water (P. J. Haringhuizen). 110
UMEZAWA, H., Quantum Field Theory (N. Kemmer) . . . 192

SUBJECT INDEX

Beta and gamma spectroscopy

Effect of distribution of nuclear charge on angular correlation in beta decay, A. Z. Dolginov and I. M. Toptigin 147
Interprétations des résultats expérimentaux de corrélation angulaire, P. C. Macq et M. de Hemptinne 160
Energy levels in Pb^{205} from the decay of Bi^{205}, M. Schmorak, R. Stockendal, J. A. Mc Donell, I. Bergström and T. R. Gerholm 193
Lifetime measurement by time to pulse height conversion, applied to the 517 keV level of ^{85}Rb, J. G. Siekman 254
Investigation of internal conversion lines in the beta spectrum of a mixture of Eu^{152} and Eu^{154} isotopes, V. M. Kelman, V. A. Romanov, R. Ya. Metskhvarishvili and V. A. Kolyunov. 395
The gamma spectrum of Sb^{124}, B. S. Dzhelepov, N. N. Zhukovsky, V. G. Nedovesov, I. F. Uchevatkin and V. G. Chumin. 408
Internal conversion coefficients for M1 transitions in $_{83}Bi^{214}$, $_{84}Po^{214}$ and $_{83}Bi^{212}$, K. O. Nielsen, O. B. Nielsen and M. A. Waggoner 476
Decay of Eu^{152} and Eu^{155m}, O. Nathan and M. A. Waggoner 548
Measurement of circularly polarized gamma radiation following polarized neutron capture, G. Trumpy 664
Directional correlation measurements in Fe^{57}, T. Lindqvist and E. Heer 680

Decay Scheme for Zr^{97} and Nb^{97}, N. N. Delyagin, A. A. Sorokin, N. V. Forafontov and V. S. Shpinel 687
On the information about β-interaction and nuclear levels derived from the polarization of X-ray quanta, A. Z. Dolginov 723

Elementary Particles

Isobaric spin and description of antiparticles, V. Votruba 98
The interaction lagrangian for fundamental particles, A. Salam 173
Ladungskonjugation und verwandte Transformationen in Nukleonenfeld, G. Györgi 267
Concerning the number of different types of K-mesons, B. Ioffe, L. Okun and I. Pomeranchuk 277
Note on the number of different types of K-mesons, I. Pomeranchuk . 281
The coupling constants of strong interactions, P. T. Matthews and A. Salam 582
On the isocovariance properties of leptons, P. Román 651

Field theory

Radially symmetric solutions of Bethe - Salpeter equation, S. N. Biswas and H. S. Green 177
Contact and core interactions according to Dirac's relativistic theory of the electron, S. T. Ma 347
Improvement of quantum electrodynamics perturbation theory with help of the renormalization group, V. Z. Blank and D. V. Shirkov 356
A model of an unstable particle, V. Glaser and G. Källén 706

Methods and instruments

Note on the isotopic effect in the fractional decomposition of potassium fluoborate, M. D'Hont and A. de Lattre 736

News Items

Nuclear physics in Hungary 111
Ford foundation grant to Cern 112
On the nomenclature of nuclear families 496
International conference on nuclear structure Rehovoth, Israël (9—13 September 1957) 640

Nuclear forces (*see also* Structure of nuclei, scattering)

On the charge independence of nuclear forces, Riazuddin 188

Nuclear states (*see also* Beta and gamma spectroscopy, Reactions induced by particles, Photonuclear reactions)

Properties of low lying levels in Mg^{25}, H. E. Gove, G. A. Bartholomew, E. B. Paul and A. E. Litherland 132
The energy levels of Pb^{205}, M. H. L. Pryce 226
Magnetic properties of F^{19} in the 197 keV nuclear level, P. B. Treacy. 239
The possible existence of rotational levels in Al^{28}, R. K. Sheline . . . 382
Repulsion of nuclear levels, I. I. Gurevich and M. I. Pevsner 575
Upper limit for the lifetimes of excited states of Fe^{56} and Ti^{46}, G. Bertolini 660

Passage of particles through matter (*see also* Cosmic radiation)

Burst production by spin-3/2 particles, A. N. Mitra 283
A quantum theory of refractive index, Čerenkov radiation and the energy loss of a fast charged particle, D. A. Tidman 289

Photonuclear reactions

Cross section of the $I^{127}(\gamma, n)I^{126}$ reaction, J. Erö and L. Keszthelyi . . 371
The (γ, n) reaction in Be^{9} at intermediate energies, R. D. Edge . . . 485

Reactions induced by particles (*see also* Nuclear states)

Investigation of Coulomb excitation of nuclei by nitrogen ions, D. G. Alkhazov, D. S. Andreyev, A. P. Greenberg and I. Kh. Lemberg . . 65
The formation of He^{5} by the deuteron bombardment of Li^{7}, A. C. Rivière 81
Energy levels of C^{11} and angular distributions of some neutron groups from the B^{10} (d, n) reaction, M. Cerineo 113
Characteristic X-rays produced by protons of 0.2 to 1.6 MeV energy, J. M. Hansteen and S. Messelt 526
Etude de la transmutation du cuivre par l'azote et l'oxygène, J. Beydon, R. Chaminade, M. Crut, H. Faraggi, J. Olkowsky et A. Papineau . 593
Transmutation du cuivre par le carbone, l'oxygène et le néon, H. Atterling, J. Beydon, M. Crut et J. Olkowsky 619
Comparaison des réactions $^{59}Co+^{20}Ne$ et $^{63}Cu+^{16}O$, M. Crut, H. Faraggi, J. Olkowsky et H. Atterling 624
Mise en évidence d'un isotope léger de Rubidium, R. Chaminade, M. Cros, I. Gratot et M. le Pape 634
Kern-Anregung durch Elektronen, H. Robl 641

Reports on conferences and congresses

Symposium on the precision determination of nuclear masses in Mainz (10—12 July 1956), A. H. Wapstra 286
International congress of theoretical physics (Seattle, 17—20 September 1956) 287

Scattering

Polarization of fast protons scattered by nuclei with inclusion of the electro-magnetic spin-orbit coupling, T. Eriksson 91
Differential elastic scattering of 14 MeV neutrons in lead, mercury and zinc, H. Nauta 124
Connection between scattering and multiple production of particles, S. Z. Belenky 259
Causality and dispersion relations in wave mechanics, E. Corinaldesi . 420

Structure of nuclei (models and theories) (*see also* Nuclear states)

The competition between nuclear shells in Mayer's model, N. Zeldes. . 1
Collective nuclear motion and the effective mass of a nucleon, R. J. Blin-Stoyle 169
Shell effects in nuclear Coulomb energy differences, O. Kofoed-Hansen . 441
Remarks on the charge distribution in nuclei, L. Rosenfeld. 450
Analysis of nuclear quadrupole moments on the basis of a kinematical model, R. K. Osborn and E. D. Klema 454
Sur les mouvements collectifs de rotation des noyaux, R. S. Nataf . . 497
Calculations in nuclear spectroscopy with the harmonic oscillator shell model, R. Thieberger 533
Magnetic moments of nuclei and the nuclear many-body problem, J. S.Bell, R. J. Eden and T. H. R. Skyrme 586

APPEAL TO CONTRIBUTORS

Among the factors delaying the appearence of a paper, the most serious is the unsatisfactory presentation of the typescript. An appeal is made to contributors to follow the simple rules and conventions laid down in the instruction sheet which has already been widely distributed and copies of which are available on request from the publishers or the members of the Editorial Board. Attention is called in particular to the writing of formulae. Authors are especially requested *not* to typewrite formulae, but to write them in long hand, very carefully, since the compositor cannot guess the meaning of a symbol which is not legible. In future, the Editor will be forced to return unsatisfactory typescripts to the authors for the necessary material improvements.

It frequently happens that after a paper has been communicated, the author sends substantial corrections or alterations. Since the publisher and printer spare no effort to achieve prompt publication, such late alterations often arrive after the paper has already been set, and inflict on them much unnecessary trouble and cost. Contributors should realise that a too hasty writing-up of a paper thus defeats the prospect of a quick publication.

Editor and publisher trust that the authors will not shun the slight trouble which the careful preparation of the typescript entails and thank them in advance for their cooperation.

Editorial Board

K. B. Adams
E. Amaldi
H. L. Anderson
K. T. Bainbridge
C. J. Bakker
P. R. Bell
R. E. Bell
S. de Benedetti
A. Berthelot
H. Brinkman
G. von Dardel
M. Deutsch
W. Gentner
P. C. Gugelot
H. Halban
O. Haxel
M. de Hemptinne
P. Huber
D. J. Hughes
S. Kikuchi
J. Koch
S. Livingston
E. M. McMillan
P. B. Moon
M. L. Oliphant
W. Paul
A. S. Rao
G. Salvini
P. Savić
P. Scherrer
C. Schmelzer
A. de Shalit
H. W. B. Skinner
R. Tangen
D. Taylor
S. du Toit
O. Wernholm
R. R. Wilson
S. D. Winter

Just out: The first issue of

NUCLEAR INSTRUMENTS

A journal on accelerators, instrumentation and techniques in nuclear physics

EDITOR: K. SIEGBAHN
UPPSALA

it contains:

K. SIEGBAHN, Editor's notice

J. B. ADAMS, The CERN symposium 1956 (I)

G. F. VON DARDEL, The CERN symposium 1956 (II)

A. LUNDBY, The CERN symposium 1956 (III)

Proceedings of the CERN symposium 1956

S. COHEN and A. V. CREWE, Regenerative action in high energy accelerators

R. W. P. DREVER, A. MOLJK and S. C. CURRAN, A proportional counter system with small wall effect

D. L. JUDD and S. A. BLUDMAN, Aberrations and fringing effects in a 180° double focusing magnetic spectrometer

R. STOCKENDAL and K. E. BERGKVIST, Evaporation device for beta-spectrometer samples

E. BREITENBERGER, Diverging electrostatic lenses in accelerators

Book Reviews

Nuclear Instruments is published in bi-monthly issues.

Subscription price 130 *sh*; $ 17.00, *postage free.*

NORTH-HOLLAND PUBLISHING COMPANY AMSTERDAM